

Supplementary information

STEREOCHEMICAL INSIGHTS IN β -AMINO-N- ACYLHYDRAZONES AND THEIR IMPACT ON DPP-4 INHIBITION

Eduardo Reina,^{a,b} Lucas Silva Franco,^{a,b} Teiliane Rodrigues Carneiro,^a Eliezer J.

Barreiro,^{a,b} and Lidia Moreira Lima^{a,b*}

^a. Instituto Nacional de Ciência e Tecnologia de Fármacos e Medicamentos (INCT-INO FAR), Laboratório de Avaliação e Síntese de Substâncias Bioativas (LASSBio[®]), Universidade Federal do Rio de Janeiro (UFRJ), CCS, Cidade Universitária, Rio de Janeiro-RJ, Brasil.

^b. Pós-graduação em Farmacologia e Química Medicinal, Instituto de Ciências Biomédicas, Universidade Federal do Rio de Janeiro, Rio de Janeiro-RJ, Brasil

Table of Contents

Supplementary Information: Molecular Modelling	4
Supplementary Information: Chemistry	10
1. Synthesis of LASSBio-2123 (5), LASSBio-2124 (6), LASSBio-2125 (7), LASSBio-2126 (9), and LASSBio-2127 (13)	11
2. Synthesis of 3-amino- <i>N'</i> -(3,4-difluorobenzyl)-4-(2,4,5-trifluorophenyl)butanehydrazide: LASSBio-2127 (13)	16
3. Synthesis of LASSBio-2128 (14)	16
4. Enantiomeric Synthesis of <i>N</i> -acylhydrazones (6-R and 6-S)	20
5. Aqueous solubility determination	27
6. Dissociation constant determination	27
7. Chemical stability studies	27
8. <i>In vitro</i> DPP-4 inhibition evaluation	28
Supplementary Information: Analytical Spectra	29
References	79

Table of Supplementary Figures and Tables

Figure S1. Sitagliptin (1) co-crystallized (yellow) in the active site of DPP4. S1 hydrophobic pocket in green. Key glutamates residues of S2 pocket in light-blue. Residues that form the “oxyanion hole” in white (Tyr659/547). Selected residues on S2 extended pocket in purple. Catalytic triad (Ser630, His740, Asp708) in orange.	5
Figure S2. a) Alignment of co-crystallographic structures of gliptins 7-16 approved for the treatment of DMT2 and the apo form with human DPP-4 b) Zoom of the active site. In yellow aminoacids without conformational differences. In purple aminoacids that presented conformational differences (Tyr547, co-crystallographic structure of vildagliptin 6b1o) and Trp629 (apo form structure of DPP-4, 1pfq) from active site of DPP-4.	5
Figure S3. Superposition of sitagliptin co-crystallized (grey) and re-docked (purple) with GOLD 5.1 program. RMSD = 0.387 Å.	6
Figure S4. Superposition of co-crystallized (<i>R</i>)-sitagliptin (purple) and docked (<i>S</i>)-sitagliptin (green) inside DPP-4 active site.	6
Figure S5. Superposition of compounds (10-R) (purple), (11-R) (orange), (12-R) (blue) and R-sitagliptin (1-R) (green) at the DPP-4 active site.	7
Figure S6. Linagliptin (11) interaction with Trp629.	8
Figure S7. Structures of LASSBio-294 and LASSBio-785 obtained by X-ray diffraction.	8
Figure S8. Superposition of compounds (13-R) (green) and R-sitagliptin (1-R) (purple) inside the DPP-4 active site.	8
Figure S9. a) ¹ H-NMR NOE-diff (400 MHz, CD ₃ OD) spectrum of 14 . Signal irradiated δ _H 7.86 (N=CH). b) ¹ H-NMR NOE-diff (400 MHz, CD ₃ OD) spectrum of 14 . Signal irradiated δ _H 3.36 (N-CH ₃).	19
Figure S10. Chemical shifts differences (Δδ ^{R-S}) between diastereoisomers (<i>R</i>)-MPA-(<i>R</i> [*])-β-aminoester (23) and (<i>S</i>)-MPA-(<i>R</i> [*])-β-aminoester (24). Representation of the model that allowed the determination of absolute stereochemistry of 20-R [*] as R	24
Figure S11. a) Energetic rotation profile of H-N-C-H bond (blue bond for diastereoisomer 23 and orange bond for diastereoisomer 24) obtained by semi-empirical method PM3 in SPARTAN program. b) Favored conformers for diastereoisomers 23 and 24 obtained by semi-empirical method PM3 in SPARTAN program.	24
Table S1. PDB codes of co-crystal structures of gliptins approved for the treatment of DMT2 and the Apo form with human DPP-4, their resolution, and type of interaction with DPP-4.	4
Table S2. GOLD 5.1 scores for (<i>R</i>)-sitagliptin (1-R) and the E and Z isomers of compound (6-R).	6
Table S3. Score values obtained with GOLD 5.1 for (<i>R</i>)-sitagliptin, (6-R), (6-S), (13-R), (13-S), (14-R) and (14-S).	7
Table S4. Physicochemical and drug-likeness properties of sitagliptin (7), LASSBio-1773 (2) and compounds 5-14 calculated by ACD/Percepta Software.	9
Table S5. Physical and spectroscopic properties of LASSBio-2123 to LASBio-2128 (5-7, 9, 13-14).	19
Table S6. ¹ H-NMR data for the MPA amides of 23 and 24 at 400 MHz, in CDCl ₃ ; δ in ppm, J in Hz.	23

Supplementary Information: Molecular Modelling

All compounds were constructed and energy-minimized at the HF/3-21G level using Spartan 14 (Wavefunction Inc.). Among the DPP-4 crystallographic structures (Table S1, Figure S1) available in the Protein Data Bank, the one with code 1X70 (resolution 2.1 Å) was used for docking runs with the GOLD 5.1 program (CCDC; License key: G/4142006). GOLD was used for addition of hydrogen atoms in the protein structure. The binding site was determined as the amino acids having atoms within 6 Å radius of the co-crystallized ligand. With the aim to obtain the more stable complex (protein-ligand) all scoring functions of GOLD program were explored, GoldScore, ChemScore, ChemPLP and ASP. All the score functions were evaluated with and without water for the re-docking of the co-crystallized sitagliptin (**7**) to identify the most adequate fitness function for docking studies into DPP-4. After docking, the RMSD between the best result for each fitness function and the crystallographic structure was calculated. The fitness function with the best performance in the re-docking test, which was ChemPLP (without water) (Figure S3 and S4), was used for the semi-rigid docking study of the compounds described in this study. Three consecutive runs were conducted, each of which generated 10 conformations. The highest-scoring conformation of each run was chosen and analyzed.

Table S1. PDB codes of co-crystal structures of gliptins approved for the treatment of DMT2 and the Apo form with human DPP-4, their resolution, and type of interaction with DPP-4.

Co-crystal Structure	PDB File	Resolution (Å)	Interaction type
<i>Sitagliptin (7)</i>	1x70	2.10	Reversible
<i>Vildagliptin (8)</i>	6b1o	1.91	Covalent Reversible
<i>Saxagliptin (9)</i>	3BJM	2.35	Covalent Reversible
<i>Alogliptin (10)</i>	3G0B	2.25	Reversible
<i>Linagliptin (11)</i>	5t4b	1.76	Reversible
<i>Anagliptin (13)</i>	3WQH	2.85	Reversible
<i>Tenagliptin (14)</i>	3VJK	2.49	Reversible
<i>Trelagliptin (15)</i>	5KBY	2.24	Reversible
<i>Omarigliptin (16)</i>	4pnz	1.90	Reversible
<i>Apo form</i>	1pfq	1.90	-

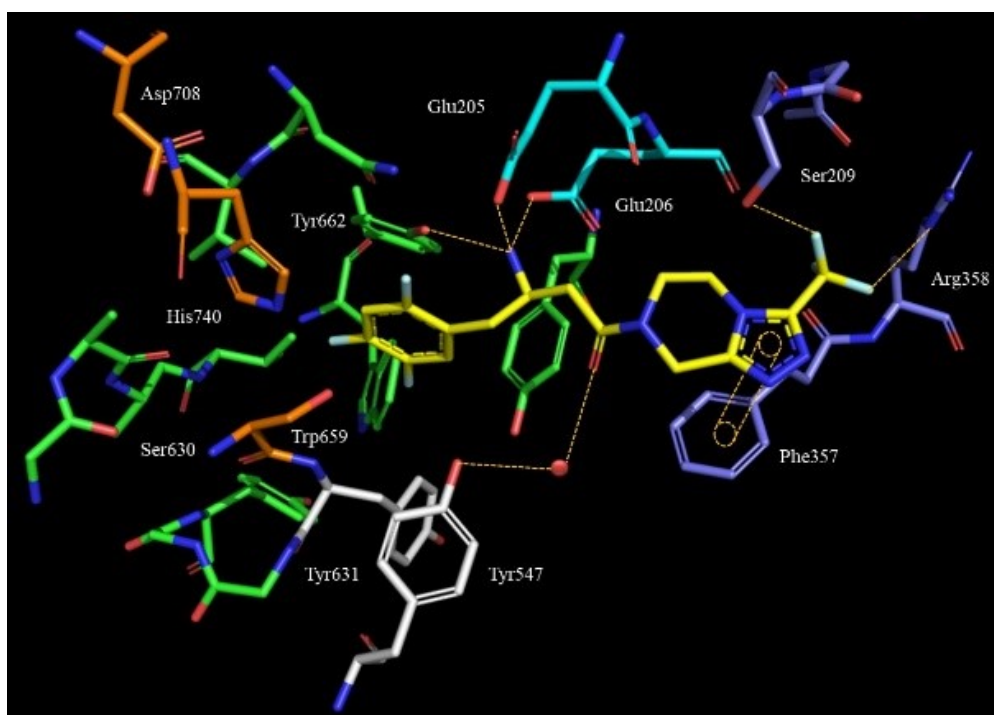


Figure S1. Sitagliptin (1) co-crystallized (yellow) in the active site of DPP4. S1 hydrophobic pocket in green. Key glutamates residues of S2 pocket in light-blue. Residues that form the “oxyanion hole” in white (Tyr659/547). Selected residues on S2 extended pocket in purple. Catalytic triad (Ser630, His740, Asp708) in orange.

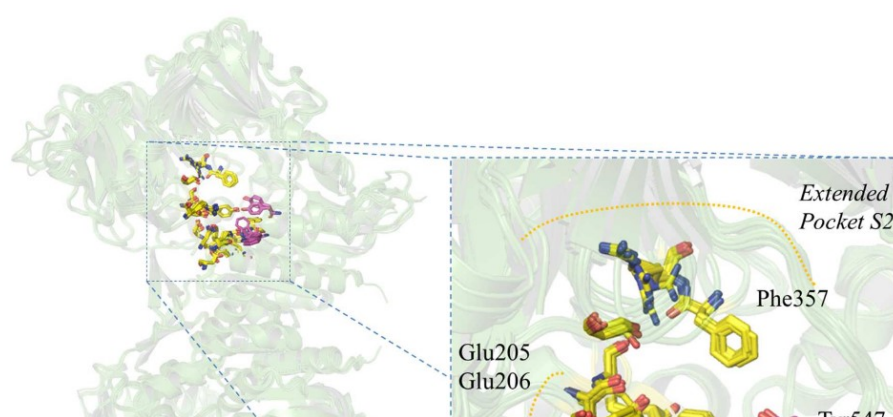


Figure S2. a) Alignment of co-crystallographic structures of gliptins 7-16 approved for the treatment of DMT2 and the apo form with human DPP-4 b) Zoom of the active site. In yellow aminoacids without conformational differences. In purple aminoacids that presented conformational differences (Tyr547, co-crystallographic structure of vildagliptin 6b1o) and Trp629 (apo form structure of DPP-4, 1pfq) from active site of DPP-4.

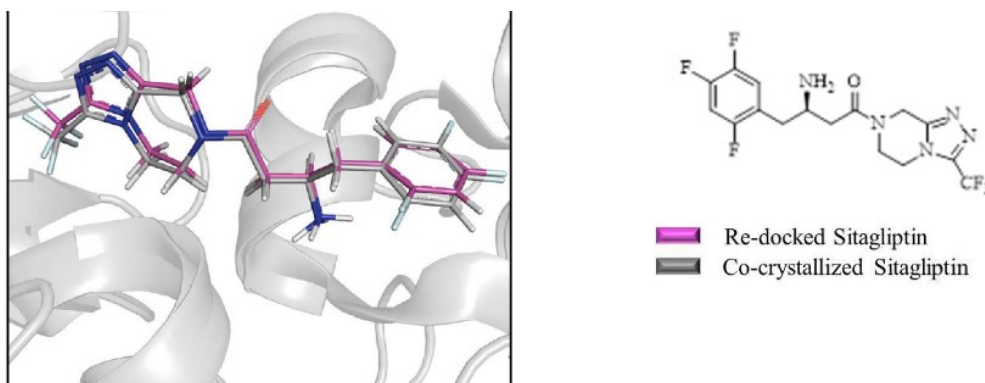


Figure S3. Superposition of sitagliptin co-crystallized (grey) and re-docked (purple) with GOLD 5.1 program. RMSD = 0.387 Å.

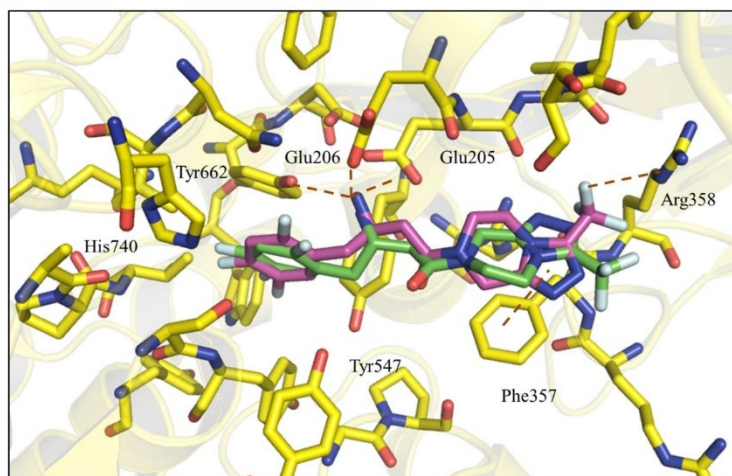
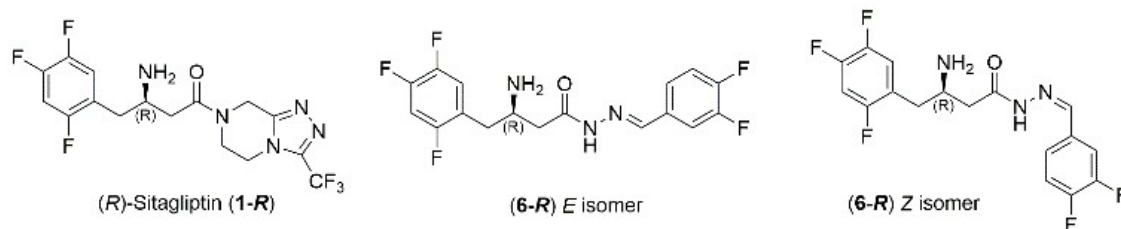


Figure S4. Superposition of co-crystallized (*R*)-sitagliptin (purple) and docked (*S*)-sitagliptin (green) inside DPP-4 active site.

Table S2. GOLD 5.1 scores for (R)-sitagliptin (**1-R**) and the E and Z isomers of compound (**6-R**).



Compound	Score Value
(R)-Sitagliptin (1-R)	88.0
(6-R) E isomer	86.9
(6-R) Z isomer	76.3

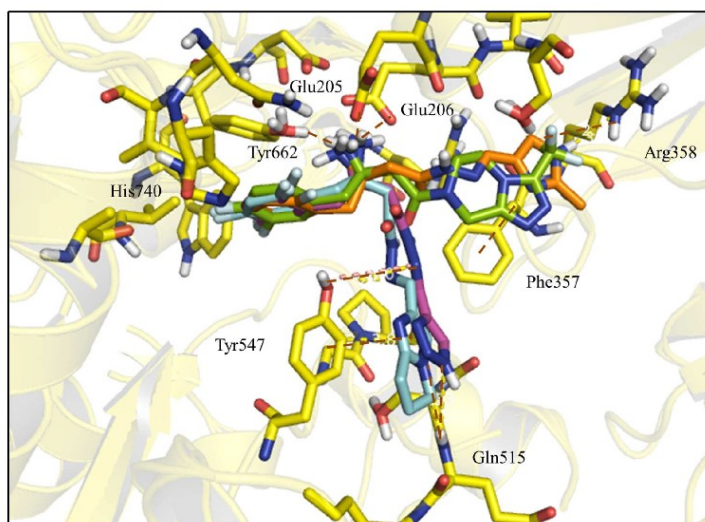
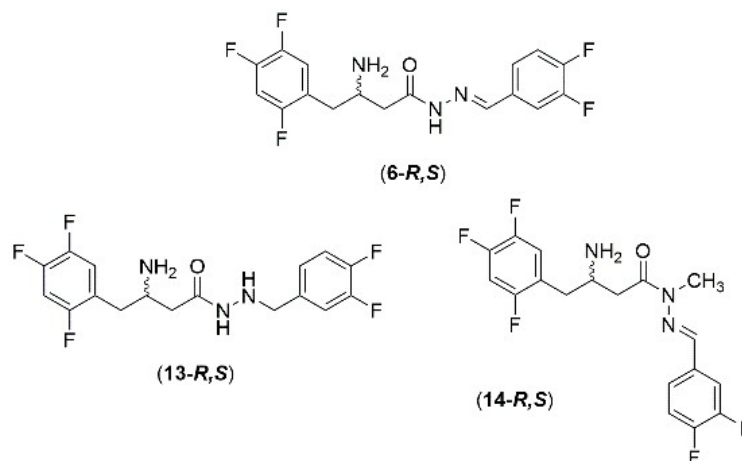


Figure S5. Superposition of compounds (**10-R**) (purple), (**11-R**) (orange), (**12-R**) (blue) and R-sitagliptin (**1-R**) (green) at the DPP-4 active site.

Table S3. Score values obtained with GOLD 5.1 for (R)-sitagliptin, (**6-R**), (**6-S**), (**13-R**), (**13-S**), (**14-R**) and (**14-S**).



<i>Compound</i>	<i>Score Value</i>
(R)-Sitagliptin (1-R)	88.0
6-R	86.9
6-S	72.01
13-R	80.0
13-S	76.2
14-R	51.0

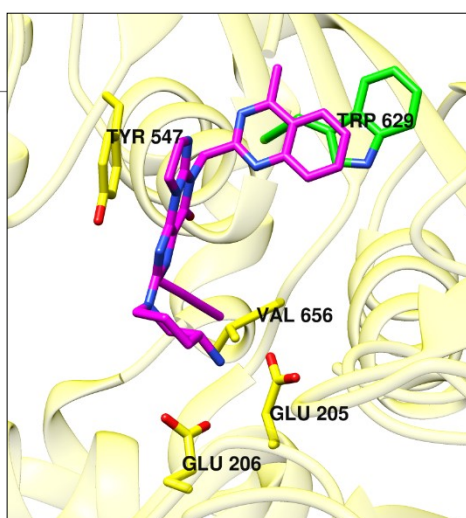
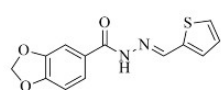
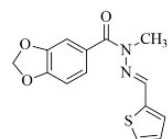


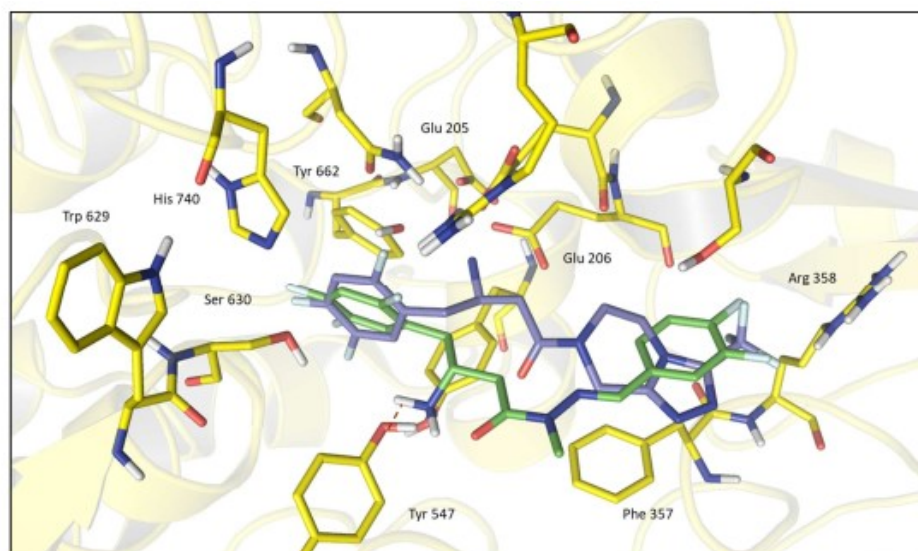
Figure S6. Linagliptin (**11**) interaction with Trp629.



LASSBio-294



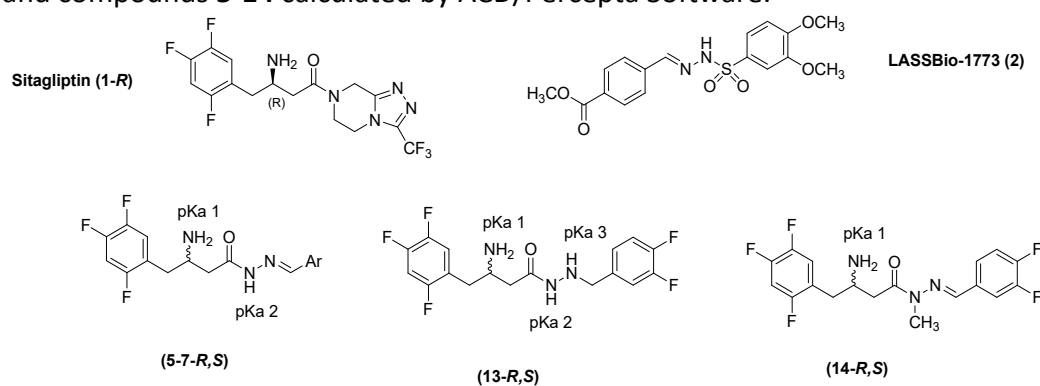
LASSBio-785



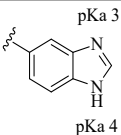
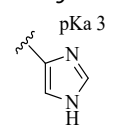
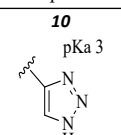
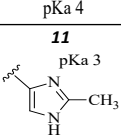
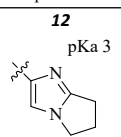
Fi

Figure S8. Superposition of compounds (**13-R**) (green) and R-sitagliptin (**1-R**) (purple) inside the DPP-4 active site.

Table S4. Physicochemical and drug-likeness properties of sitagliptin (**7**), LASSBio-1773 (**2**) and compounds **5-14** calculated by ACD/Percepta Software.



Compound	cLog P	LogD		pKa	PPB	BBB	Bioavailability (F)	Permeation (CaCo-2) (cm/s)	HIA	Solubility (mg/mL)
		4.6	7.4							
Sitagliptin (1)	1.17 (1.5 ^a)	-	-	7.2 (7.7 ^a)	68% (38% ^a)	-2.97 (Penetrant)	(87% ^a) 77%	Pe = 49E ⁻⁶	100% (90% ^{ab})	0.09 Insoluble
LASSBio-1773 (2)	2.79	2.36	2.36	8.7; - 3.7	98%	-3.34 (weak)	98%	Pe = 206E ⁻⁶	100%	0.003 Insoluble
5 	2.39	- 1.14	0.2	7.0; 12.9	87%	-2.97 (Penetrant)	82%	Pe = 84E ⁻⁶	100%	0.02 Insoluble
6 	2.74	- 0.92	0.43	7.1; 12.6	90%	-3.24 (weak)	89%	Pe = 114E ⁻⁶	100%	0.008 Highly insoluble
7 	4.00	0.47	1.82	7.1; 12.7	96%	-2.70 (Penetrant)	48%	Pe = 156E ⁻⁶	100%	0.0002 Insoluble
8	2.04	- 2.18	0.08	7.1; 13.6; 4.4;	89%	-3.38 (weak)	48%	Pe = 29E ⁻⁶	100%	0.007 Insoluble

				11.9						
9 	1.00	-4.53	-1.59	7.1; 14.3; 3.9; 11.5	58%	-3.33 (weak)	17%	Pe = 8E ⁻⁶	70%	0.36 Soluble
10 	0.52	-3.0	-1.68	7.6; 13.5; 0.5; 9.22	47%	-4.02 (Non-penetrant)	14%	Pe = 1E ⁻⁶	50%	1.35 Soluble
11 	1.29	-4.07	-1.33	7.5; 12.0; 5.1; 14.9	58%	-3.47 (weak)	15%	Pe = 5E ⁻⁶	43%	0.15 Soluble
12 	1.95	-3.15	-0.55	7.4; 12.4; 5.2	49%	-2.82 (Penetrant)	19%	Pe = 35E ⁻⁶	91%	0.1 Soluble
13	1.66	-0.49	0.88	8.0; 0.5	77%	-3.88 (Non-penetrant)	63%	Pe = 8E ⁻⁶	87%	0.28 Soluble
14	2.59	-1.26	0.97	9.1	92%	-4.33 (Non-penetrant)	98%	Pe = 48E ⁻⁶	100%	0.69 Soluble

^{a)}Experimental data from literature report¹. ^{b)}In dogs¹²

PPB=Protein plasma binding; BBB=Blood-brain barrier; CaCo-2=Human epithelial colorectal adenocarcinoma cells; HIA=Human intestinal absorption.

Supplementary Information: Chemistry

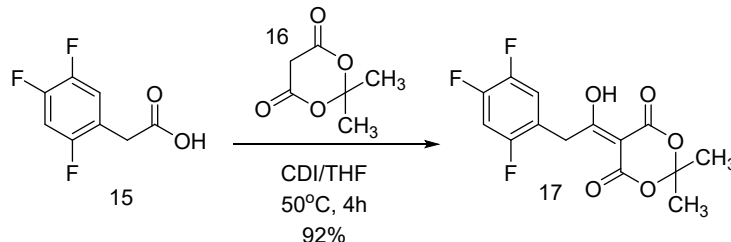
General Remarks

Unless otherwise noted, all the materials were obtained from commercially available sources and were used without purification. Reactions were routinely monitored by thin-layer chromatography (TLC) in silica gel (KieselGel 60 F254 Merck); the products were visualized with UV lamps (254 nm & 365 nm), or using the following color reagents: iodine, 2,4-dinitrophenylhydrazine or 4-dimethylaminobenzaldehyde. Purifications by column chromatography were carried out in silica gel 230-400 Mesh (Merck). Melting points (m.p.) were determined in a melting point system MP70 Mettler Toledo and the values obtained were not corrected. ¹H- and ¹³C-Nuclear Magnetic Resonance (NMR) spectra were determined in deuterated solutions using a Varian model MR400 spectrometer with 400 MHz for ¹H- and 100 MHz for ¹³C (LAMAR, Laboratório Multiusuários de Análises por RMN (LAMAR). Núcleo de Pesquisas de Produtos Naturais, Universidade Federal do Rio de Janeiro; UFRJ, Brazil), or Varian Mercury-300 spectrometer with 300 MHz for ¹H and 75 MHz for ¹³C (IMA, Laboratório de Ressonância Magnética Nuclear (RMN) de Alta Resolução. Instituto de Macromoléculas, Universidade Federal do Rio de Janeiro; UFRJ, Brazil) or Bruker AC-200 spectrometer with 200 MHz for ¹H and 50 MHz for ¹³C (LABRMN, Laboratório de Ressonância Magnética Nuclear (LABRMN). Instituto de Química (IQ). Universidade Federal do Rio de Janeiro (UFRJ), Brazil). The chemical shifts are given in parts per million (δ) from solvent residual peaks and the coupling constant values (J) are given in Hertz. Signal multiplicities are represented as s

(singlet), d (doublet), t (triplet), q (quartet) and m (multiplet). Deuterated solvents like CDCl₃, DMSO-*d*₆ and CD₃OD were used for the determinations. High performance liquid chromatography (HPLC) for purity determinations were conducted using Shimadzu LC-20AD equipped with a SIL-20A autosampler, with a Shimadzu CBM-20A interface and a Shimadzu SPD-M20A detector (Diode Array) at substance-specific wavelengths. The column used was Kromasil 100-5 C18 (4.6 mm x 250 mm) and the solvent system for HPLC purity analyses was conducted in mobile phase MeCN-H₂O-NH₄OH (5.0 N) 60:40:0.01 (pH = 9), with 1 mL/min flow, sample concentration of 1 mg/mL, injection volume of 20 μL, and run time = 15 min. Data were acquired by software "LC solution" version 4.0. Mass spectra were obtained in electrospray ionization (EI) mode on Bruker AmaZon SL ion-trap MS. Spectra were analyzed using Compass 4.0 software. Infrared (IR) spectra were obtained in a Thermo Nicolet's iS 10 FT-IR spectrometer, equipped with smart iTR ATR for direct measurements. All described products showed MS spectra, IR spectra and ¹H- and ¹³C-NMR spectra according to the assigned structures and obtained a purity ranging from 95.0 % to 99.8 % determined by HPLC. Optical rotation was measured with a Perkin-Elmer polarimeter model 341 using a sodium lamp (589 nm) at 20°C (Central Analítica - Núcleo de Pesquisas de Produtos Naturais, Universidade Federal do Rio de Janeiro; UFRJ, Brazil).

1. Synthesis of LASSBio-2123 (5), LASSBio-2124 (6), LASSBio-2125 (7), LASSBio-2126 (9), and LASSBio-2127 (13)

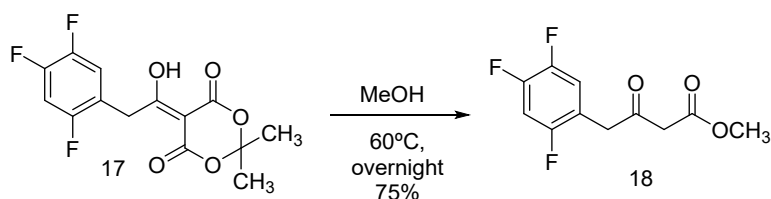
1.1. (5-(1-hydroxy-2-(2,4,5-trifluorophenyl)ethylidene)-2,2-dimethyl-1,3-dioxane-4,6-dione) (17)



Adapted from Sun et al (2011)³. In a 25 mL two necked round-bottom flask equipped with a reflux condenser, a magnetic stirrer and under argon atmosphere, 2 g (10.52 mmol) of 2,4,5-trifluorophenylacetic acid (**15**) was dissolved in 15 mL of dry THF. Next, 1.1 equivalents of CDI were added. The reaction was heated to 50°C and then 1.1 equivalents of Meldrum's acid (**16**) were added, keeping the stirring and temperature for 4 hours. Completion of the reaction was verified by TLC. Next, the reaction mixture was concentrated under reduced pressure and then, the residue was dissolved in DCM followed by a partition with cold water. pH was adjusted to 2 with HCl 10% and the aqueous phase was separated. The organic phase was washed with HCl 0.1 N and brine, respectively. The organic phase was then dried with anhydrous Na₂SO₄, filtered, and concentrated under vacuum to yield the Meldrum's adduct (**17**).

Appearance: white pale solid; **Yield:** 92%; **TLC conditions:** DCM/MeOH 98:2 (R_f: 0.75); **mp:** 102 - 103°C (lit. 101.5 - 103.5°C)⁴; **NMR-¹H** (400 MHz, CDCl₃) δ (ppm): 7.18-7.12 (1H, m); 6.99-6.93 (1H, m); 4.44 (2H, s); 1.76 (6H, s).

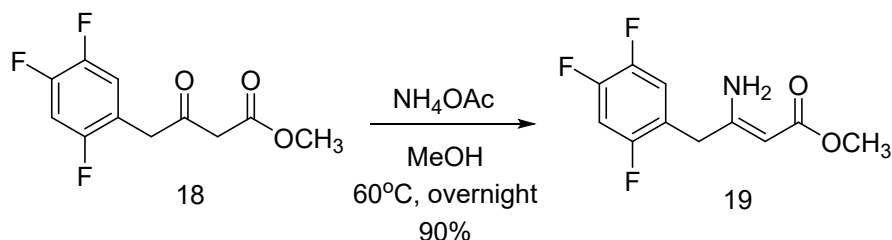
1.2. Synthesis of methyl 3-oxo-4-(2,4,5-trifluorophenyl)butanoate (18)



Adapted from Gore et al (2010)⁴. In a 100 mL round-bottom flask equipped with a reflux condenser, a magnetic stirrer and under argon atmosphere, 3.0 g (9.48 mmol) of Meldrum's adduct **17** was dissolved in 20 mL of dry MeOH. The resulting solution was stirred at 60°C overnight. After verifying total consumption of starting material (monitoring by TLC), the reaction mixture was concentrated under reduced pressure and the residue was treated with Na₂CO₃ 10% aqueous solution, achieving pH = 8, then it was extracted with DCM (3x40 mL). The organic phase was dried with anhydrous Na₂SO₄, filtered, and concentrated under vacuum to yield compound **18**.

Appearance: yellow oil; **Yield:** 75%; **TLC conditions:** Hexane/CHCl₃ 3:7 (Rf: 0.6); **MS (ESI):** [M+H]⁺, 247,23; **NMR-¹H** (400 MHz, CDCl₃) δ (ppm): 7.08-7.02 (1H, m); 6.99-6.92 (1H, m); 3.85 (2H, s); 3.76 (3H, s); 3.55 (2H, s); **NMR-¹³C** (100 MHz, CDCl₃) δ (ppm): 198.0 (C8); 167.3 (C14); 158.6/153.7 (C4); 152.1/147.1 (C2); 149.2/144.4 (C1); 119.3 (C3); 116.9 (C5); 105.6 (C6); 52.6 (C15); 48.5 (C7); 42.1 (C3).

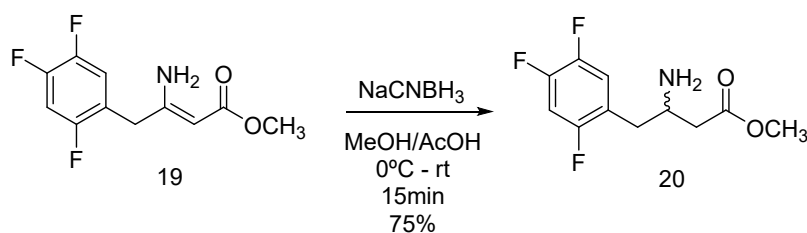
1.3. Synthesis of (Z)-methyl 3-amino-4-(2,4,5-trifluorophenyl)but-2-enoate (**19**)



Adapted from Kubryk et al (2006)⁵ and Gore et al (2010)⁴. In a 100 mL round-bottom flask equipped with a reflux condenser, a magnetic stirrer and under argon atmosphere, 1.8 g (7.31 mmol) of β-ketoester **18** and 10 equivalents of NH₄OAc were dissolved in 25 mL of dry MeOH. The resulting mixture was stirred and heated at 60 °C overnight. After end of the reaction, it was concentrated under reduced pressure until obtaining a pale-yellow oil, which was dissolved in EtOAc and stirred at 25 - 30 °C for 15 min. The white precipitate was filtered, and the solvent distilled until ¼ of initial volume. Next, hexane was added to the residue and stirred to 30 - 35°C for 1h. Finally, the mixture was filtered, dried over anhydrous Na₂SO₄, and concentrated under vacuum to yield compound **19**.

Appearance: white pale solid; **Yield:** 90%; **TLC conditions:** Hexane/CHCl₃ 3:7 (Rf: 0.5); **MS (ESI):** [M+H]⁺, 246,05; **NMR-¹H** (400 MHz, CDCl₃) δ (ppm): 7.15-7.02 (1H, m); 7.02-6.89 (1H, m); 4.57 (1H, s); 3.65 (3H, s); 3.41 (2H, s); **NMR-¹³C** (100 MHz, CDCl₃) δ (ppm): 170.4 (C14); 159.4 (C8); 158.5/153.5 (C4); 151.9/146.9 (C2); 149.4/144.4 (C1); 120.0 (C3); 118.5 (C5); 105.7 (C6); 85.0 (C13); 50.4 (C15); 34.7 (C7).

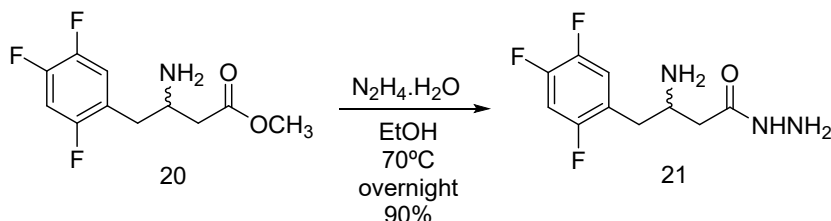
1.4. Synthesis of methyl 3-amino-4-(2,4,5-trifluorophenyl)butanoate (**20**)



Adapted from Gore et al (2010)⁴. In a 100 mL round-bottom flask equipped with a magnetic stirrer and under argon atmosphere, 1.6 g (6.53 mmol) of β -enamine ester **19** was dissolved in 20 mL of dry MeOH, followed by addition of AcOH until pH 4-5. The resulting solution was stirred at 0°C for 15 min. Subsequently, 3 equivalents of NaCNBH_3 were added and the reaction was stirred overnight. After completion of the reaction (monitored by TLC) the solvent was distilled, and the residue was treated with HCl 10% until pH 2. The resulting suspension was stirred for 15 min and extracted with DCM (3 x 20 mL). The organic phase was separated, and the aqueous phase was basified with NaOH 10% until pH 8-9. Then, the product was isolated with EtOAc (3 x 50 mL). The organic phase was dried over anhydrous Na_2SO_4 , filtered, and concentrated to yield **20**.

Appearance: dark yellow oil; **Yield:** 75%; **TLC conditions:** DCM/MeOH/ NH_4OH 95:5:0.025 (Rf: 0.3); **MS (ESI):** $[\text{M}+\text{H}]^+$, 247,98; **NMR- ^1H** (400 MHz, CDCl_3) δ (ppm): 7.11-6.98 (1H, m); 6.97-6.84 (1H, m); 3.68 (3H, s); 3.44 (1H, bs); 2.72-2.30 (4H, m); **NMR- ^{13}C** (100 MHz, CDCl_3) δ (ppm): 172.6 (C14); 158.9/153.9 (C4); 151.4/146.5 (C2); 149.1/144.4 (C1); 122.0 (C3); 119.1 (C5); 105.7 (C6.); 51.8 (C15); 48.6 (C8); 41.5 (C13); 36.4 (C7).

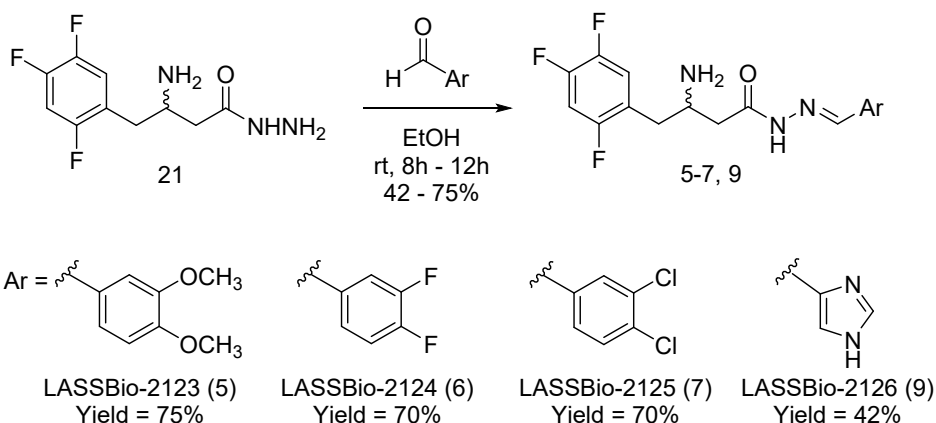
1.5. Synthesis of 3-amino-4-(2,4,5-trifluorophenyl)butanehydrazide (**21**)



Adapted from Kümmerle et al. (2012)⁶. In a 25 mL round-bottom flask equipped with a magnetic stirrer and reflux condenser, 700 mg (2.83 mmol) of β -aminoester **20** was dissolved in 15 mL of EtOH and heated at 70°C . Next, 10 equivalents of hydrazinium hydroxide (about 100% $\text{N}_2\text{H}_5\text{OH}$) were slowly added to the reaction mixture, which was constantly stirred at 70°C overnight. After completion of the reaction (verified by TLC) the solvent was completely distilled and the residue dissolved in brine solution (40 mL), followed by exhaustive extraction with DCM (6 x 50 mL). Subsequently, the organic phase was dried with anhydrous Na_2SO_4 , filtered, and concentrated under vacuum to yield compound **21**.

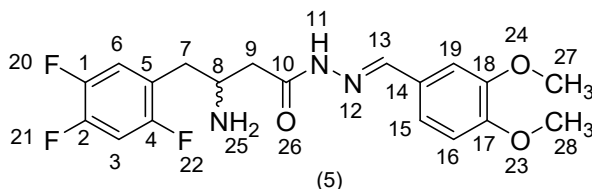
Appearance: yellow oil; **Yield:** 90%; **TLC conditions:** DCM/MeOH/ NH_4OH 90:10:0.05 (Rf: 0.45); **HPLC purity:** 96%; **MS (ESI):** $[\text{M}+\text{H}]^+$, 248,79; **NMR- ^1H** (400 MHz, CDCl_3) δ (ppm): 8.27 (1H, s); 7.06-7.00 (1H, m); 6.97-6.90 (1H, m); 3.39 (1H, m); 2.75 (1H, dd, $J=6.0, 14.0$); 2.63 (1H, dd, $J=8.0, 13.6$); 2.39 (1H, dd, $J=3.2, 15.6$), 2.16 (1H, dd, $J=9.2, 15.2$); **NMR- ^{13}C** (100 MHz, CDCl_3) δ (ppm): 172.1 (C14); 158.0/154.6 (C4); 150.6/147.3 (C2); 148.2/145.1 (C1); 121.6 (C5); 119.1 (C3); 105.7 (C6); 49.1 (C8); 41.3 (C7); 37.5 (C13).

1.6. General Synthetic Procedure for the Target Compounds LASSBio-2123 –2126 (5-7, 9)



Adapted from Kümmerle et al. (2012)⁶. In a 25 mL round-bottom flask equipped with a magnetic stirrer, 1 mmol of hydrazide **21** was dissolved in 5-10 mL of EtOH. After 15 min of stirring 1.1 equivalents of the corresponding aldehyde was added. The reaction mixture was stirred at room temperature until TLC analysis showed complete consumption of the hydrazide. Subsequently, the solvent was completely distilled. The target products were purified as described next:

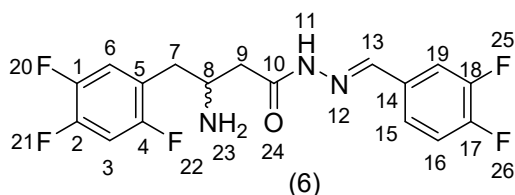
1.6.1. (*E*)-3-amino-*N'*-(3,4-dimethoxybenzylidene)-4-(2,4,5-trifluorophenyl)butanehydrazide: LASSBio-2123 (5)



After completion of the reaction (9h), the residue was concentrated and partitioned with water and EtOAc. The organic phase was washed with brine (3 x 30 mL), dried with anhydrous Na₂SO₄, filtered, and concentrated under vacuum. The product was purified by column chromatography (Hexane/EtOAc 1:1 → EtOAc/MeOH 9:1) yielding compound **5**.

Appearance: yellow oil; **Yield:** 75%; **TLC conditions:** DCM/MeOH/NH₄OH 90:10:0.05 (Rf: 0.65); **Purity:** 95.7%; **MS (ESI):** [M+H]⁺, 396.01; **NMR-¹H** (300 MHz, DMSO-*d*₆) δ (ppm): 8.06 (0.9H, s, H-13')/7.87 (1H, s, H-13); 7.51-7.40 (2H, m, H-6, H-3); 7.27 (0.9H, d, J= 4.0, H-19')/7.21 (1H, d, J=4.0, H-19); 7.15 (0.9H, dd, J=2.4, 11.2, H-15')/7.10 (1H, dd, J=2.4, 11.2, H-15); 7.00 (1H, d, J=6.8, H-16)/6.97 (0.9H, d, J=6.8, H-16'); 3.79 (12H, s, H-27, H-28, H-27', H-28'); 3.42-3.27 (m, H-8); 2.76- 2.56 (8H, m, H-7a, H-7a', H-7b, H-7b', H-9a', H-9b); 2.27 (1H, dd, J=6.0, 19.2, H-9a)/2.16 (1H, dd, J=11.2, 19.2, H-9b'); **NMR-¹³C** (75 MHz, DMSO-*d*₆) δ (ppm): 171.7/165.7 (C-10); 157.4/154.3 (C-4); 150.6 (C-17); 149.3/147.4 (C-2); 149.0 (C-18); 146.1/142.6 (C-13); 146.0/144.2 (C-1); 127.0 (C-14); 123.4 (C-5); 121.7/120.7 (C-15); 119.5 (C-3); 111.5 (C-16); 108.5/108.1 (C-19); 105.5 (C-6); 55.5 (C-27, C-28); 49.1/48.5 (C-8), 42.2/40.4 (C-9); 36.0 (C-7).

1.6.2. (E)-3-amino-N'-(3,4-difluorobenzylidene)-4-(2,4,5-trifluorophenyl) butanehydrazide: LASSBio-2124 (6)

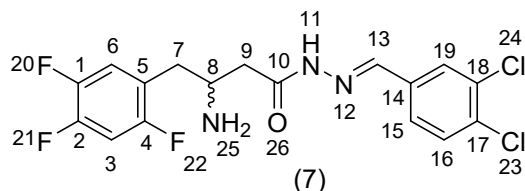


After completion of the reaction (8h), the residue was concentrated and partitioned with water and EtOAc. The organic phase was washed with brine (3 x 30 mL), dried with anhydrous Na₂SO₄, filtered, and concentrated under vacuum. The product was purified by column chromatography (Hexane/EtOAc 1:1 → EtOAc/MeOH 9:1) yielding compound **6**.

Appearance: yellow oil; **Yield:** 70%; **TLC conditions:** DCM/MeOH/NH₄OH 90:10:0.05 (Rf: 0.7); **Purity:** 99.4%; **MS (ESI):** [M+H]⁺, 372.15; **NMR-¹H** (300 MHz, DMSO-d₆) δ (ppm): 8.13 (0.7H, s, H-13)/7.91 (1H, s, H-13); 7.73-7.61 (1.8H, m, H-3); 7.53-7.41 (7H, m, H-6, H-15, H-16, H-19); 3.35 (overlapping with water H-8); 2.77/2.61 (5.8H, m, H-7a, H-7b, H-9a); 2.32/2.14 (1.72H, m, H-9b);

NMR-¹³C (75 MHz, DMSO-d₆) δ (ppm): 173.3/167.5 (C-10); 157.5/154.6 (C-4); 151.9/148.6 (C-18); 151.4/148.2 (C-17); 148.3/146.0 (C-2); 147.3/144.1 (C-1); 143.7/140.2 (C-13); 132.2 (C-14); 124.0 (C-15); 123.3 (C-5); 119.5 (C-19); 118.0 (C-16); 115.0 (C-3); 105.5 (C-6); 49.0/48.7 (C-8); 42.0 (C-7), 36.0 (C-9).

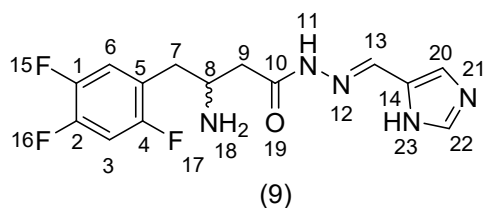
1.6.3. (E)-3-amino-N'-(3,4-dichlorobenzylidene)-4-(2,4,5-trifluorophenyl) butanehydrazide: LASSBio-2125 (7)



After completion of the reaction (8h), the residue was concentrated and partitioned with water and EtOAc. The organic phase was washed with brine (3 x 30 mL), dried with anhydrous Na₂SO₄, filtered, and concentrated under vacuum. The product was purified by column chromatography (Hexane/ EtOAc 1:1 → EtOAc /MeOH 9:1) yielding compound **7**.

Appearance: yellow oil; **Yield:** 70%; **TLC conditions:** DCM/MeOH/NH₄OH 90:10:0.05 (Rf: 0.75); **Purity:** 99.7%; **MS (ESI):** [M+H]⁺, 404.09; **NMR-¹H** (300 MHz, DMSO-d₆) δ (ppm): 8.18 (0.7 H, s, H-13')/7.97 (1H, s, H-13); 7.93 (0.7H, s, H-19')/7.87 (1H, d, J= 4, H-19); 7.70-7.68 (2.4 H, m, H-15', H-16, H-16'); 7.60 (1H, dd, J=12, 4, H-15); 7.50-7.42 (3.7H, m, H-3, H-6); 3.40 (m, H-8); 2.82-2.63 (5.9H, m, H-7a, H-7a', H-7b, H-7b', H-9a', H-9b); 2.38-2.20 (1H, dd, J=8, 12, H-9a)/2.20 (0.8H, dd, J=12, 20, H-9b'); **NMR-¹³C** (75 MHz, DMSO-d₆) δ (ppm): 173.3/167.6 (C-10); 157.4/154.2 (C-4); 149.3/146.0 (C-2); 147.2/144.0 (C-1); 143.2/139.9 (C-13); 135.1 (C-14); 132.0 (C-18); 131.8 (C-17); 131.0 (C-15); 128.1 (C-19); 126.4 (C-16); 123.3 (C-5); 119.4 (C-3); 105.5 (C-6); 49.0/48.6 (C-8); 42.1 (C-7), 35.9 (C-9).

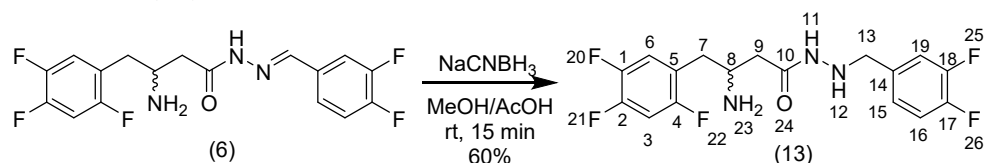
1.6.4. (E)-N'-((1H-imidazol-4-yl)methylene)-3-amino-4-(2,4,5-trifluorophenyl)butanehydrazide: LASSBio-2126 (9)



After completion of the reaction (12h), the residue was concentrated and directly subjected to column chromatography in reverse phase (C-18) starting with MeCN 100%, followed by MeCN/H₂O (pH 3-4) 95:5 → MeCN/H₂O (pH 3-4) 40:60 yielding compound **9**.

Appearance: white solid; **Yield:** 42%; **TLC conditions:** DCM/MeOH/NH₄OH 90:10:0.05 (Rf: 0.45); **Purity:** 95.2%; **mp:** 145 - 147°C; **MS (ESI):** [M+H]⁺, 325.99; **NMR-¹H** (300 MHz, DMSO-d₆) δ (ppm): 11.1 (2H, bs, H-imidazole); 8.10 (0.9H, s, H-13')/7.91 (1H, s, H-13); 7.62 (1H, s, H-22); 7.48-7.32 (5 H, m, H-20', H-3, H-6)/7.20 (1H, s, H-20); 3.46-3.31 (m, H-8); 2.28 (1H, dd, J=3.0, 6.0, H-9a')/2.17 (0.8H, dd, J=9.0, 9.0, H-9b'); **NMR-¹³C** (75 MHz, DMSO-d₆) δ (ppm): 172.4/166.8 (C-10); 157.4/154.2 (C-4); 149.2/145.9 (C-2); 147.3/143.9 (C-1); 140.0/136.8 (C-13); 135.4 (C-14); 123.2 (C-5); 131.8 (C-22), 120.6/121.0 (C-20); 119.4 (C-3); 105.3 (C-6); 48.9/48.2 (C-8), 42.9/41.0 (C-9), 35.4 (C-7).

2. Synthesis of 3-amino-N'-(3,4-difluorobenzyl)-4-(2,4,5-trifluorophenyl)butanehydrazide: LASSBio-2127 (13)



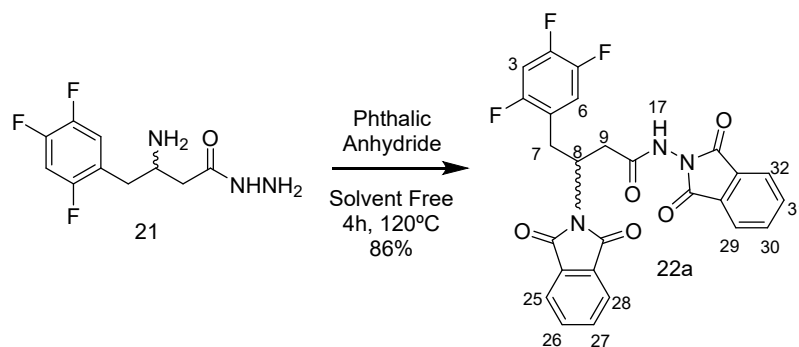
Adapted from Gore et al (2010) ⁴. In a 25 mL round-bottom flask equipped with a magnetic stirrer and under argon atmosphere, 100 mg (0.270 mmol) of *N*-acylhydrazone **6** (LASSBio-2124) was dissolved in 7 mL of MeOH, then, 12 equivalents of NaBH₃CN were added and the solution was stirred for 15 min. Subsequently, AcOH was added until pH 3-4 and the reaction mixture was stirred until total consumption of the starting material (monitored by TLC). Next, the solvent was distilled, and the residue was treated with HCl 10% until pH 2. The resulting suspension was stirred for 15 min and extracted with DCM (3 x 20 mL). The organic phase was separated, and the aqueous phase was basified with NaOH 10% until pH 8-9. Then, the product was isolated with EtOAc (3 x 50 mL). The organic phase was dried over anhydrous Na₂SO₄, filtrated and concentrated. The resulting oil was purified by column chromatography (Hexane/AcOEt 1:1 → AcOEt/MeOH 9:1) yielding compound **13**.

Appearance: transparent oil; **Yield:** 60%; **Purity:** 95.7%; **MS (ESI):** [M+H]⁺, 374.18; **NMR-¹H** (300 MHz, CDCl₃) δ (ppm): 7.19-7.01 (4H, m, H-6, H-15, H-16, H-19); 6.93-6.83 (1H, m, H-3); 3.90 (2H, s, H-13); 3.70 (1H, m, H-8); 2.96-2.84 (2H, m, H-7); 2.47-2.38 (2H, m, H-9); **NMR-¹³C** (75 MHz, CDCl₃) δ (ppm): 170.1 (C-10); 158.1/154.7 (C-4); 152.2/148.4 (C-18); 151.0/148.6 (C-

17); 151.7/147.9 (C-2); 148.7/145.3 (C-1); 134.6 (C-14); 124.8 (C-19); 120.0 (C-5); 119.6 (C-6); 117.2 (C-16); 115.8 (C-15); 106.0 (C-3); 54.6 (C-13); 49.3 (C-8); 73.7 (C-9); 33.8 (C-7).

3. Synthesis of LASSBio-2128 (14)

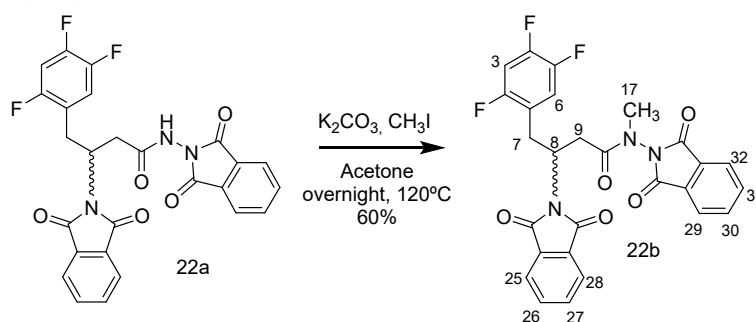
3.1. Synthesis of *N*,3-bis(1,3-dioxoisindolin-2-yl)-4-(2,4,5-trifluorophenyl)butanamide (22a)



Adapted from Rodrigues et al. (2016)⁷. In a 10 mL round-bottom flask, equipped with a magnetic stirrer, 130 mg (0.526 mmol) of hydrazide **21** were added and temperature was adjusted to 80°C. Next, four equivalents of phthalic anhydride were added without any added solvent. The reaction mixture was stirred at 130°C for 4h (monitored by TLC). Subsequently, the reaction was cooled, Na₂CO₃ (10%) solution was added, and the suspension was sonicated for 15min. Then, the solid was filtered and washed with water and hexane to yield **22a**.

Appearance: white solid; **Yield:** 86%; **mp:** 223 - 225°C; **MS (ESI):** [M+Na]⁺, 530.20; **NMR-¹H** (300 MHz, DMSO-d₆) δ (ppm): 8.18 (1H, bs, H-17); 7.80-7.82 (8H, m, H-25-32); 7.49-7.30 (2H, m, H-6, H-3); 4.80 (1H, m, H-8); 3.35 (2H, overlapped with water signal, H-7a, H-7b); 3.09-3.03 (2H, m, H-9a, H-9b).

3.2. Synthesis of *N*,3-bis(1,3-dioxoisindolin-2-yl)-*N*-methyl-4-(2,4,5-trifluorophenyl)butanamide (22b)

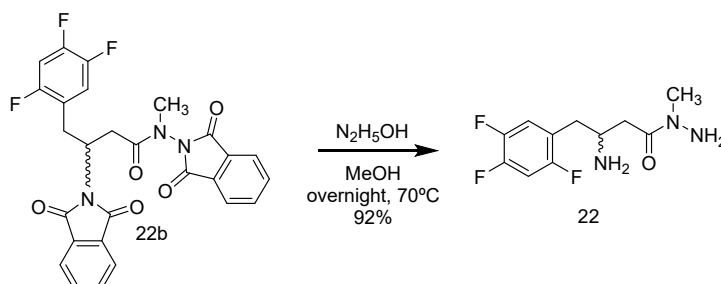


Adapted from Rodrigues et al. (2016)⁷. In a 10 mL round-bottom flask, equipped with a magnetic stirrer, 230 mg (0.454 mmol) of phthalimide **22a** and 3 equivalents of K₂CO₃ were suspended in 10 mL of acetone. The suspension was thoroughly mixed under vigorous stirring for 5 min, and 2 equivalents of methyl iodide were subsequently added. The reaction was heated at 50°C and maintained under stirring overnight. At the end of the reaction (monitored by TLC), the solvent was evaporated under reduced pressure, and the residual solid was suspended in 2 mL of ethanol and poured into cold water. The solid was collected through filtration and dried under vacuum for 16h to yield **22b**.

Appearance: white solid; **Yield:** 60%; **Melting Point:** 216 - 218°C; **NMR-¹H** (300 MHz, DMSO-d₆) δ (ppm): 7.77-8.04 (8H, m, H-25-32); 7.28-7.44 (2H, m, H-3, H-6); 4.70 (1H, m, H-8); 3.19-3.32

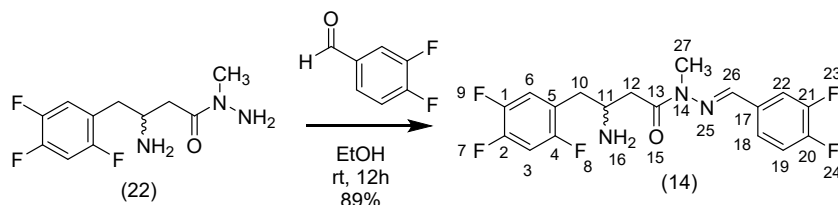
(2H, m, H-7a, H-7b); 3.10 (3H, s, H-17); 2.76 (1H, dd, J= 4.0, 16.0, H-9a); 2.95 (1H, dd, J=8.0, 16.0, H-9b).

3.3. Synthesis of 3-amino-*N*-methyl-4-(2,4,5-trifluorophenyl)butanehydrazide (**22**)



Adapted from Khan et al (1995)⁸ and Rodrigues et al. (2016)⁷. In a 10 mL round-bottom flask, equipped with a magnetic stirrer and reflux condenser, 126 mg (0.161 mmol) of phthalimide **22b** was dissolved in 7 mL of MeOH, followed by the addition of 10 equivalents of hydrazine hydroxide. The reaction mixture was stirred at 70°C for 8h. After completion of the reaction (monitored by TLC) the solvent was completely distilled and the residue was treated with 10 mL of a saturated Na_2CO_3 solution, then it was partitioned with DCM (5 x 12 mL). The organic extracts were washed with water and brine, subsequently dried over sodium sulfate, filtrated and concentrated under reduced pressure to yield **22**. **Appearance:** yellow oil; **Yield:** 92%; **MS (ESI):** $[\text{M}+\text{H}]^+$, 262.25.

3.4. Synthesis of 3-amino-*N'*-(3,4-difluorobenzyl)-*N*-methyl-4-(2,4,5-trifluorophenyl)butanehydrazide: LASSBio-2128 (**14**)



Adapted from Kümmerle et al. (2012)⁶. In a 25 mL round-bottom flask equipped with a magnetic stirrer, 1 mmol of 3-amino-*N*-methyl-4-(2,4,5-trifluorophenyl)butanehydrazide **22** was dissolved in 5mL of EtOH. After 15min of stirring 1.1 equivalents of 3,4-difluorobenzaldehyde was added. The reaction mixture was stirred at room temperature until TLC analysis showed complete consumption of the hydrazide (12h). Subsequently, the solvent was completely distilled. The product was, partitioned with water and EtOAc. The organic phase was washed with brine (3 x 30 mL), dried with anhydrous Na_2SO_4 , filtered, and concentrated under vacuum. The product was purified by column chromatography (Hexane/AcOEt 9:1 \rightarrow AcOEt/MeOH 9:1) yielding compounds **14**.

Appearance: yellow oil; **Yield:** 89%; **Purity:** 98.3%; **MS (ESI):** $[\text{M}+\text{H}]^+$, 385.12; **NMR-¹H** (300 MHz, CD_3OD) δ (ppm): 7.87 (1H, s, H-13); 7.62-7.56 (1H, m, H-19); 7.49-7.43 (1H, m, H-15); 7.35-7.26 (2H, m, H-6, H-16); 7.19-7.10 (1H, m, H-3); 3.79 (1H, m, H-8); 3.34 (3H, s, H-27); 3.23 (1H, m, H-9a); 3.06-2.97 (3H, m, H-9b, H-7a, H-7b); **NMR-¹³C** (75 MHz, CD_3OD) δ (ppm): 173.7 (C-10); 159.4/156.2 (C-4); 154.3/150.8 (C-18); 153.7/150.2 (C-17); 152.2/148.9 (C-2);

149.7/146.4 (C-1); 140.3 (C-13); 133.8 (C-14); 125.4 (C-15); 121.9 (C-5); 120.6 (C-16); 118.6 (C-6); 116.0 (C-19); 106.7 (C-3); 50.0 (C-8); 38.0 (C-9); 34.5 (C-7); 28.2 (C-27).

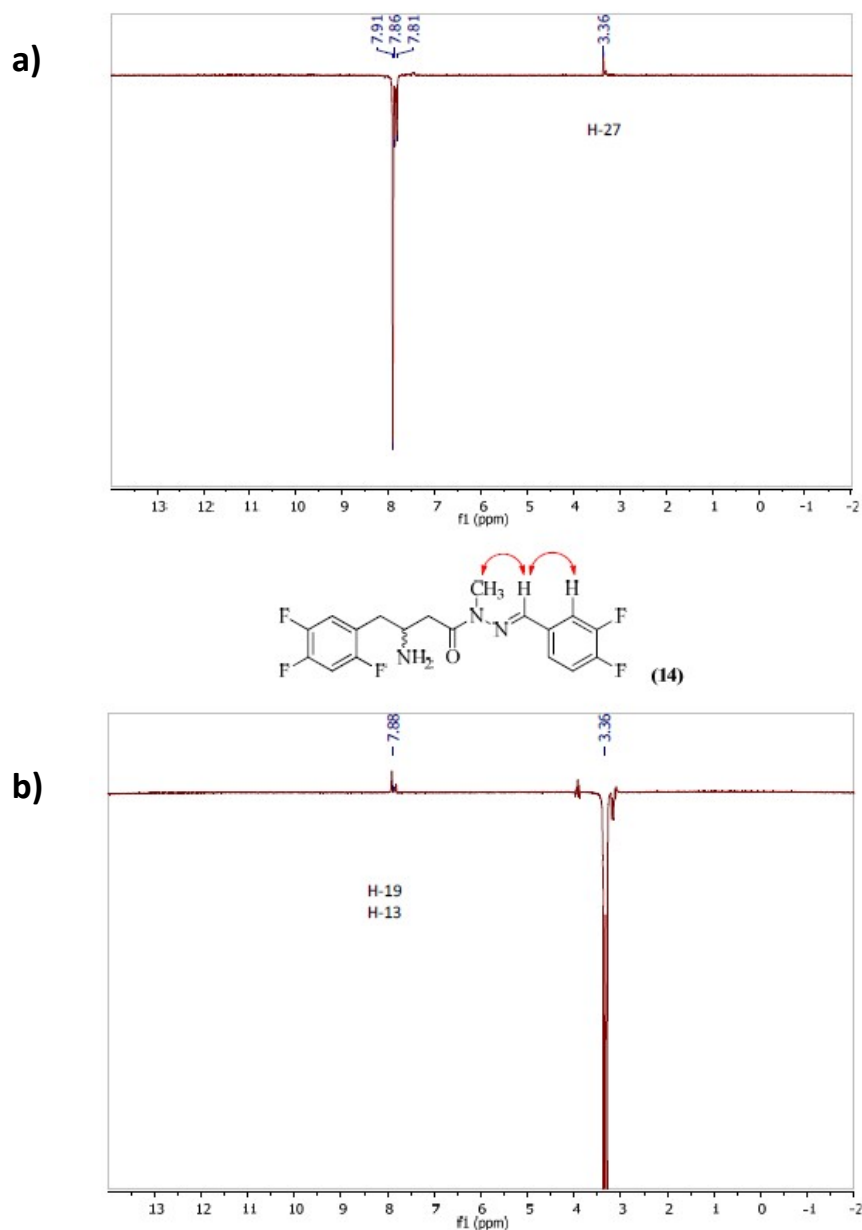


Figure S9. a) ¹H-NMR NOE-diff (400 MHz, CD₃OD) spectrum of **14**. Signal irradiated δ_H 7.86 (N=CH). b) ¹H-NMR NOE-diff (400 MHz, CD₃OD) spectrum of **14**. Signal irradiated δ_H 3.36 (N-CH₃).

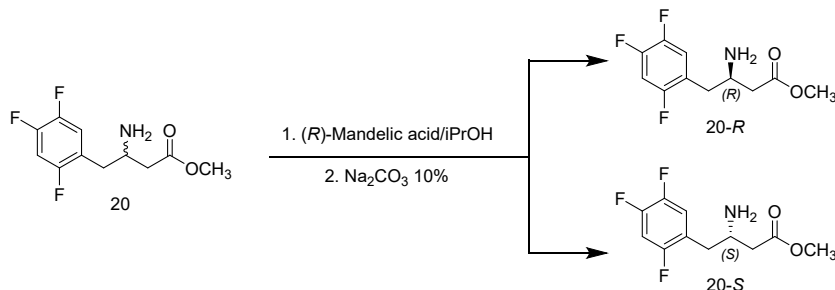
Table S5. Physical and spectroscopic properties of LASSBio-2123 to LASBio-2128 (5-7, 9, 13-14).

Compound	R	Appearance	Overall Yield (%)	Purity ^a (%)	Melting point ^b (°C)	MS-ESI ^c [M+H] ⁺ (m/z)	δ_H iminic	δ_C iminic
LASSBio-2123 (5)	OCH ₃	Transparent Oil	29.3	95.7	-	396.01	8.06/7.87	146.1/142.6
LASSBio-2124 (6)	F	Transparent Oil	31.4	99.4	-	372.15	8.13/7.91	143.7/140.2
LASSBio-2125 (7)	Cl	Transparent Oil	29.3	99.7	-	404.09	8.18/7.97	143.2/139.9
LASSBio-2126 (9)	-	White Solid	17.6	95.2	145-147	325.99	8.10/7.91	140.0/136.8
LASSBio-2127 (13)	-	Light yellow oil	18.2	95.7	-	374.18	3.90	54.6
LASSBio-2128 (14)	-	Light yellow solid	18.4	98.3	81-83	386.18	7.87	140.3

^a Relative purity determined by HPLC. ^b Melting point determined on an apparatus Melt Point System MP70, Mettler Toledo (values obtained were not corrected). ^c Direct injection.

4. Enantiomeric Synthesis of *N*-acylhydrazones (6-*R* and 6-*S*)

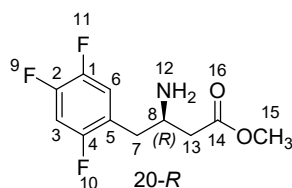
4.1. Resolution of the β -aminoester intermediate (20-*R* and 20-*S*)



Adapted from Gore et al (2010)⁴. In a 50 mL round-bottom flask equipped with a magnetic stirrer, 1.62 mmol of β -Aminoester (**20**) was dissolved in 5 mL of isopropanol (IPA). Then, 2 equivalents of (*R*)-mandelic acid dissolved in 6 mL of IPA were added to the mixture reaction. The resulting solution was stirred at 25 - 30°C for 5 h. At the end of the reaction, the white precipitate formed was filtered and washed with 12 mL of cold IPA. The supernatant was concentrated under reduce pressure, dissolved in 40 mL of water, and treated with Na₂CO₃ (10%) until pH 9. Subsequently, it was extracted with EtOAc (3x40 mL), dried with anhydrous Na₂SO₄, filtered, and concentrated under vacuum to yield a transparent oil **20-(S)**.

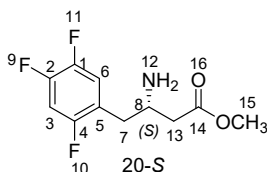
The solid obtained from the filtration, was dried in a desiccator for 24 and weighted (Rend. 89%), next, it was subjected to recrystallization in a mixture IPA/water (18 mL/1 mL) at 25 - 30°C. The mixture was heated at 75 - 80°C for 1 h, and it was cooled gradually until room temperature. The white precipitate was filtered, washed with 5 mL of cold IPA, dried in a desiccator for 24 h and weight (Rend. 66%). Subsequently, the solid was dissolved in 30 mL of water and treated with Na₂CO₃ (10%) until pH 9. This solution was extracted with EtOAc (3 x 40 mL), dried with anhydrous Na₂SO₄, filtered, and concentrated under vacuum to yield a transparent oil **20-(R)**.

4.1.1. (*R*)-methyl 3-amino-4-(2,4,5-trifluorophenyl)butanoate (20-*R*)



Appearance: transparent oil; **Yield:** 66%; **TLC conditions:** Same as racemate; **MS (ESI):** Same as racemate; **NMR-¹H** (400 MHz, CDCl₃) δ (ppm): Same as racemate; **NMR-¹³C** (100 MHz, CDCl₃) δ (ppm): Same as racemate; **Optical Rotation ($[\alpha]_D^{25}$):** - 6.83 (c 0.3 in MeOH); **ee** > 99%.

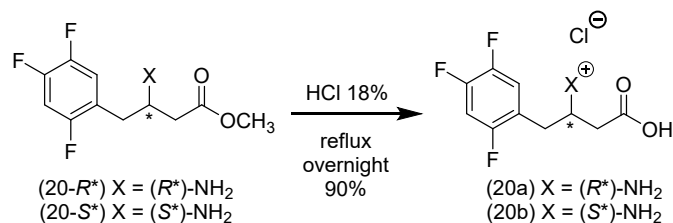
4.1.2. (*S*)-methyl 3-amino-4-(2,4,5-trifluorophenyl)butanoate (20-*S*)



Appearance: transparent oil; **Yield:** 89%; **TLC conditions:** Same as racemate; **MS (ESI):** Same as racemate; **NMR-¹H** (400 MHz, CDCl₃) δ (ppm): Same as racemate; **NMR-¹³C** (100 MHz, CDCl₃) δ (ppm): Same as racemate; **Optical Rotation ([α]_D²⁵):** + 9.75 (c 0.3 in MeOH); **ee:** 82%.

4.2. Determination of absolute stereochemistry of β-amino ester (20-*R*) and (20-*S*)

4.2.1. Tasnadi and colleagues (2010)⁹ method evaluating carboxylic β-aminoacids (20a) and (20b)

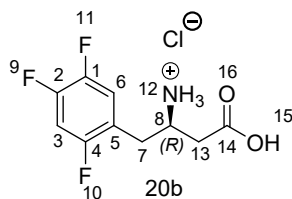


To establish a methodology useful to determine the absolute stereochemistry of target compounds, we selected β-aminoester intermediate (20-*R,S*) as a template. This selection was made considering we could easily convert esters (20-*R,S*) in the carboxylic β-aminoacids (20a and 20b), which absolute stereochemistry has been previously reported Tasnadi and colleagues (2010)⁹. Therefore, once synthesized the (*R*)- and (*S*)-β-aminoacid (20a and 20b), it would be feasible to compare their specific rotation values with those previously described by Tasnadi and co-workers (2010).

In a 10 mL round-bottom flask equipped with a reflux condenser and a magnetic stirrer, 25 mg (0.0929 mmol) of the corresponding β-aminoester's 20-*(R*)* and 20-*(S*)* were added to 2.5 mL of 18% aqueous HCl. Then, the reaction mixture was stirred at reflux overnight. When TLC analysis showed total consumption of the starting material, the solvent was azeotropically distilled under reduced pressure and the residue dried for 24h to give compounds 20a and 20b.

Once obtained, the carboxylic (*R*)- and (*S*)-β-aminoacids were characterized by ¹H- and ¹³C-NMR, and the specific rotation of the β-amino acids 20a and 20b was measured. The (*R**)-1-carboxy-3-(2,4,5-trifluorophenyl)propan-2-aminium chloride 20a has shown [α]_D²⁵ = - 7.42 (c 0.3 in H₂O); while compound (*S**)-1-carboxy-3-(2,4,5-trifluorophenyl)propan-2-aminium chloride 20b has displayed [α]_D²⁵ = + 8.87 (c 0.3 in H₂O). Surprisingly, these results contrasted to those reported by Tasnadi and coworkers (2010)⁹, who have reported a specific rotation of [α]_D²⁵ = + 10.6 (c 0.3 in H₂O) to (*R*)-1-carboxy-3-(2,4,5-trifluorophenyl)propan-2-aminium chloride (20a) and [α]_D²⁵ = - 9.8 (c 0.3 in H₂O) to (*S*)-1-carboxy-3-(2,4,5-trifluorophenyl)propan-2-aminium chloride (20b).

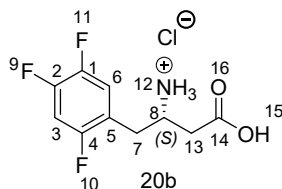
4.2.1.1. (*R*)-1-carboxy-3-(2,4,5-trifluorophenyl)propan-2-aminium chloride (20a)



Chemical Formula: C₁₀H₁₁ClF₃NO₂; **Appearance:** white solid; **Yield:** 90%; **Purity:** 95.2%; **NMR-¹H** (400 MHz, D₂O) δ (ppm): 7.30-7.25 (1H, m, H-3); 7.19-7.14 (1H, m, H-6); 3.95-3.90 (1H, m, H-8); 3.08 (1H, dd, *J* = 8.0, 12.0, H-13a); 3.03 (1H, dd, *J* = 4.0, 12.0, H-13b); 2.80 (1H, dd, *J* = 8.0, 12.0,

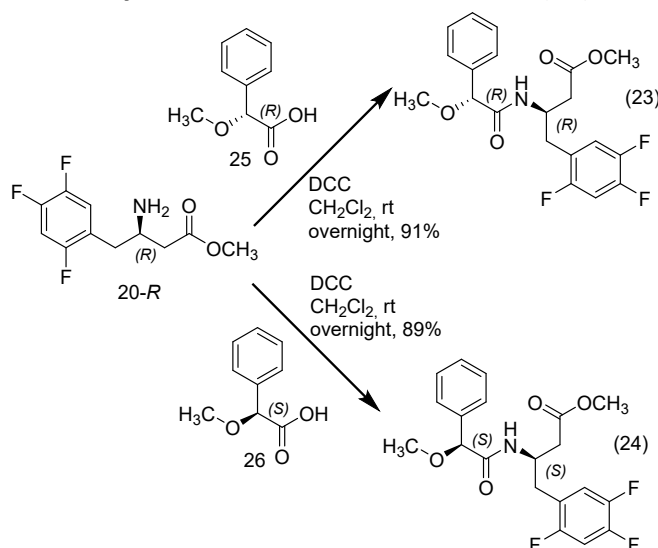
H-7a); 2.72 (1H, dd, $J = 8.0, 16.0$, H-7b); **NMR-¹³C (100 MHz, D₂O) δ (ppm):** 173.9 (C-14); 157.4/155.5 (C-4); 150.4/148.5 (C-2); 147.6/145.7 (d, C-1); 119.2 (C-3); 105.9 (C-6); 48.1 (C-8), 35.4 (C-7); 30.9 (C-13); **Optical Rotation ($[\alpha]_D^{25}$):** - 7.42 (c 0.3 in H₂O).

4.2.1.2. (S)-1-carboxy-3-(2,4,5-trifluorophenyl)propan-2-aminium chloride (20b)



Chemical Formula: C₁₀H₁₁ClF₃NO₂; **Appearance:** white solid; **Yield:** 90%; **Purity:** 95.2%; **NMR-¹H (400 MHz, D₂O) δ (ppm):** 7.30-7.25 (1H, m, H-3); 7.19-7.14 (1H, m, H-6); 3.95-3.90 (1H, m, H-8); 3.08 (1H, dd, $J = 8.0, 12.0$, H-13a); 3.03 (1H, dd, $J = 8.0, 12.0$, H-13b); 2.80 (1H, dd, $J = 4.0, 16.0$, H-7a); 2.72 (1H, dd, $J = 8.0, 16.0$, H-7b); **NMR-¹³C (100 MHz, D₂O) δ (ppm):** 173.9 (C-14); 157.4/155.5 (C-4); 150.4/148.5 (C-2); 147.6/145.7 (d, C-1); 119.2 (C-3); 105.9 (C-6); 48.1 (C-8), 35.4 (C-7); 30.9 (C-13); **Optical Rotation ($[\alpha]_D^{25}$):** + 8.87 (c 0.3 in MeOH).

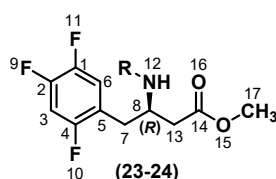
4.2.2. Mosher's method by chiral derivatization to obtain (23) and (24)



Intrigued by those controversial data regarding the specific rotation, we decided to study another methodology to determine the absolute stereochemistry. The approach adopted was the so-called modified Mosher's method, which is based on the chemical shift differences obtained in the NMR spectra of the diastereoisomeric products (usually esters and/or amides) obtained by reaction of the target substrate with chiral derivatizing reagents^{10,11}. Accordingly, the methoxyphenylacetic acid (MPA) amides **23** and **24** were obtained separately through *N,N'*-dicyclohexylcarbodiimide (DCC) coupling between (*R*)-MPA (**25**) and (*S*)-MPA (**26**) with the (*R*)- β -amino ester (**20-R***). In a 10 mL round-bottom flask equipped with a magnetic stirrer, 20 mg (0.0810 mmol) of the β -aminoester's (**20-R**) were treated with (*R*)-MPA (**25**) and (*S*)-MPA (**26**) acids separately in the presence of DCC (0.05 mmol) in CH₂Cl₂ (10 mL). The reactions were monitored by TLC, purified by CC on silica gel (hexane 100% - EtOAc 100%), to yield amides **23** and **24**.

Once obtained and characterized by ^1H , ^{13}C , HMBC and HSQC NMR experiments, the absolute stereochemistry of intermediate (**20-*R**) has been determined establishing the differences in the chemical shifts between the diastereoisomers (*R*)-MPA-(*R**)- β -amino ester (**23**) and (*S*)-MPA-(*R**)- β -amino ester (**24**), ($\Delta\delta^{R-S}$), where it was found negative $\Delta\delta$ values for hydrogens H-3, H-6, H-7a and H-7b, and positive $\Delta\delta$ values for hydrogens H-8, H-13a, H-13b and H-17 (Table S6 and Figures S10 and S11). Thus, it was possible to observe that the shielding effects of the aromatic ring fits with an *R*-configuration in the asymmetric centre and not with an *S*-configuration. These results allowed to propose an absolute configuration of *R* for the asymmetric carbon 8.**

Table S6. ^1H -NMR data for the MPA amides of **23** and **24** at 400 MHz, in CDCl_3 ; δ in ppm, J in Hz.



<i>C</i> #	(<i>R</i>)-MPA-(<i>R</i> *)- β - aminoester (23) $\delta(\text{H})$	(<i>S</i>)-MPA-(<i>R</i> *)- β - aminoester (24) $\delta(\text{H})$	$\Delta\delta^{R-S}$
1	-	-	-
2	-	-	-
3	6.88	7.00	0.12
4	-	-	-
5	-	-	-
6	6.77	6.89	0.12
7a	2.84	2.93	0.09
7b	2.84	2.93	0.09
8	4.47	4.38	0.09
9	-	-	-
10	-	-	-
11	-	-	-
12	-	-	-
13a	2.64	2.56	0.08
13b	2.57	2.54	0.03
14	-	-	-
15	-	-	-
16	-	-	-
17	3.71	3.62	0.09

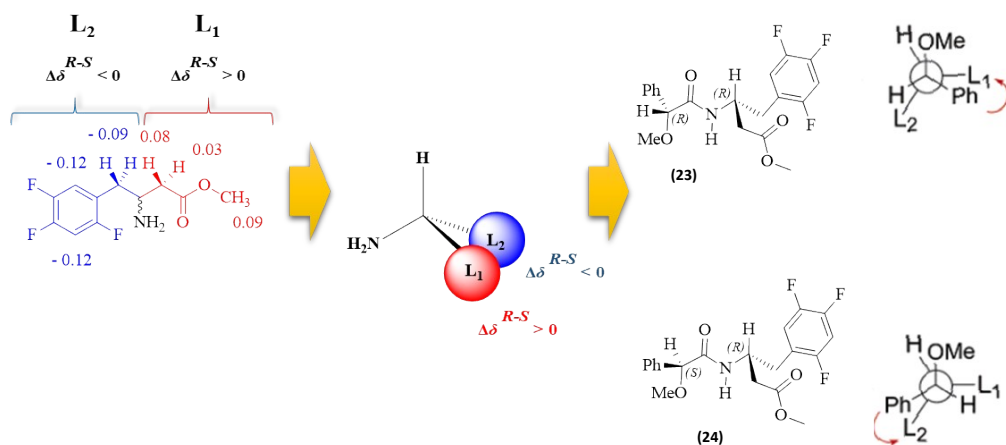


Figure S10. Chemical shifts differences ($\Delta\delta^{R-S}$) between diastereoisomers (R)-MPA-(R*)- β -aminoester (**23**) and (S)-MPA-(R*)- β -aminoester (**24**). Representation of the model that allowed the determination of absolute stereochemistry of **20-R*** as **R**.

It is important to mention, that a suitable spatial disposition of the more stable conformer of the Mosher's amides is mandatory for the correct interpretation of the results obtained experimentally from this methodology. Hence, a conformational analysis of both MPA-amides **23** and **24** using a semiempirical model (PM3) in SPARTAN program was carried out. The *in silico* approach has supported the NMR results obtained here and, in consequence, the proposed absolute stereochemistry of the (R)-methyl 3-amino-4-(2,4,5-trifluorophenyl)butanoate (**20-R**).

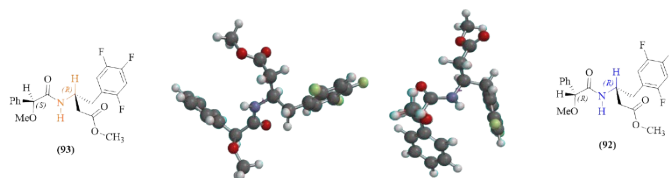
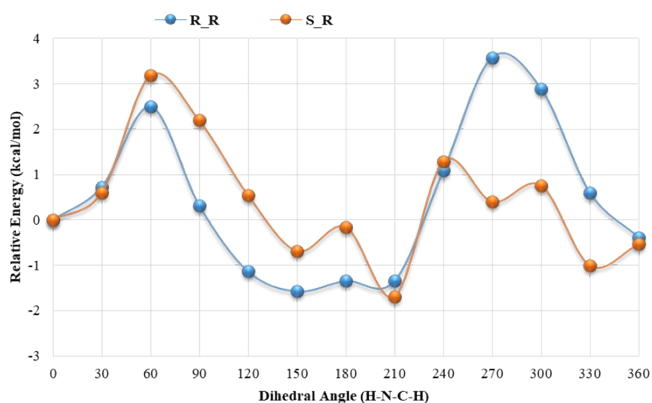
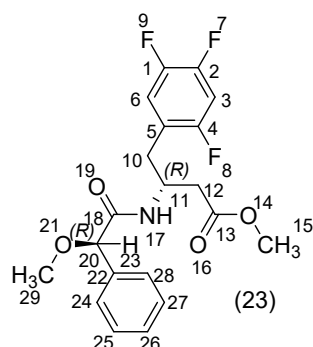


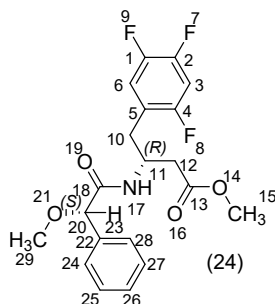
Figure S11. a) Energetic rotation profile of H-N-C-H bond (blue bond for diastereoisomer **23** and orange bond for diastereoisomer **24**) obtained by semi-empirical method PM3 in SPARTAN program. **b)** Favored conformers for diastereoisomers **23** and **24** obtained by semi-empirical method PM3 in SPARTAN program.

4.2.2.1. (R)-methyl 3-((R)-2-methoxy-2-phenylacetamido)-4-(2,4,5-trifluorophenyl)butanoate (23)



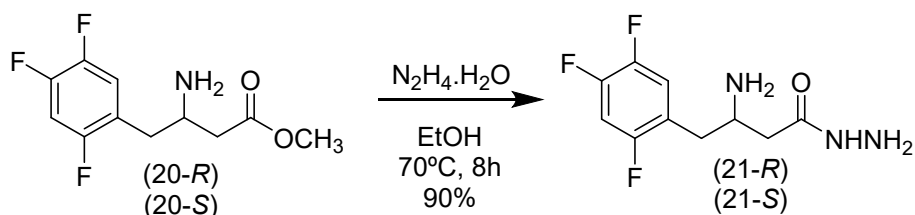
Chemical Formula: C₂₀H₂₀F₃N₅O₄; **Appearance:** white solid; **Yield:** 91%; **HPLC Purity:** 95.2%; **NMR-¹H** (400 MHz, CDCl₃) δ (ppm): 7.31-7.28 (3H, m, H-28, H-27, H-26); 7.24-7.22 (2H, m, H-4, H-25); 6.90-6.85 (1H, m, H-6); 6.80-6.74 (1H, m, H-3); 4.53 (1H, s, H-20); 4.51-4.44 (1H, m, H-1); 3.71 (3H, s, H-15); 3.33 (3H, s, H-29); 2.84 (2H, d, J=4.0, H-10) 2.64 (1H, dd, J=4.0, 16.0, H-12a); 2.57 (1H, dd, J=4.0, 12.0, H-12b); **NMR-¹³C** (100 MHz, CDCl₃) δ (ppm): 171.8 (C-13); 170.4 (C-18); 136.9 (C-22); 128.5, (C-24, C-25); 126.7 (C-26, C-27, C-28); 120.9 (C-5); 119.0 (C-6); 105.4 (C-3), 83.7 (C-20); 57.4 (C-29); 52.0 (C-15); 45.8 (C-11); 37.9 (C-12); 32.7 (C-10).

4.2.2.2. (R)-methyl 3-((S)-2-methoxy-2-phenylacetamido)-4-(2,4,5-trifluorophenyl)butanoate (24)



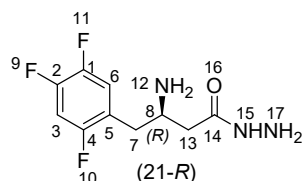
Chemical Formula: C₂₀H₂₀F₃N₅O₄; **Appearance:** white solid; **Yield:** 89%; **HPLC Purity:** 95.2%; **NMR-¹H** (400 MHz, CDCl₃) δ (ppm): 7.33-7.31 (4H, m, H-28, H-27, H-26, H-24); 7.24-7.22 (1H, d, J=8.0, H-25); 7.03-6.97 (1H, m, H-6); 6.92-6.86 (1H, m, H-3); 4.52 (1H, s, H-20); 4.43-4.34 (1H, m, H-11); 3.62 (3H, s, H-15); 3.32 (3H, s, H-29); 2.93 (2H, m, H-7a, H-10b) 2.56 (1H, dd, J=8.0, 16.0, H-12a), 2.54 (1H, dd, J=4.0, 12.0, H-12b); **NMR-¹³C** (100 MHz, CDCl₃) δ (ppm): 171.7 (C-13); 170.4 (C-18); 137.0 (C-22); 128.6 (C-24, C-25); 126.9 (C-26, C-27, C-28); 121.2 (C-5); 119.2 (C-6); 105.5 (C-3); 83.8 (C-20); 57.4 (C-29); 51.9 (C-15); 46.5 (C-11); 37.5 (C-12); 32.6 (C-10).

4.3. Synthesis of (S) and (R)-hydrazide intermediates (21-R, 21-S)



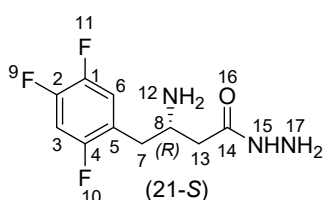
Compounds were obtained according to Kümmerle et al (2012)⁶ by the synthetic procedure previously reported on item 1.5 (compound 21).

4.3.1. (R)-3-amino-4-(2,4,5-trifluorophenyl)butanehydrazide (21-R)



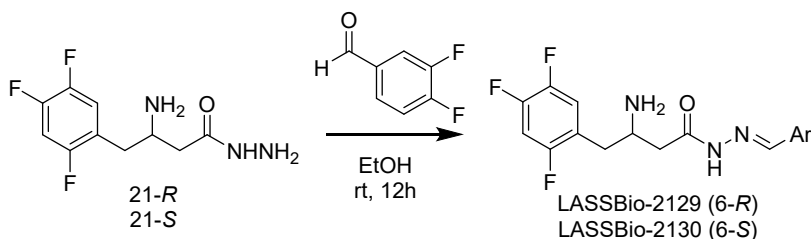
Chemical Formula: C₁₀H₁₂F₃N₃O; **Appearance:** transparent oil; **Yield:** 90%; **MS (ESI):** same as racemate; **NMR-¹H** (400 MHz, CDCl₃) δ (ppm): same as racemate; **NMR-¹³C** (100 MHz, CDCl₃) δ (ppm): same as racemate; **Optical Rotation ([α]_D²⁵):** - 6.21 (c 0.3 in H₂O).

4.3.2. (S)-3-amino-4-(2,4,5-trifluorophenyl)butanehydrazide (21-S)



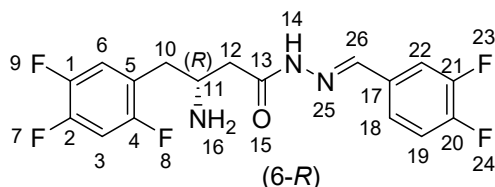
Chemical Formula: C₁₀H₁₂F₃N₃O; **Appearance:** transparent oil; **Yield:** 90%; **MS (ESI):** same as racemate; **NMR-¹H** (400 MHz, CDCl₃) δ (ppm): same as racemate.; **NMR-¹³C** (100 MHz, CDCl₃) δ (ppm): same as racemate; **Optical Rotation ([α]_D²⁵):** + 9.73 (c 0.3 in MeOH).

4.4. General Synthetic Procedure for the (R)- (S)- N-acylhydrazones: LASSBio-2129 (6-(R)) and LASSBio-2130 (6-(S)) (KUMMERLE et al, 2012)



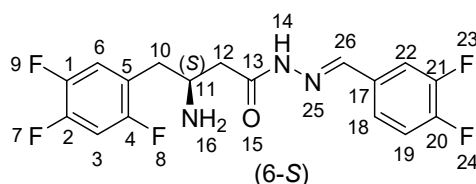
Compounds were obtained according to Kümmerle et al (2012)⁶ by the synthetic procedure previously reported on item 1.6 (compounds 5-7, 9).

4.4.1. (R,E)-3-amino-N'-(3,4-difluorobenzylidene)-4-(2,4,5-trifluorophenyl)butanehydrazide: LASSBio-2129 (6-(R))



Appearance: same as racemate; **Yield:** 75%; **HPLC purity:** 98.8%; **MS (ESI):** same as racemate; **NMR-¹H** (300 MHz, DMSO-d₆) δ (ppm): same as racemate; **NMR-¹³C** (75 MHz, DMSO- d₆) δ (ppm): same as racemate; **Optical Rotation ([α]_D²⁵):** - 21.18 (c 0.3 in MeOH); **ee** > 99.9 %.

4.4.2. (S,E)-3-amino-N'-(3,4-difluorobenzylidene)-4-(2,4,5-trifluorophenyl)butanehydrazide: LASSBio-2130 (6-(S))



Appearance: same as racemate; **Yield:** 73%; **HPLC Purity:** 98.2%; **MS (ESI):** same as racemate; **NMR-¹H** (300 MHz, DMSO-d₆) δ (ppm): same as racemate; **NMR-¹³C** (75 MHz, DMSO-d₆) δ (ppm): same as racemate; **Optical Rotation ([α]_D²⁵):** + 25.86 (c 0.3 in MeOH).

5. Aqueous solubility determination

Solubility was measured by spectrophotometric assay. The solubility was determined by constructing a calibration curve as follows: 1 mg of analyte was dissolved in MeOH and transferred to a 20 mL volumetric glass (stock solution). Six solutions of different concentrations (200 μM - 0.5 μM) were prepared by dilution of the stock solution. Data were obtained in triplicate and the mean values were used for the graphs. The values of the correlation coefficient (R²) were between 0.9972 and 0.9999. Saturated aqueous solutions of the analytes were prepared at 0.01 mg/ml and kept at 37°C for 4 hours with stirring. The supernatant was filtered through 0.45 mm filters and transferred to a quartz cuvette (10 mm) for spectral acquisition. Adapted method from Schneider et al. (2009)¹².

6. Dissociation constant determination

Phosphate buffer solutions were prepared using Na₂HPO₄ (10 mM) and NaH₂PO₄ (10 mM). These buffers were first filtered through a 0.45 μm membrane filter and degassed in an ultrasonic bath before use. The mobile phases consisted of mixtures of acetonitrile-phosphate buffer 20:80 (v/v) and 30:70 (v/v) adjusted by the addition of H₃PO₄ (10 mM) or NaOH (10 mM). The ionic strength of the diluted buffers used was close to 1. The final pH of the mobile phases was measured before and after each chromatographic run at 25°C. The column was equilibrated by rinsing with the mobile phase at the defined pH for 15 min at a flow rate of 1.0 mL/min. Solutions containing the analytes were prepared in MeCN/H₂O 1:1 to a final concentration of 0.1 mg/mL. A 20 μL injection of each compound was made in triplicate into the chromatographic system. The chromatographic separations were performed at a flow rate of 1 ml/min. The dead time value (t₀) was measured by injecting Uracile (0.1 mg/ml), which was determined for each mobile phase composition and pH studied. For each mobile phase composition, the retention factor k was calculated according to $k=(rt - t_0)/t_0$, where rt and t₀ are the retention time of the analyte and the dead time, respectively. Observed retention factors were plotted against mobile phase pH using a non-linear least squares program (Prism 3.0). Computer generated plots of k vs. pH were obtained and the pH at the inflection point (V50) was used as a valuable index of pKa. Sitagliptin was used as a positive control. Adapted method from Wiczling et al. (2004)¹³.

7. Chemical stability studies

Two microlitres (0.01 mmol) of a concentrated solution of the compound of interest (40 mM stock solution solubilised in DMSO) and 248 μL acid (0.2 M potassium chloride and 0.2 M HCl; pH 2.0) or neutral (phosphate dibasic, pH 7.4) buffer were added to a 2 mL Eppendorf microtube. After vortexing, the mixture was placed in a water bath at 37°C with vigorous stirring for 0, 30, 60, 120 and 240 min. After each reaction, 248 μL of basic buffer (phosphate

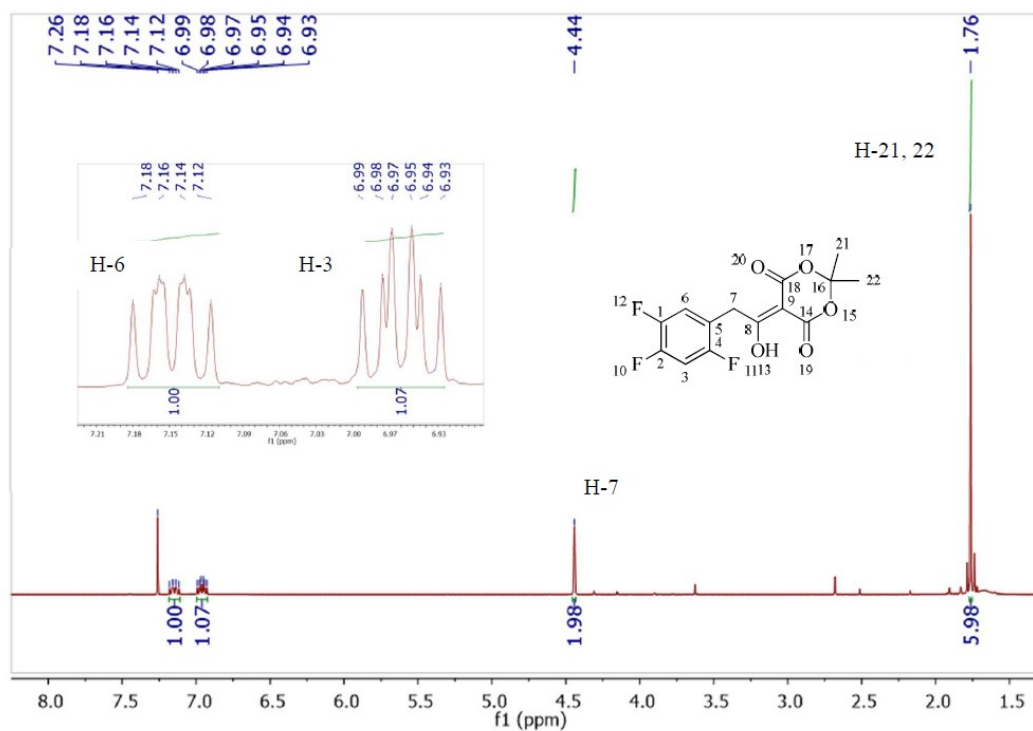
buffer, pH 8.4) was added to neutralise the pH of the medium in experiments using acidic buffer. The compound was extracted with 1 mL of acetonitrile, followed by vigorous vortexing and freezing of the aqueous phase (-10°C). The organic phase was separated, filtered and analysed by HPLC-PDA (acetonitrile/water 1:1, 0.05% TFA). Adapted method from Konsoula et al. (2008)¹⁴.

8. *In vitro* DPP-4 inhibition evaluation

A fluorogenic assay was used to measure the activity of DPP-4 using a DPP-4 Inhibitor Screening Test Assay Kit (item number 700210) from Cayman Chemical (Miami, USA). Inhibition of human recombinant DPP-4 was measured using the chromogenic substrate H-Gly-Pro-AMC, which is cleaved by DPP-4 to release the fluorescent AMC leaving group, according to the following protocol: 30 µL buffer (20 mM Tris-HCl, pH 8, 100 mM NaCl, 1 mM EDTA), 10 µL enzyme and 10 µL DMSO were added to three wells (100% activity wells). 40 µL buffer and 10 µL DMSO were added to three plates (background wells). 30 µL buffer, 10 µL enzyme and 10 µL inhibitor (compounds and sitagliptin as positive control) were added to 90 wells. The reaction was initiated by adding 50 µL of substrate solution (5 mM) to all wells used, followed by incubation at 37°C for 30 minutes. DPP-4 activity, resulting in the formation of fluorescent aminomethylcoumarin, was monitored by excitation at 360 nm and emission at 465 nm. The inhibitors (compounds and sitagliptin) dissolved in DMSO were tested in five concentrations (10 µM, 1 µM, 0.1 µM, 0.01 µM, 0.001 µM and 0.0001 µM) and in triplicate. The percentage of inhibition was obtained according to the following formula % inhibition = [(initial activity - inhibitor)/(initial activity)] x 100.

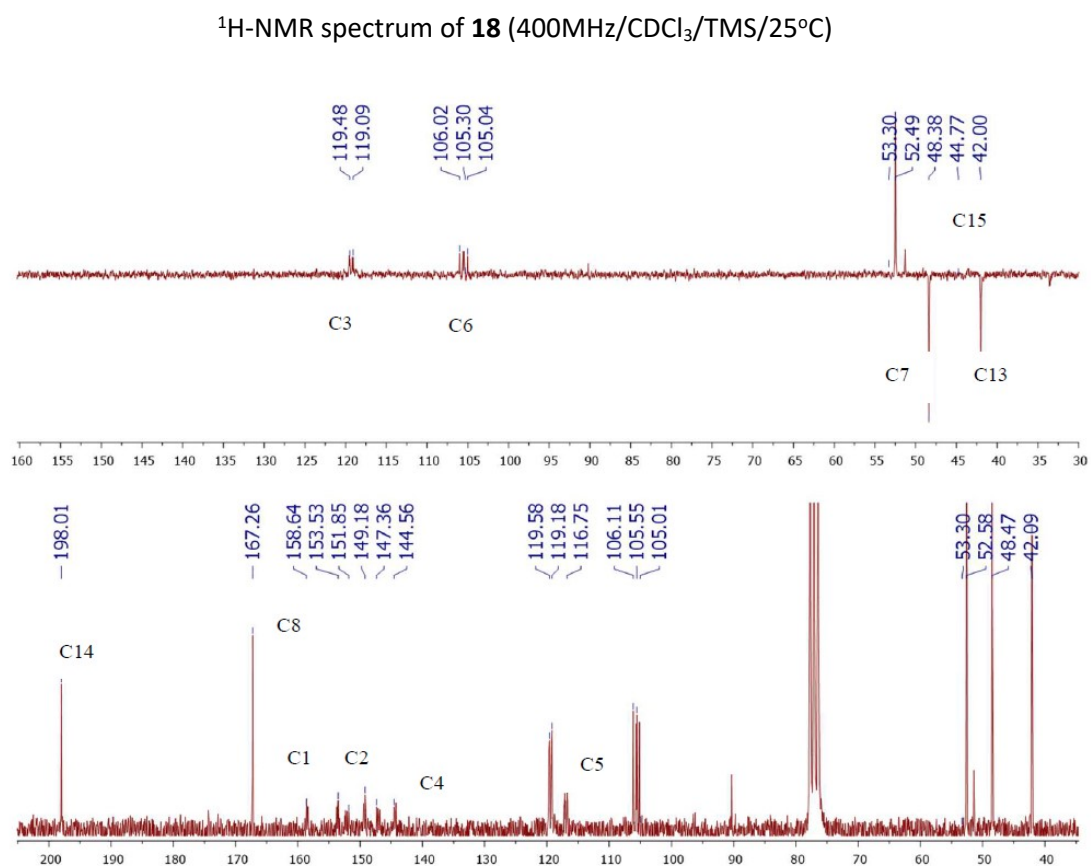
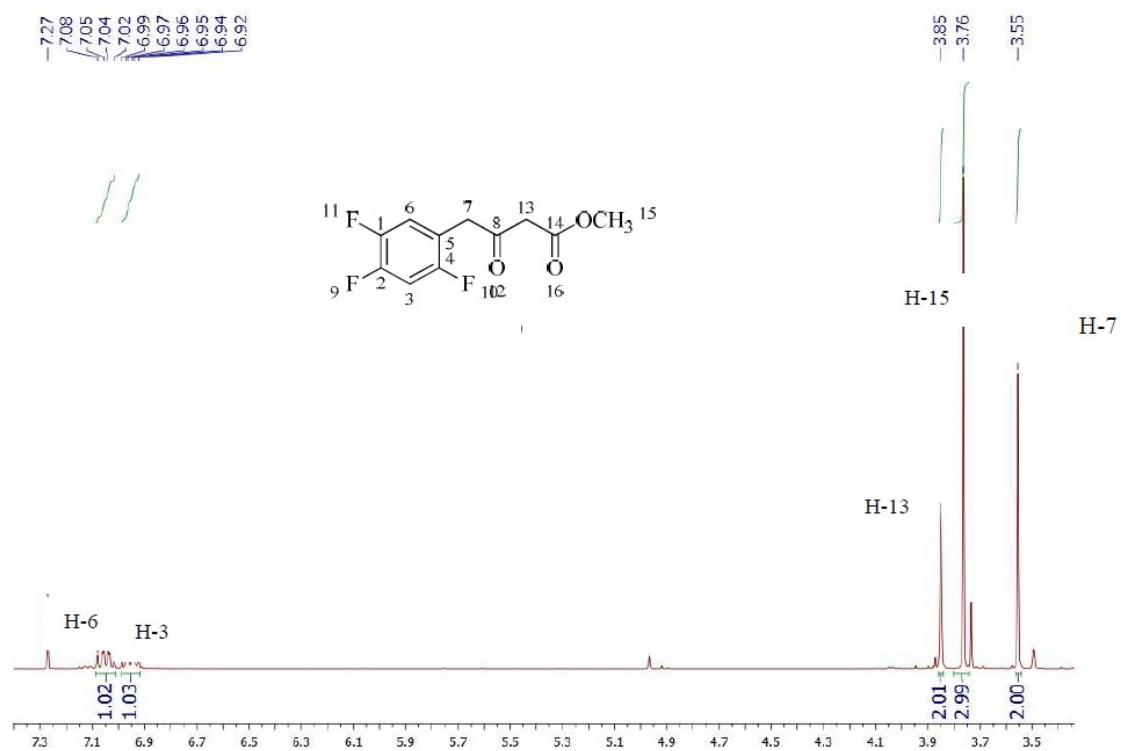
Supplementary Information: Analytical Spectra

(5-(1-hydroxy-2-(2,4,5-trifluorophenyl)ethylidene)-2,2-dimethyl-1,3-dioxane-4,6-dione) (17)

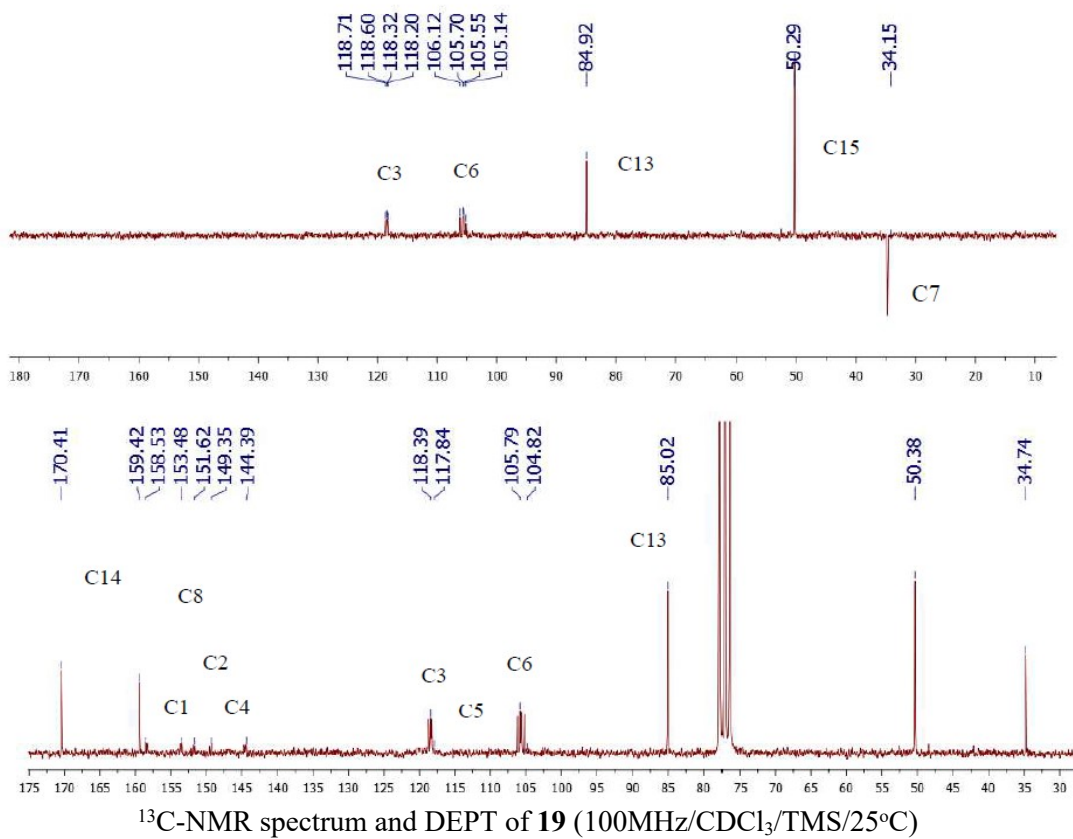
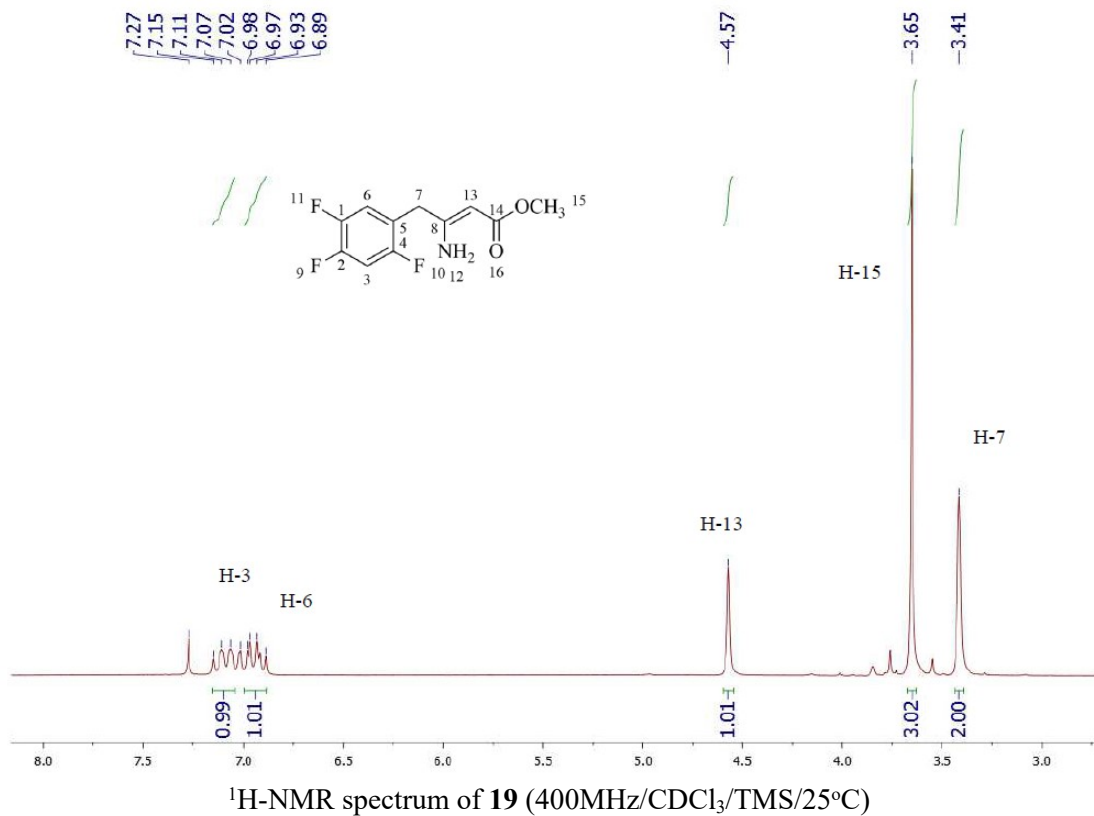


¹H-NMR spectrum of Meldrum's adduct **17** (400MHz/CDCI₃/TMS/25°C)

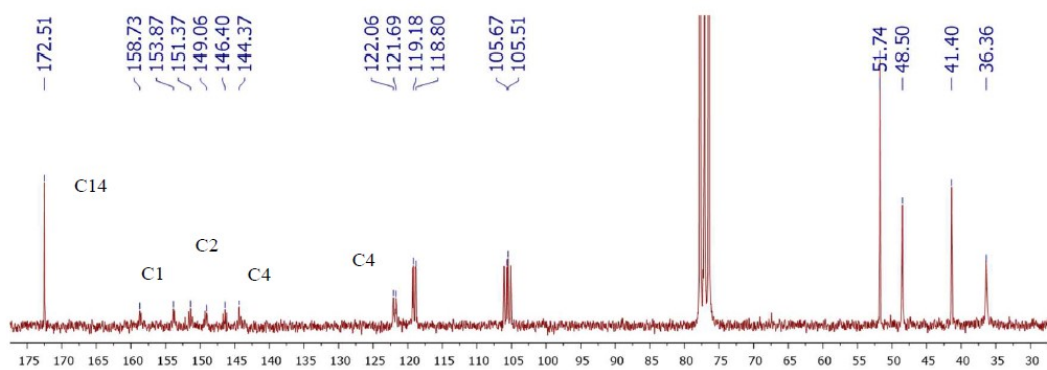
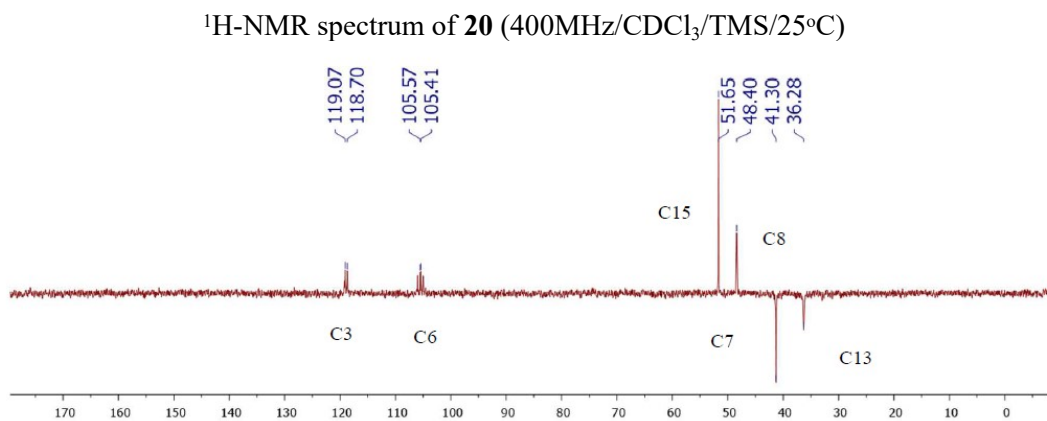
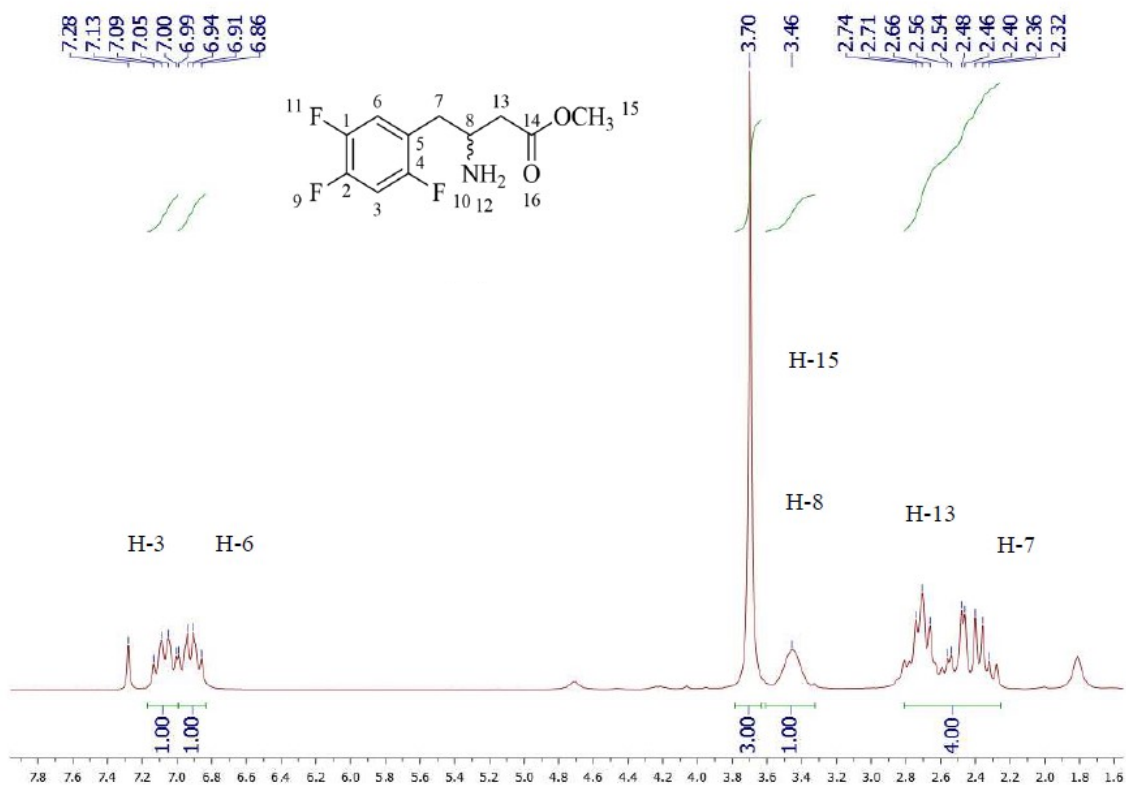
Methyl 3-oxo-4-(2,4,5-trifluorophenyl)butanoate (18)



(Z)-methyl 3-amino-4-(2,4,5-trifluorophenyl)but-2-enoate (19)

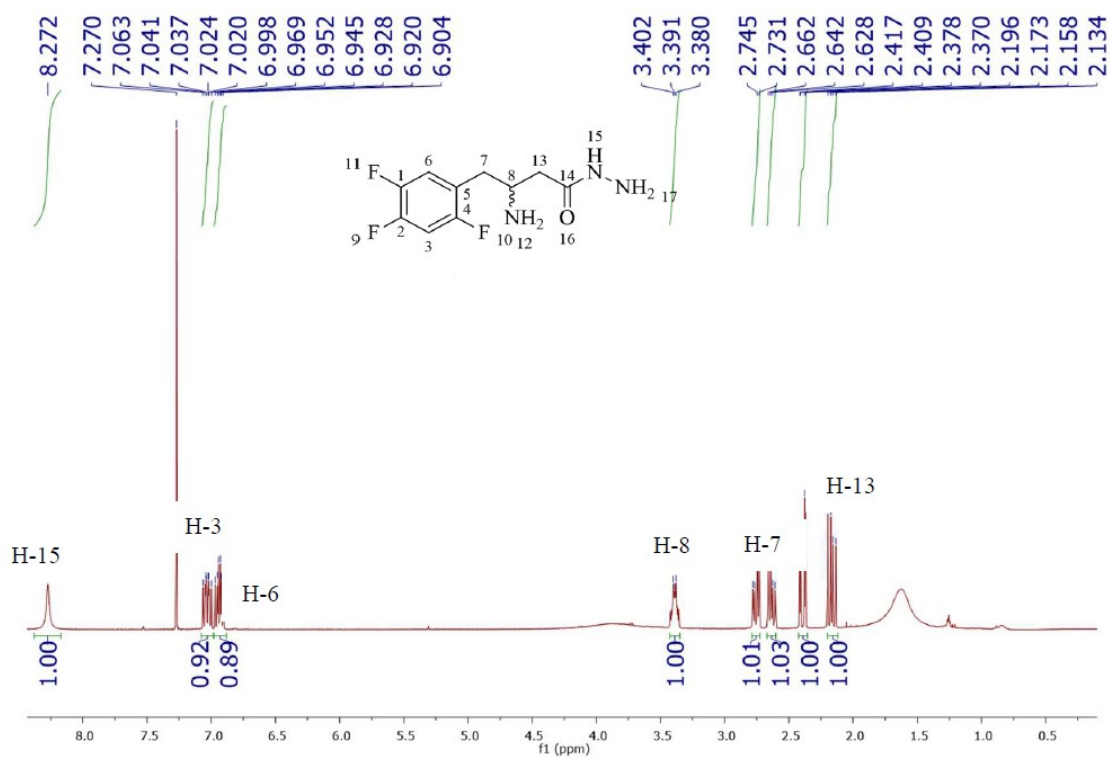


3-amino-4-(2,4,5-trifluorophenyl)butanoate (20)

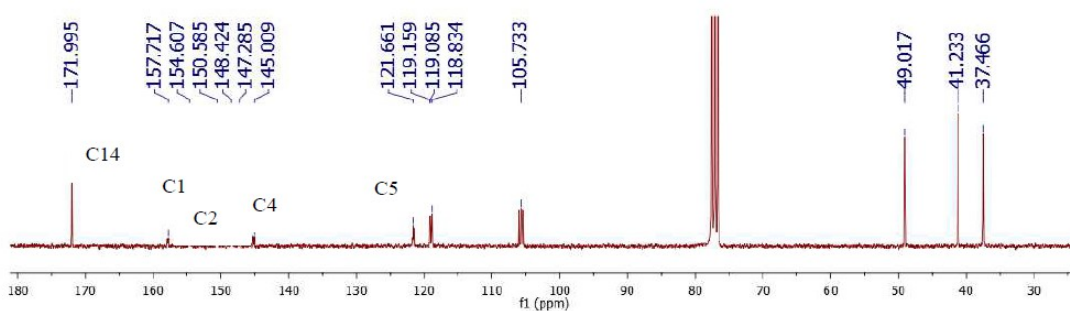
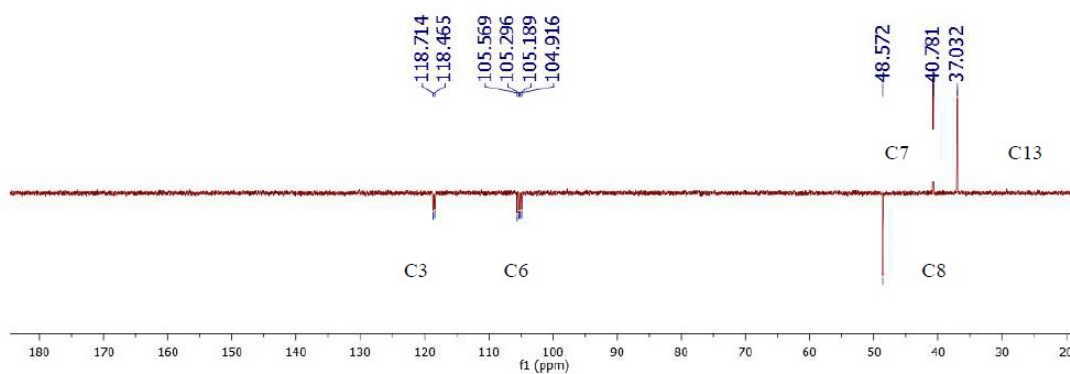


¹³C-NMR spectrum and DEPT of **20** (100MHz/CDCl₃/TMS/25°C)

8.1.3-amino-4-(2,4,5-trifluorophenyl)butanehydrazide (**21**)

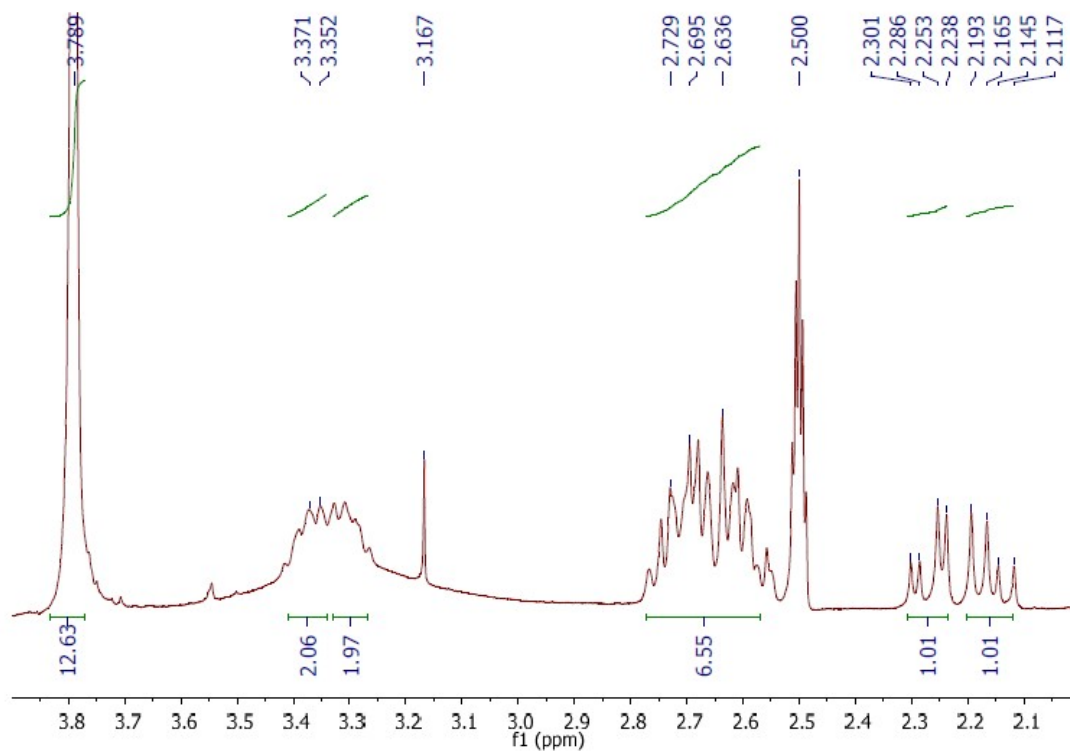
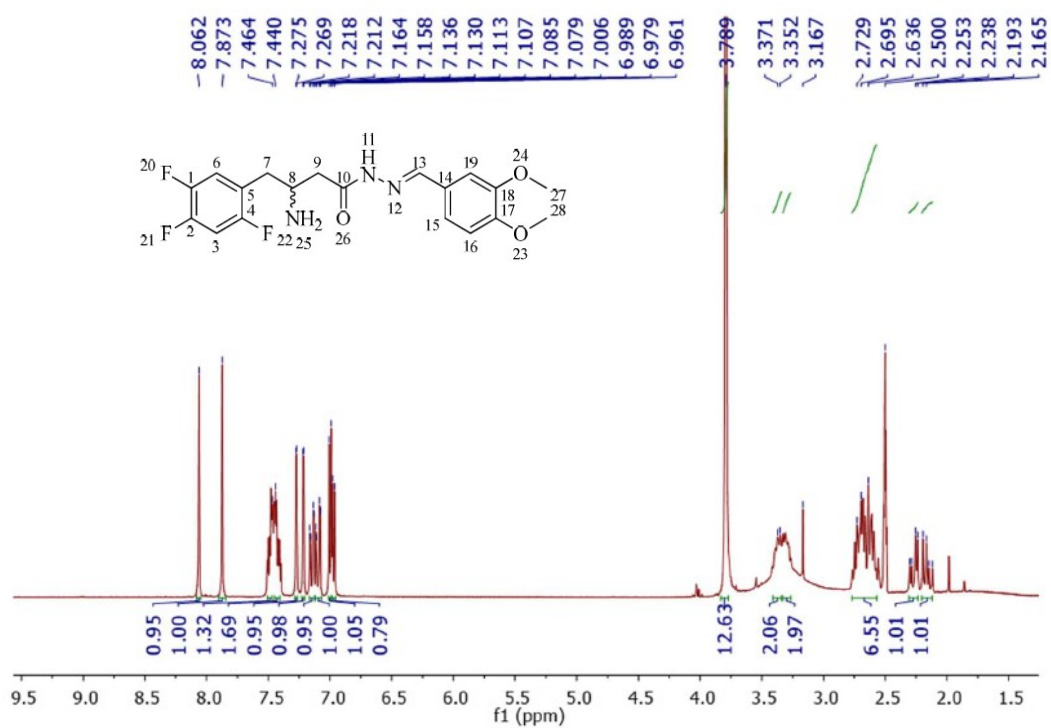


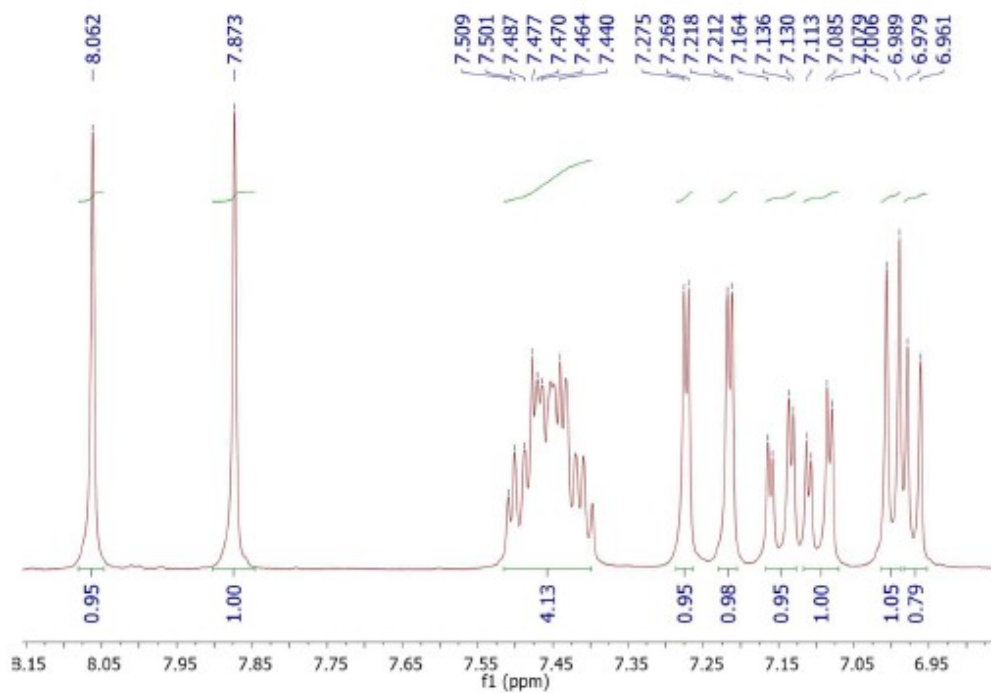
¹H-NMR spectrum of **21** (400MHz/CDCl₃/TMS/25°C)



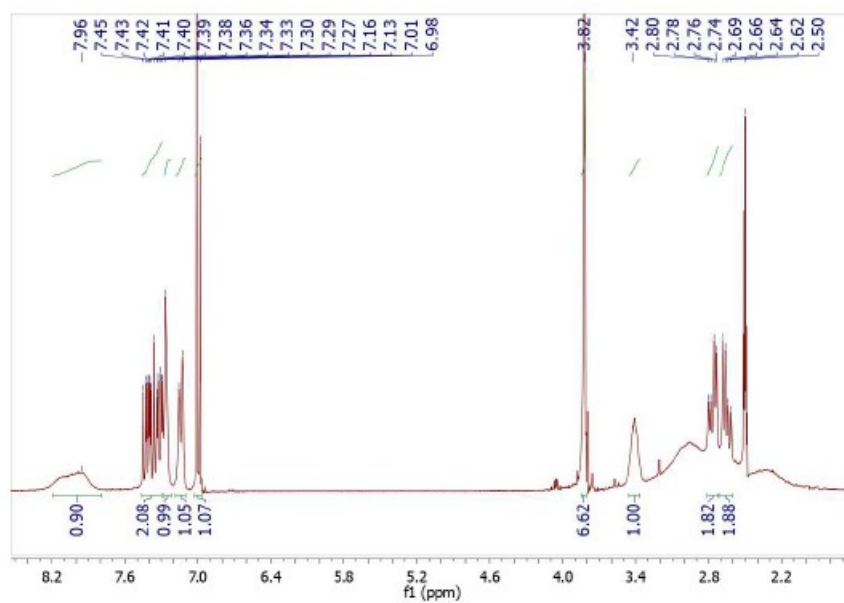
¹³C-NMR spectrum and DEPT of **21** (100MHz/CDCl₃/TMS/25°C)

(E)-3-amino-N'-(3,4-dimethoxybenzylidene)-4-(2,4,5-trifluorophenyl)butanehydrazide:
LASSBio-2123 (5)

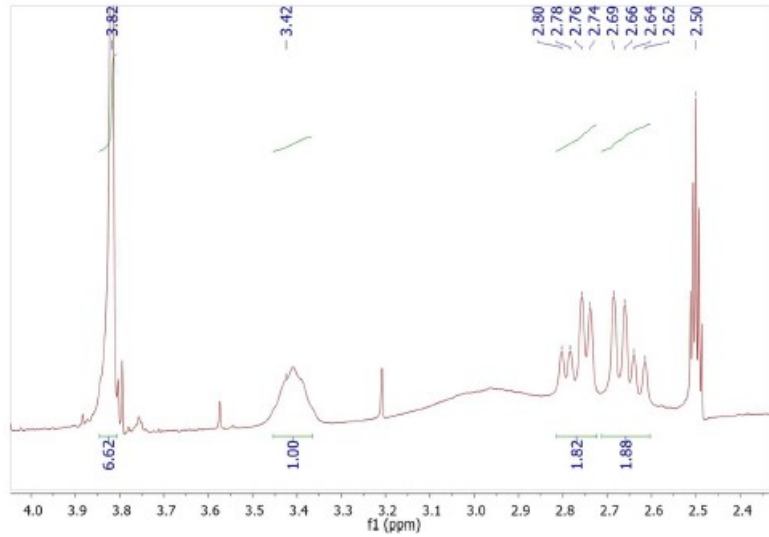




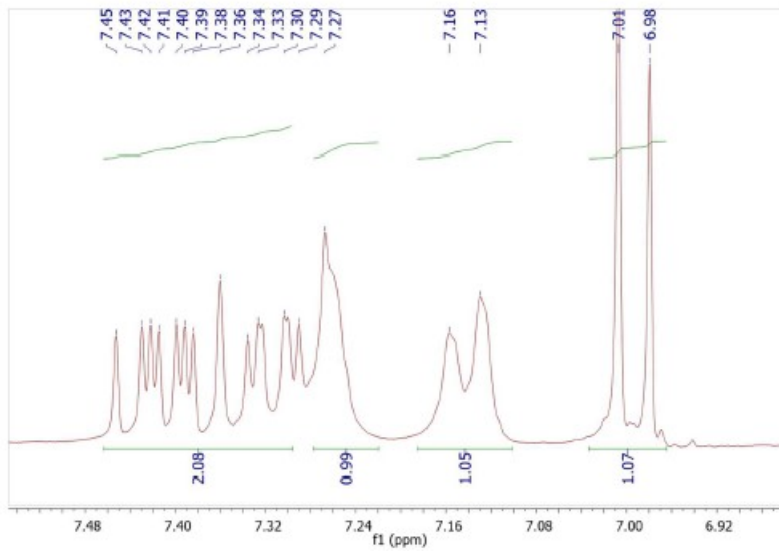
Expansion of $^1\text{H-NMR}$ spectrum of **5** (400MHz/DMSO- d_6 /TMS/25°C)



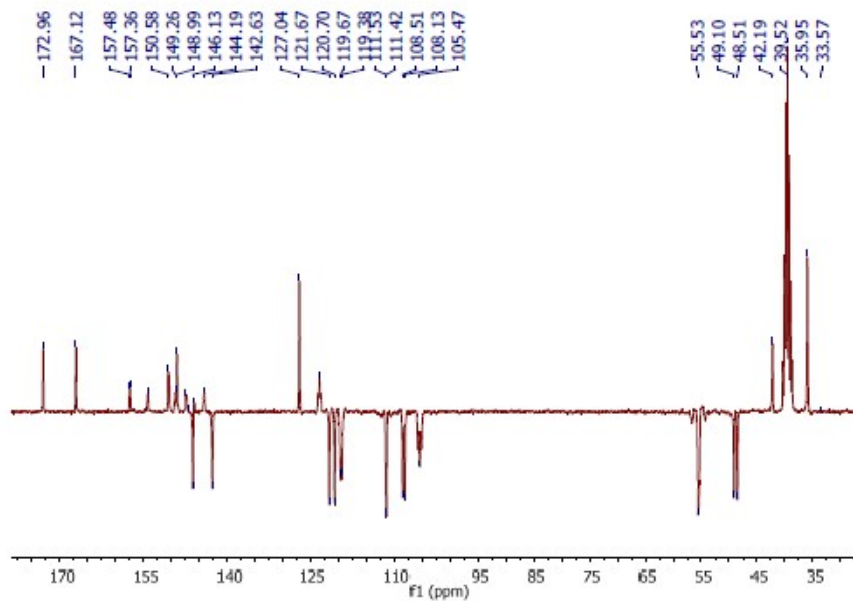
$^1\text{H-NMR}$ spectrum of **5** (400MHz/DMSO- d_6 /TMS/90°C)



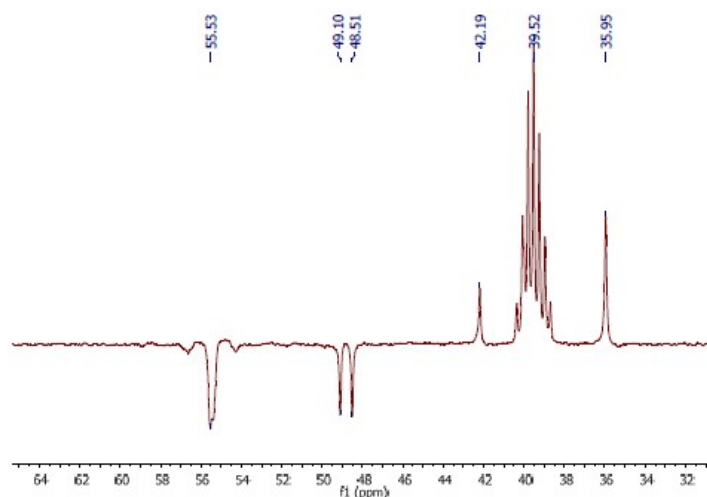
Expansion of ¹H-NMR spectrum of **5** (400MHz/DMSO-d₆/TMS/90°C)



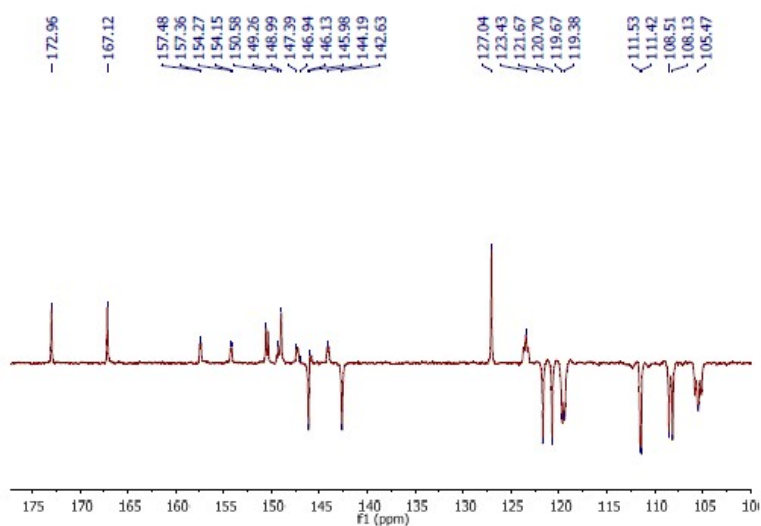
Expansion of ¹H-NMR spectrum of **5** (400MHz/DMSO-d₆/TMS/90°C)



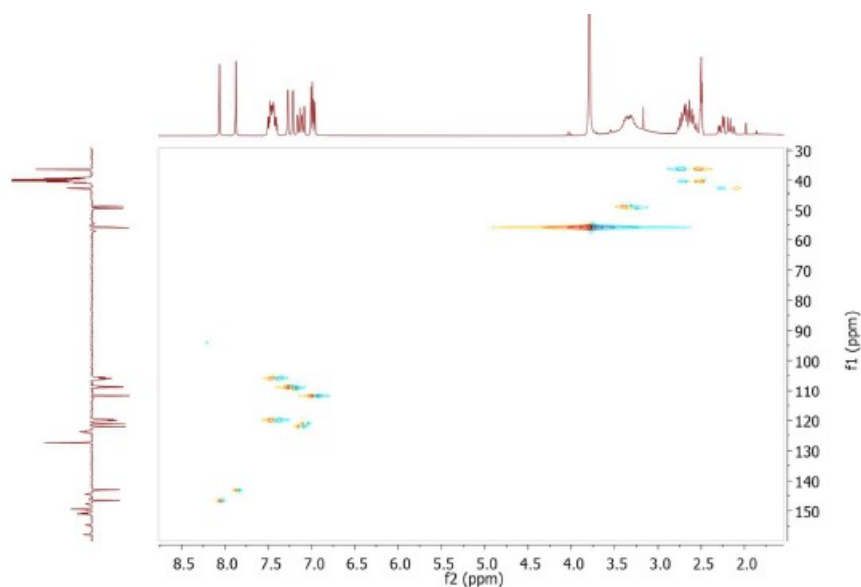
APT of **5** (100MHz/ DMSO-d₆/TMS/25°C)



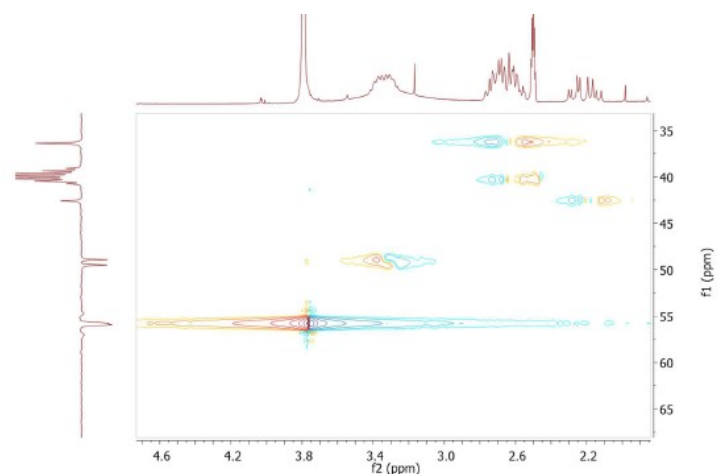
Expansion of APT of **5** (100MHz/DMSO-d₆/TMS/25°C)



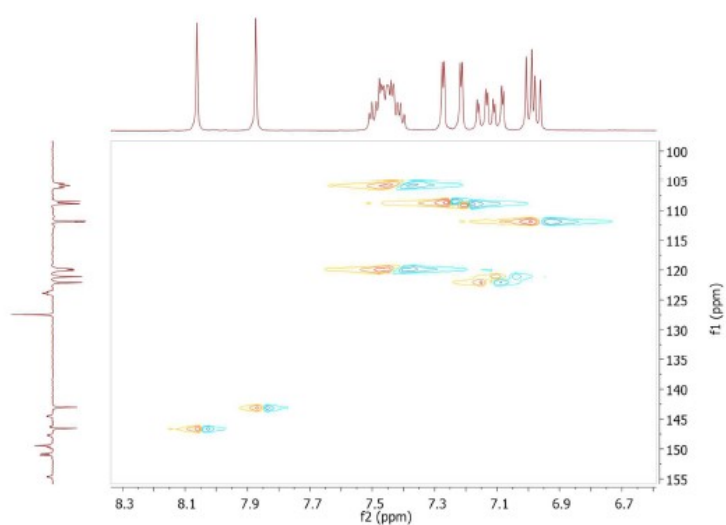
Expansion of APT of **5** (100MHz/DMSO-d₆/TMS/25°C)



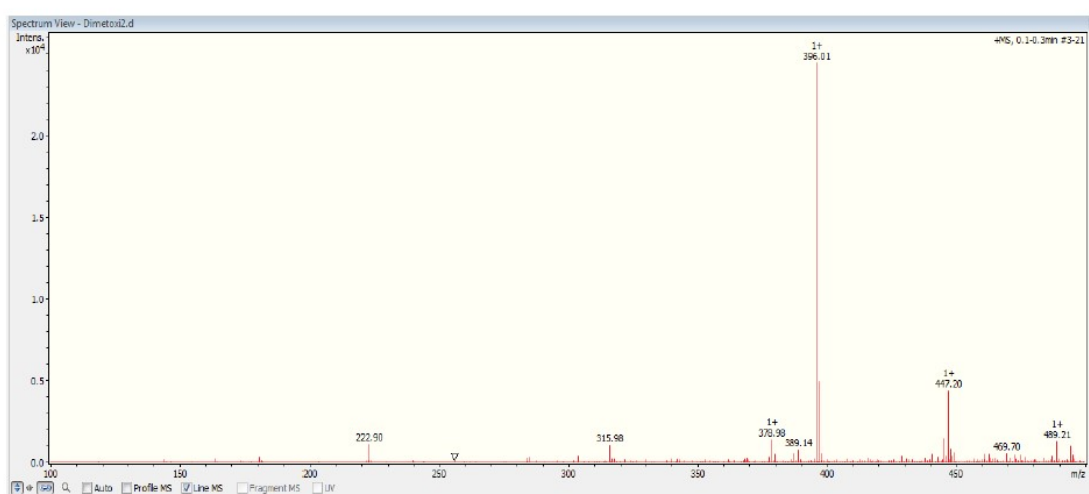
HSQC of **5** (DMSO-d₆/TMS/25°C)



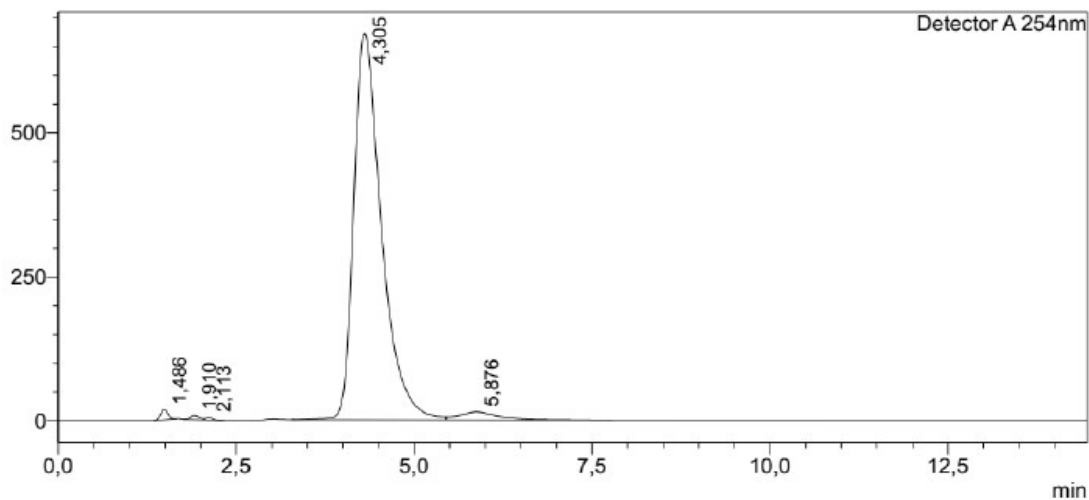
Expansion of HSQC of **5** (DMSO- d_6 /TMS/25°C)



Expansion of HSQC of **5** (DMSO- d_6 /TMS/25°C)



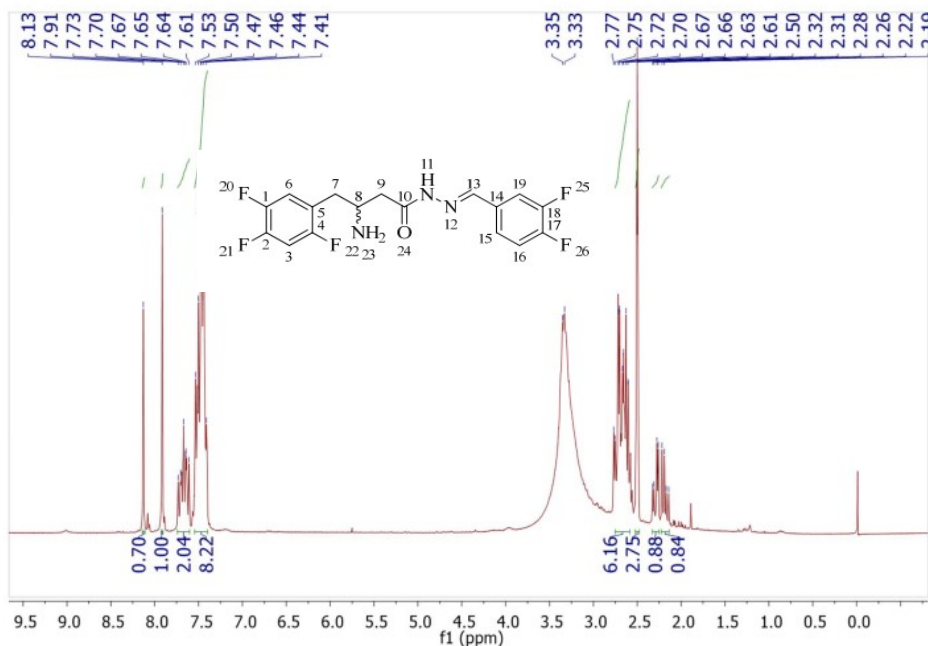
Mass spectrum of **5** in positive mode (ESI, direct injection)



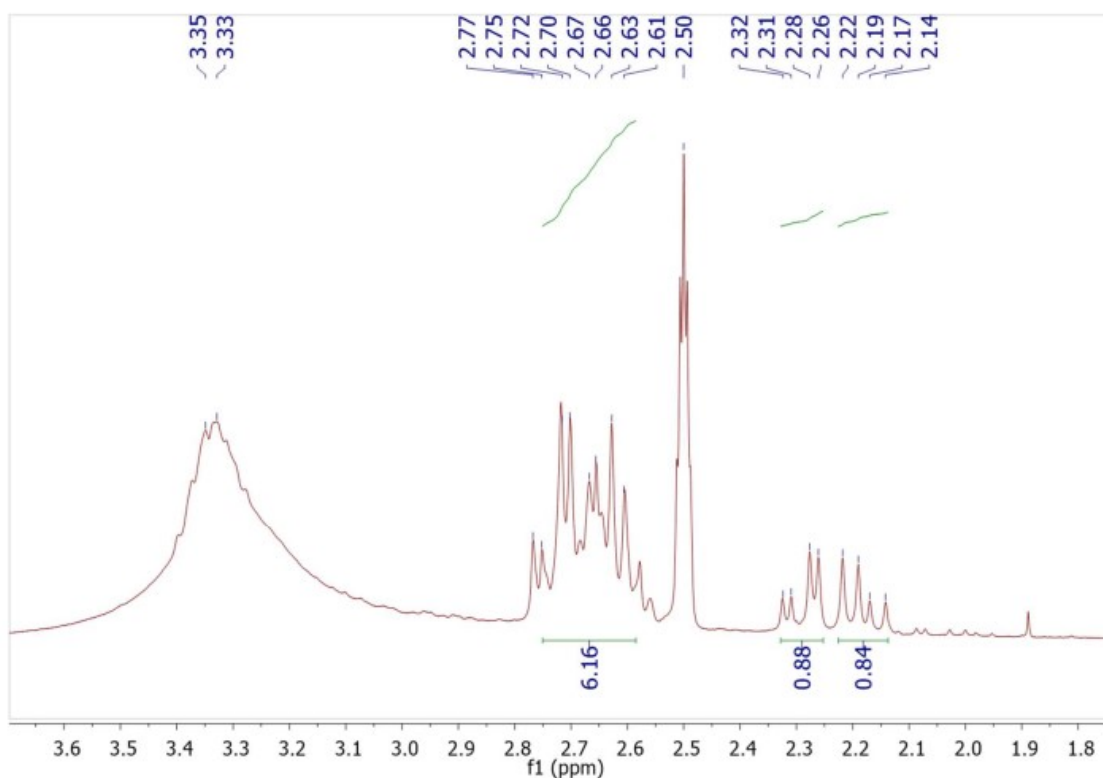
Detector A 254nm					
Peak#	Ret. Time	Area	Height	Height%	Area%
1	1,486	130111	18387	2,571	0,683
2	1,910	67947	7533	1,053	0,357
3	2,113	31535	4197	0,587	0,166
4	4,305	18229542	670704	93,788	95,676
5	5,876	594223	14308	2,001	3,119
Total		19053358	715130	100,000	100,000

HPLC Purity: Kromasil Column C18 [4,6 mm x 250 mm]; detector SPD-M20A [Diode Array]; flux: 1mL/min; injection volume: 20 μ L, mobile phase: 6:4 MeCN/H₂O (pH = 9).

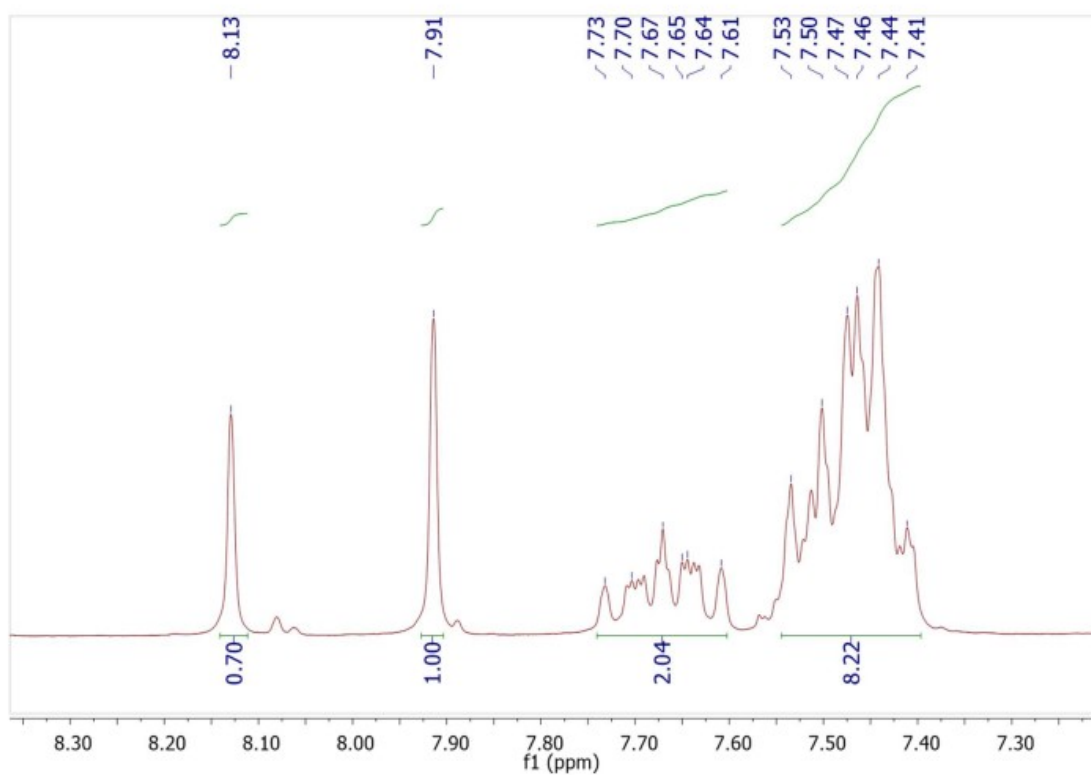
(*E*)-3-amino-N'-(3,4-difluorobenzylidene)-4-(2,4,5-trifluorophenyl) butanehydrazide:
LASSBio-2124 (6)



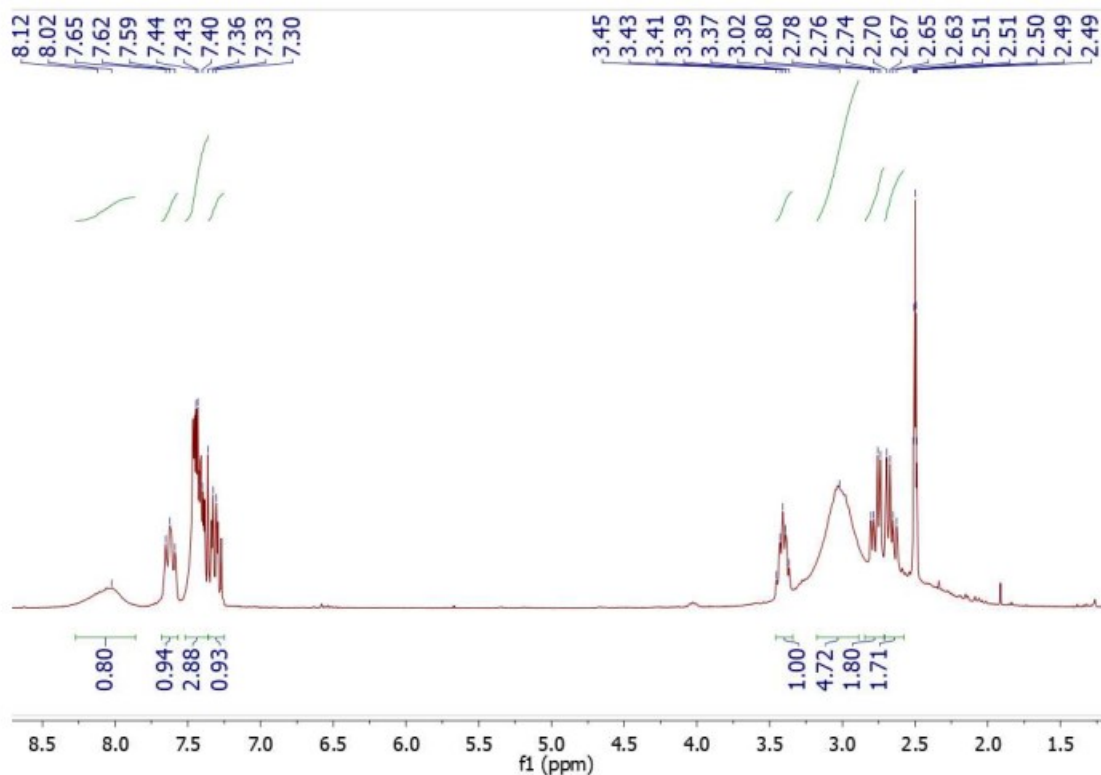
¹H-NMR spectrum of **6** (300MHz/DMSO-d₆/TMS/25°C)



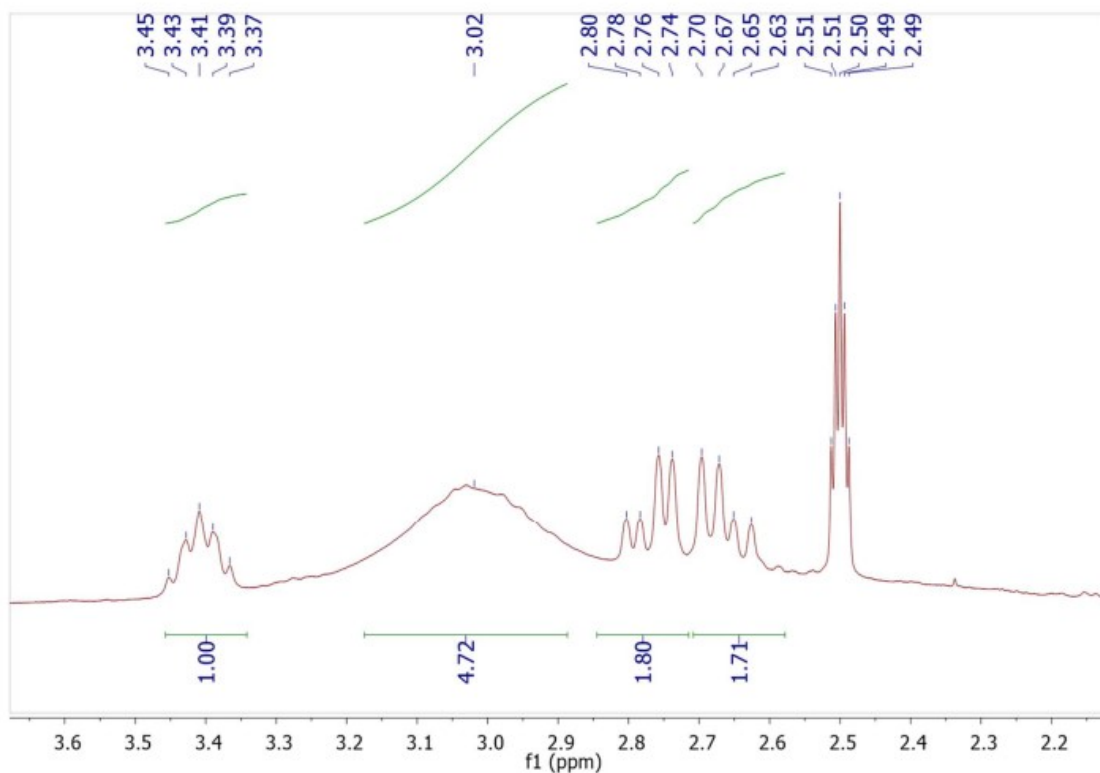
Expansion of $^1\text{H-NMR}$ spectrum of **6** (300MHz/DMSO- d_6 /TMS/25°C)



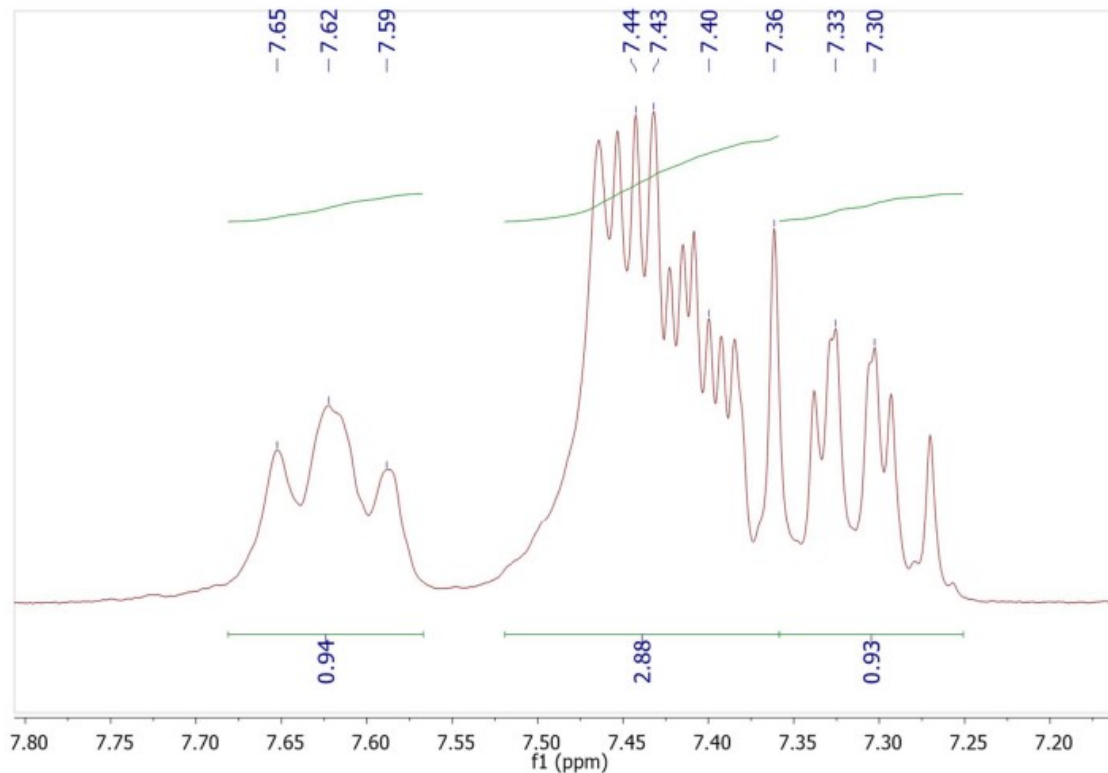
Expansion of $^1\text{H-NMR}$ spectrum of **6** (300MHz/DMSO- d_6 /TMS/25°C)



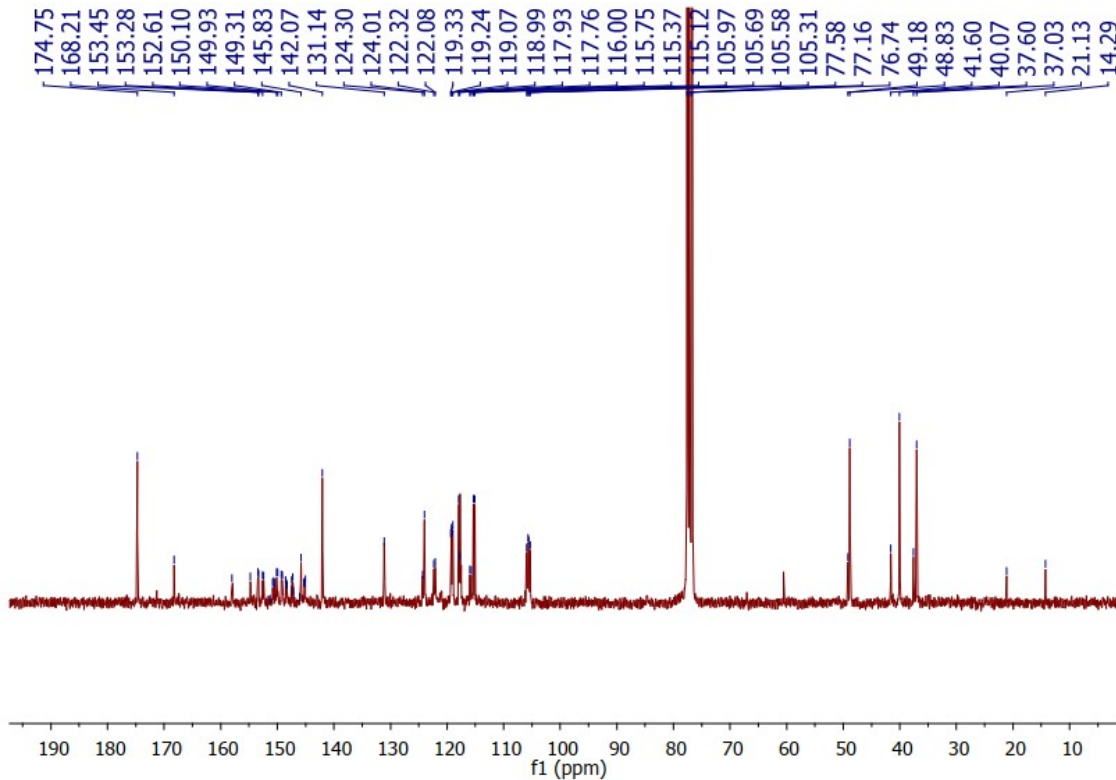
$^1\text{H-NMR}$ spectrum of **5** (400MHz/DMSO- d_6 /TMS/90°C)



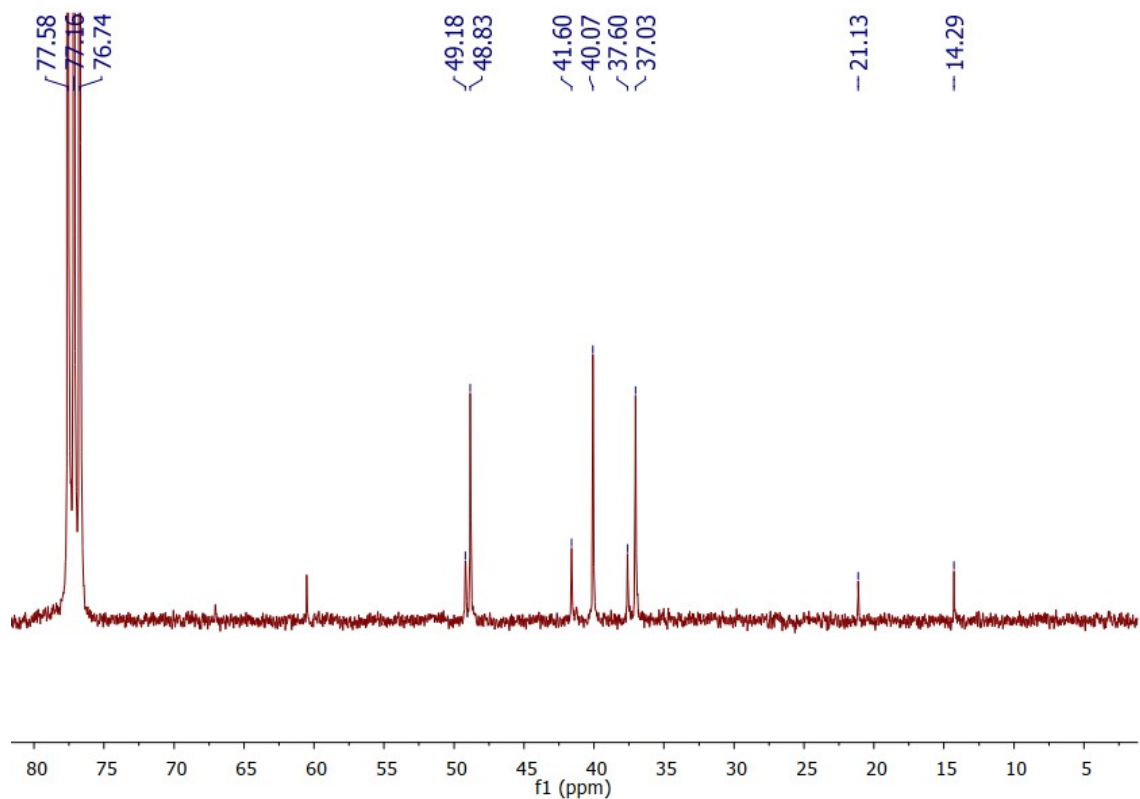
Expansion of $^1\text{H-NMR}$ spectrum of **5** (400MHz/DMSO- d_6 /TMS/90°C)



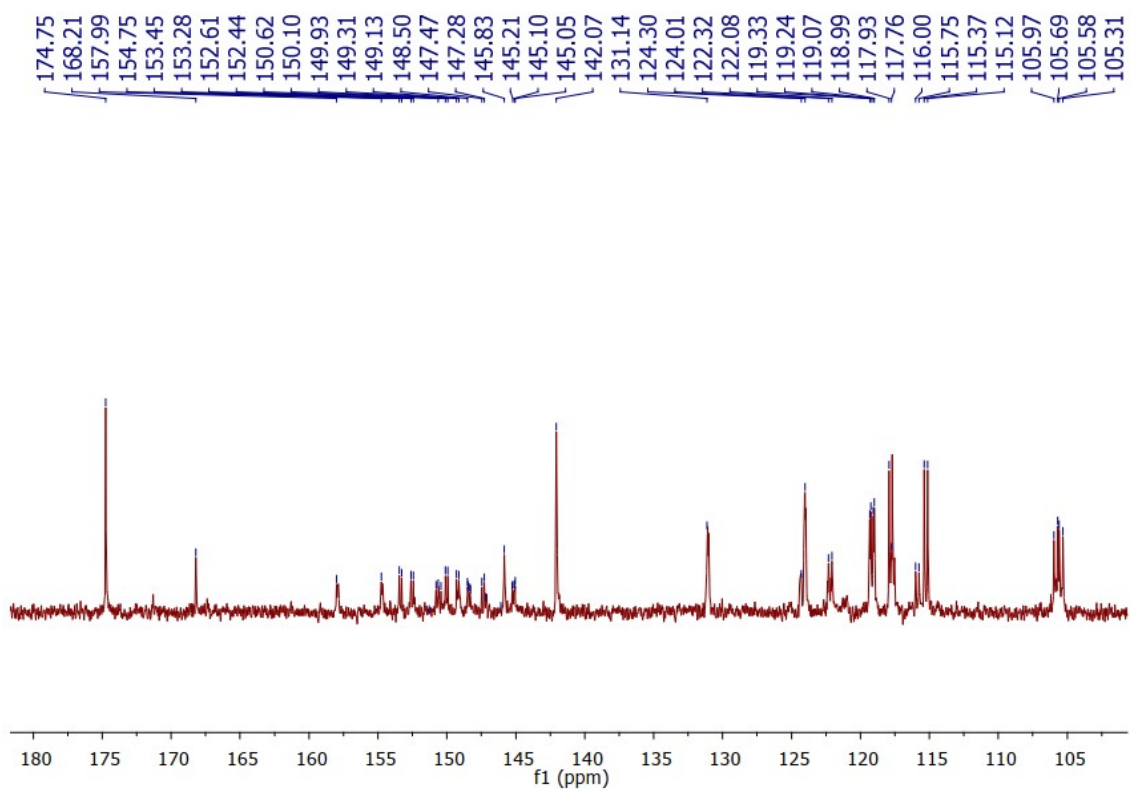
Expansion of ^1H -NMR spectrum of **5** (400MHz/DMSO- d_6 /TMS/90°C)



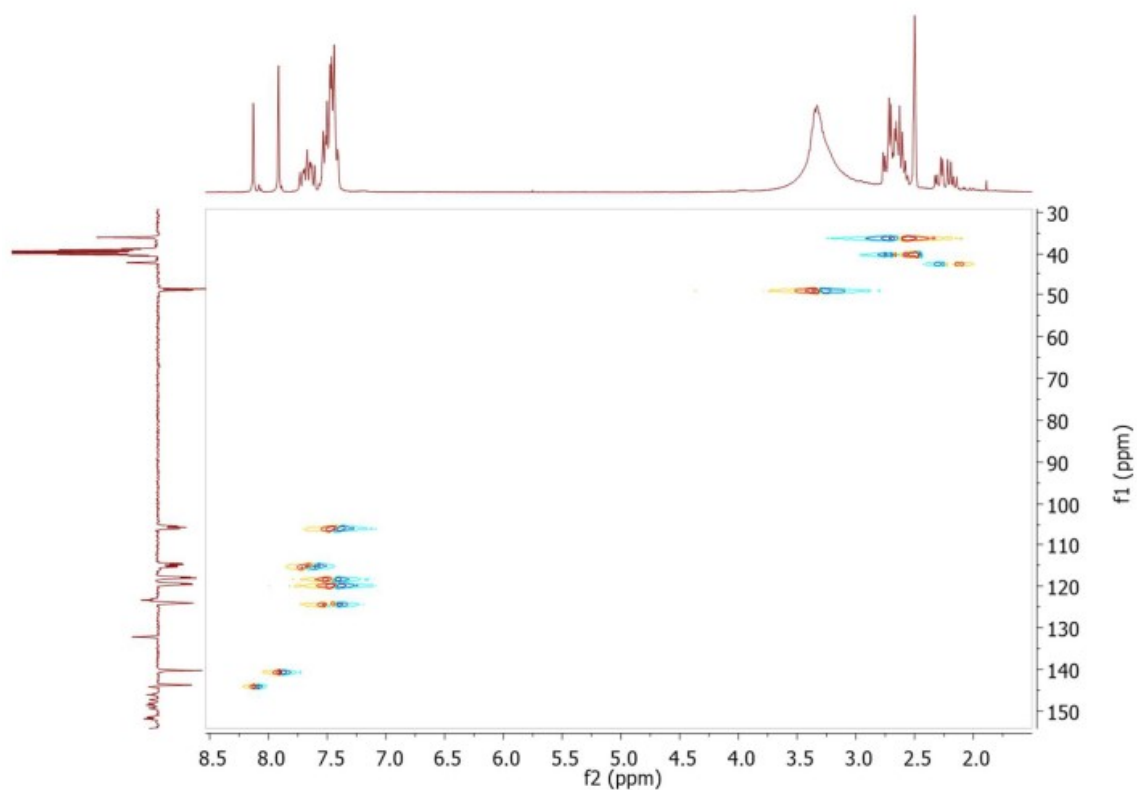
^{13}C -NMR of **6** (100MHz/ CDCl_3 /TMS/25°C)



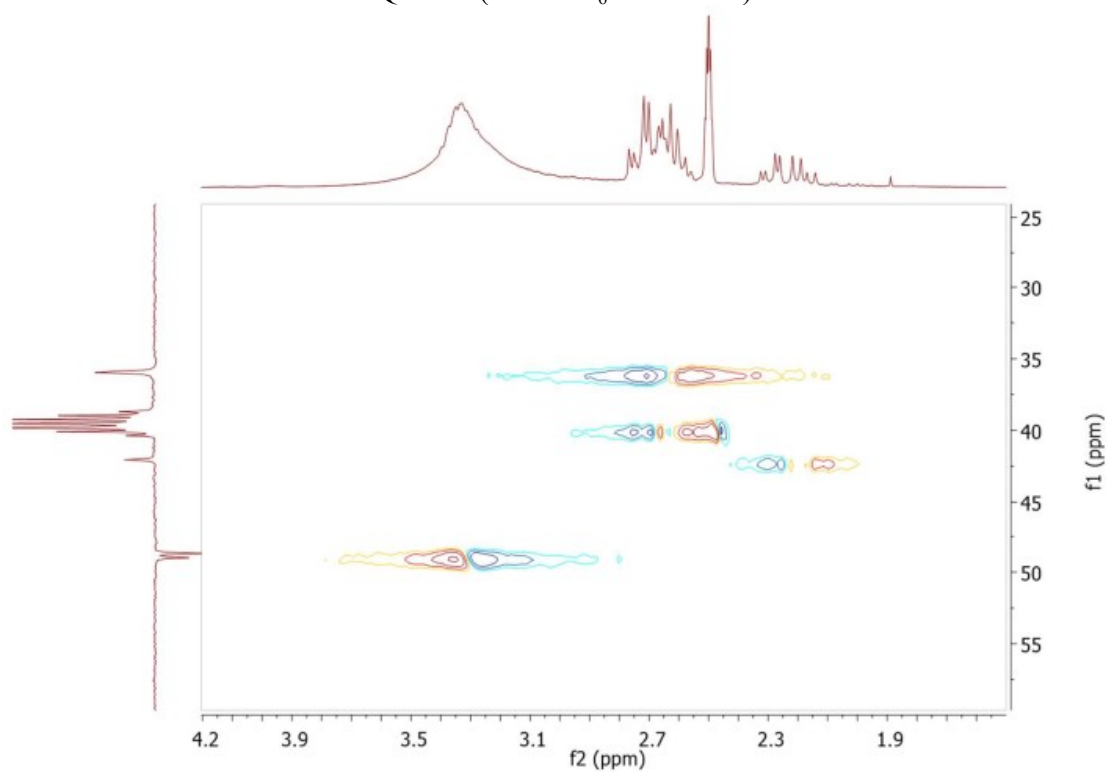
Expansion of ¹³C-NMR of **6** (100MHz/CDCl₃/TMS/25°C)



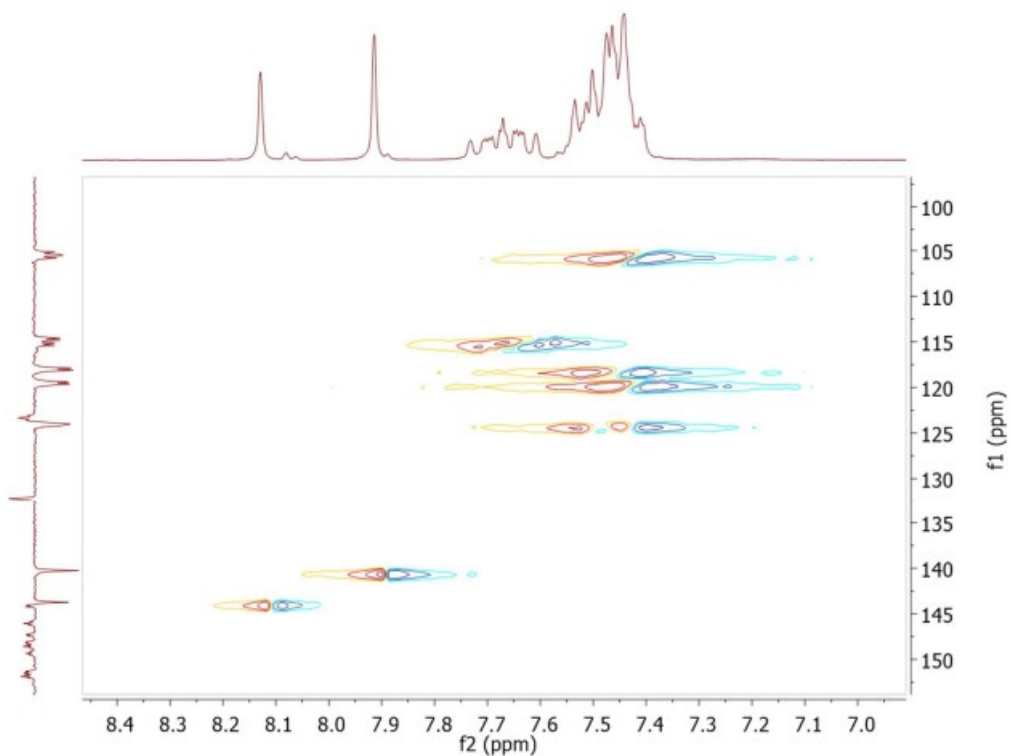
Expansion of ¹³C-NMR of **6** (100MHz/CDCl₃/TMS/25°C)



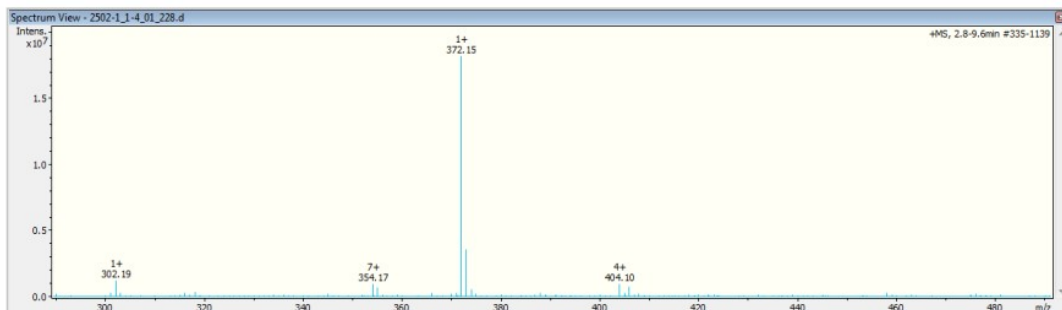
HSQC of **6** (DMSO- d_6 /TMS/25°C)



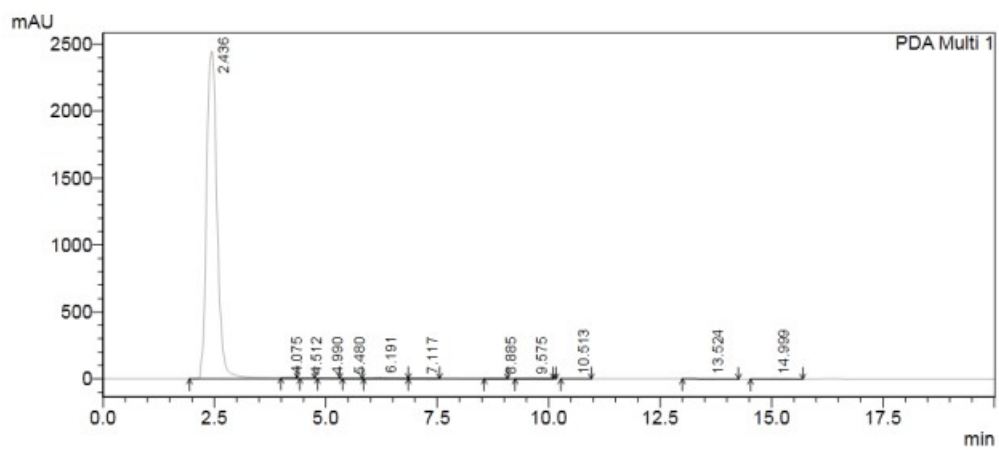
Expansion of HSQC of **6** (DMSO- d_6 /TMS/25°C)



Expansion of HSQC of **6** (DMSO- d_6 /TMS/25°C)



Mass spectrum of **6** in positive mode (ESI, direct injection)

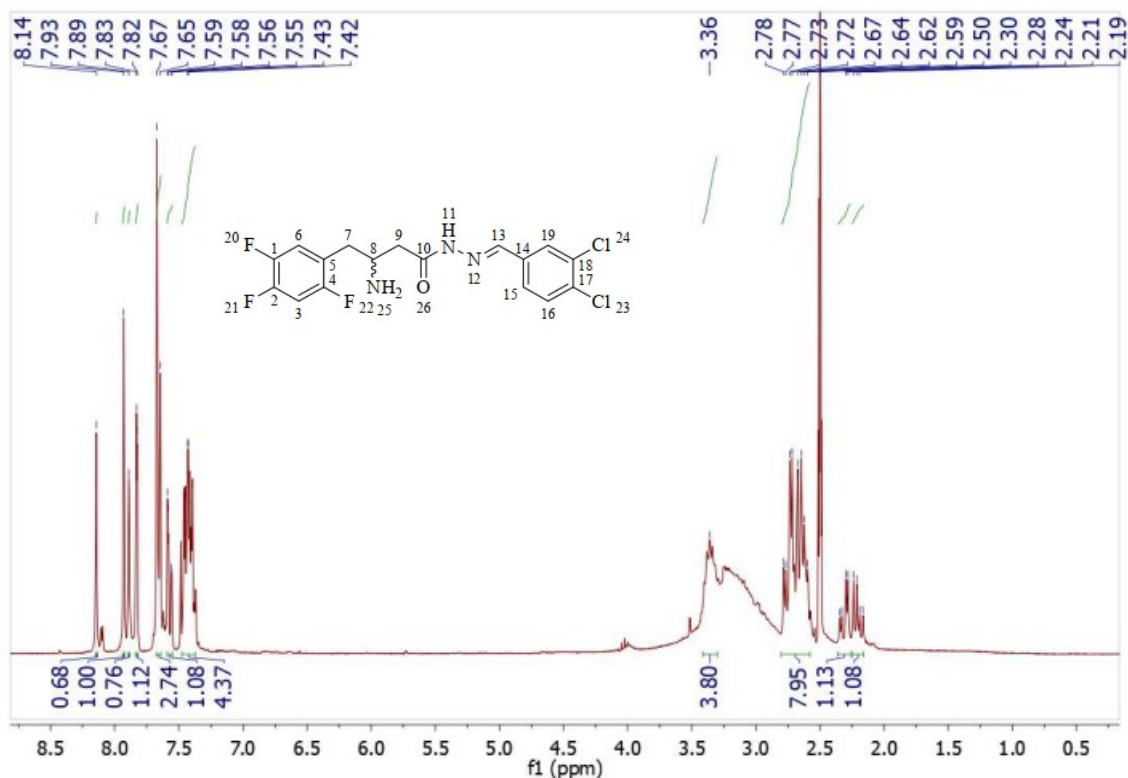


PDA Ch1 281nm 4nm

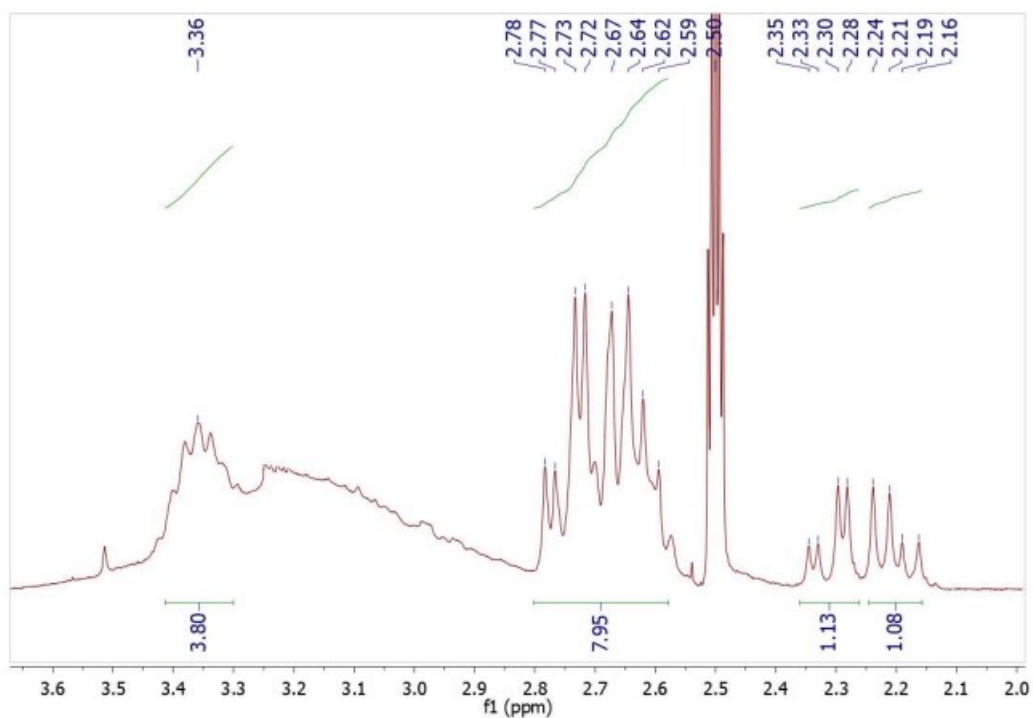
Peak#	Ret. Time	Area	Height	Area %	Height %
1	2.436	41020256	2448472	99.355	99.568
2	4.075	4113	301	0.010	0.012
3	4.512	1987	184	0.005	0.007

HPLC Purity: Kromasil Column C18 [4,6 mm x 250 mm]; detector SPD-M20A [Diode Array]; flux: 1mL/min; injection volume: 20 μ L, mobile phase: 6:4 MeCN/H₂O (pH = 9).

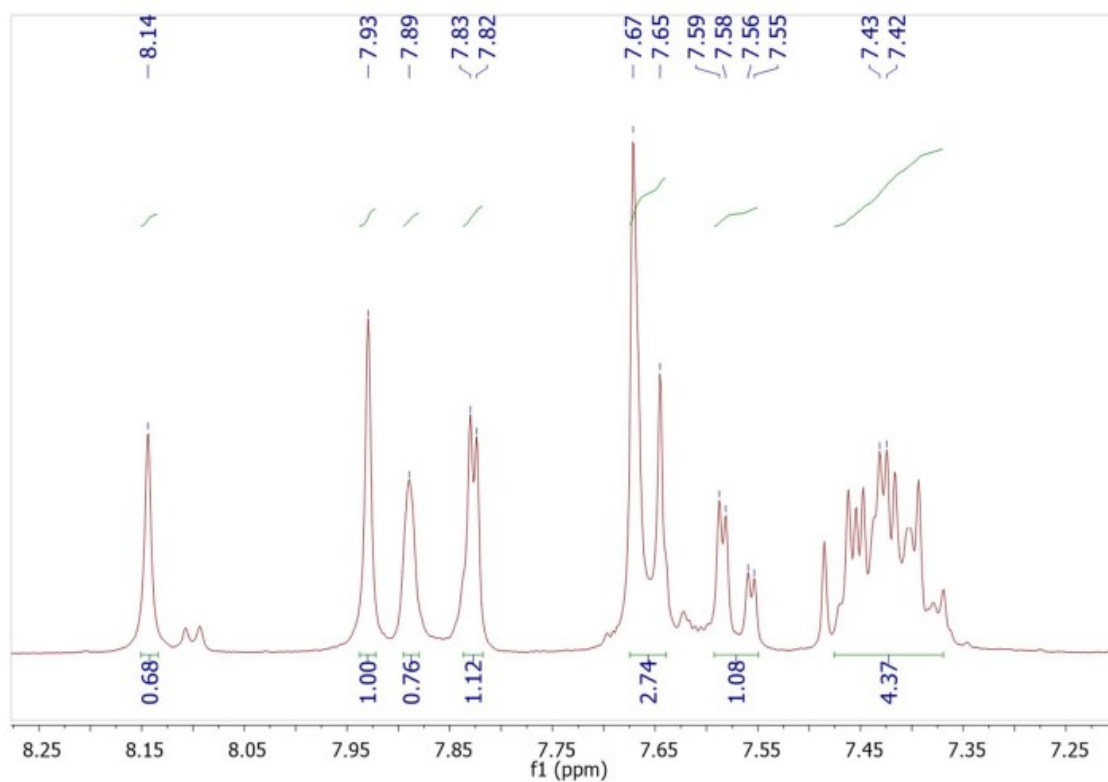
(E)-3-amino-N'-(3,4-dichlorobenzylidene)-4-(2,4,5-trifluorophenyl) butanehydrazide:
LASSBio-2125 (7)



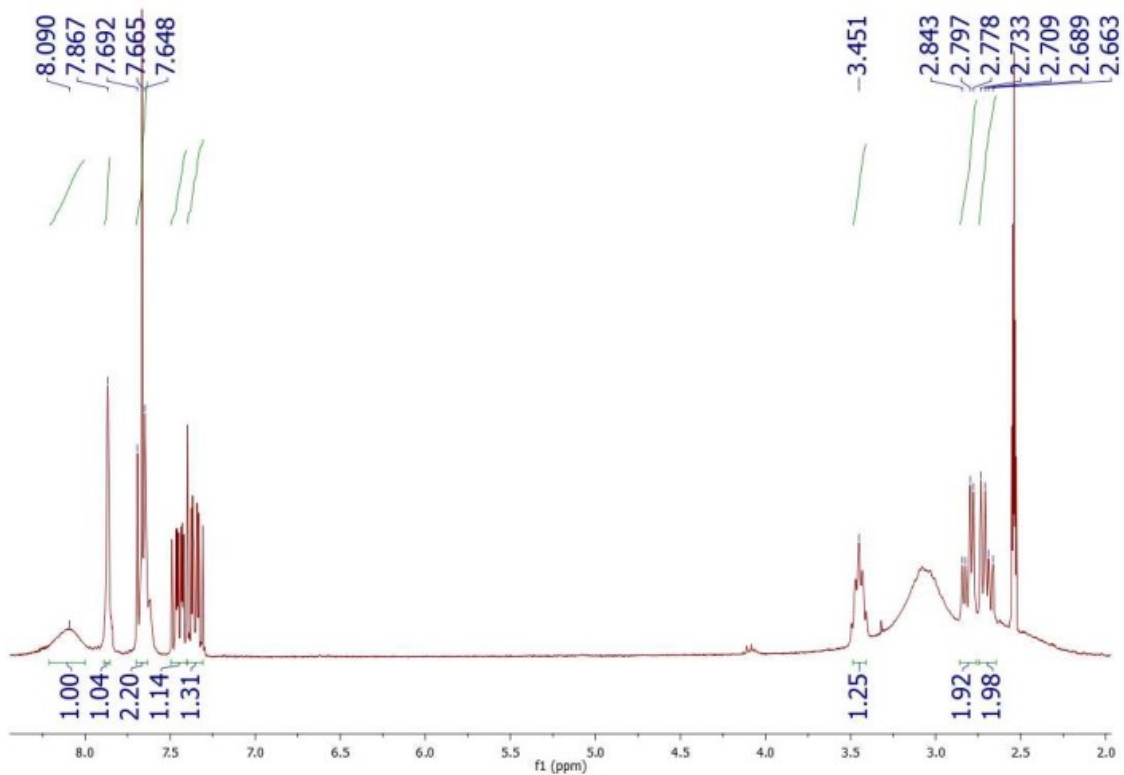
¹H-NMR spectrum of 7 (300MHz/DMSO-d₆/TMS/25°C)



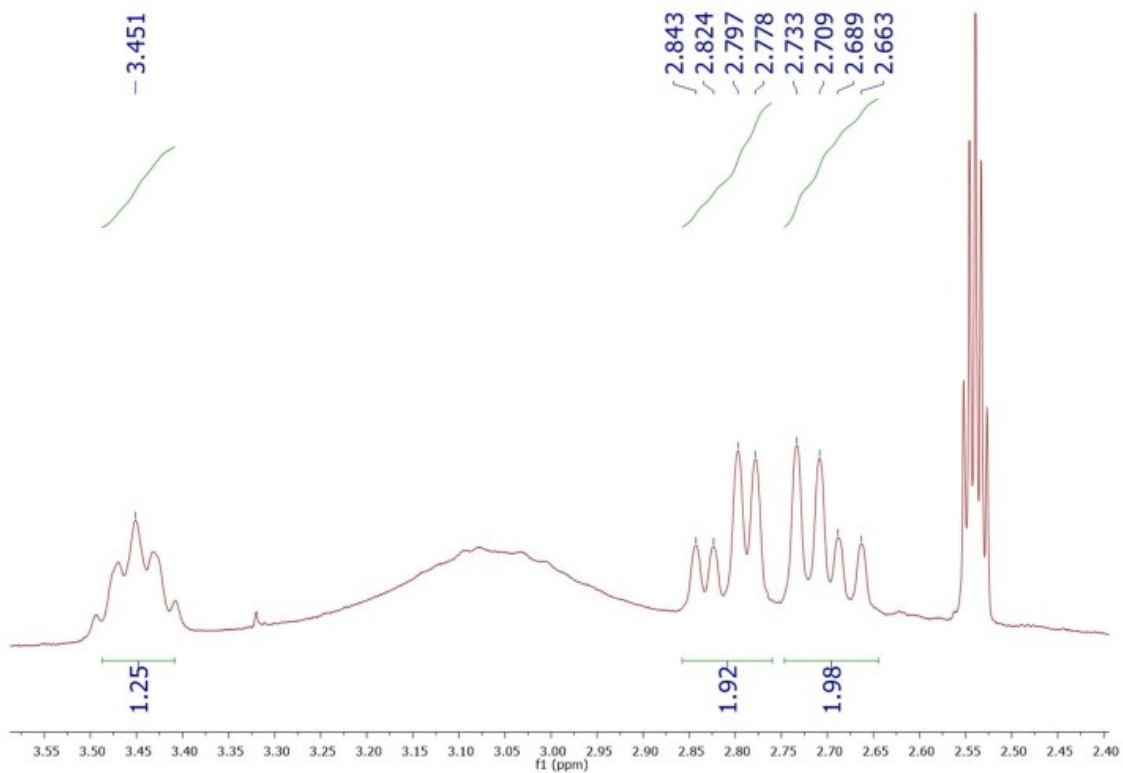
Expansion of $^1\text{H-NMR}$ spectrum of **6** (300MHz/DMSO- d_6 /TMS/25°C)



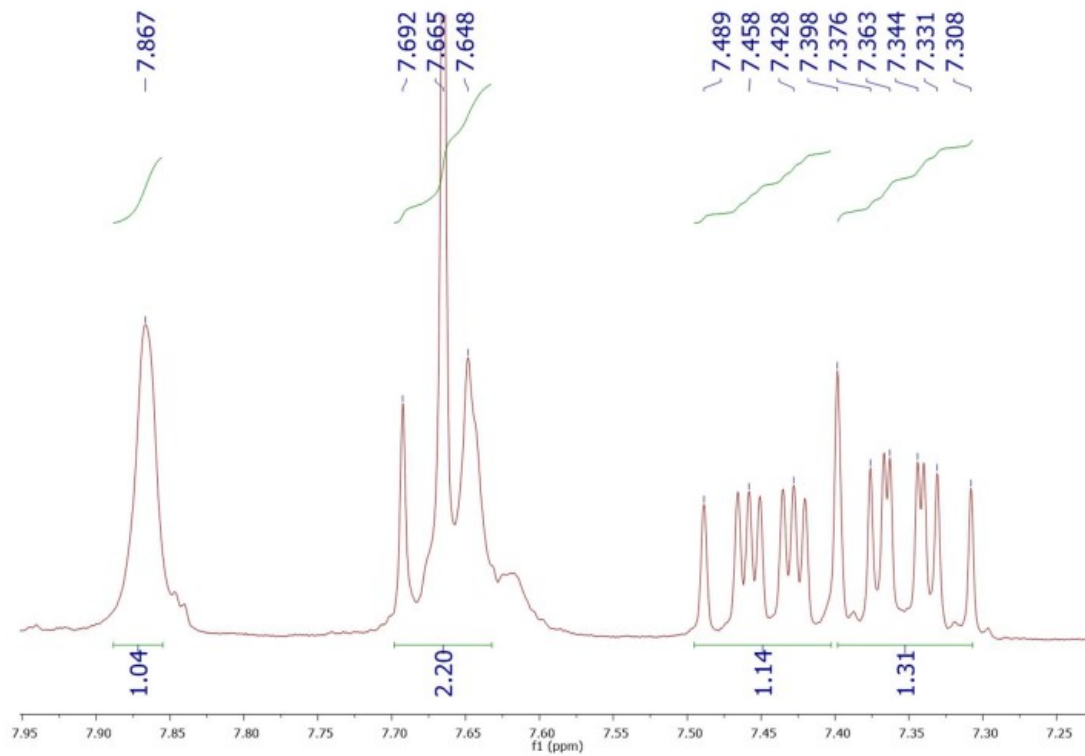
Expansion of $^1\text{H-NMR}$ spectrum of **6** (300MHz/DMSO- d_6 /TMS/25°C)



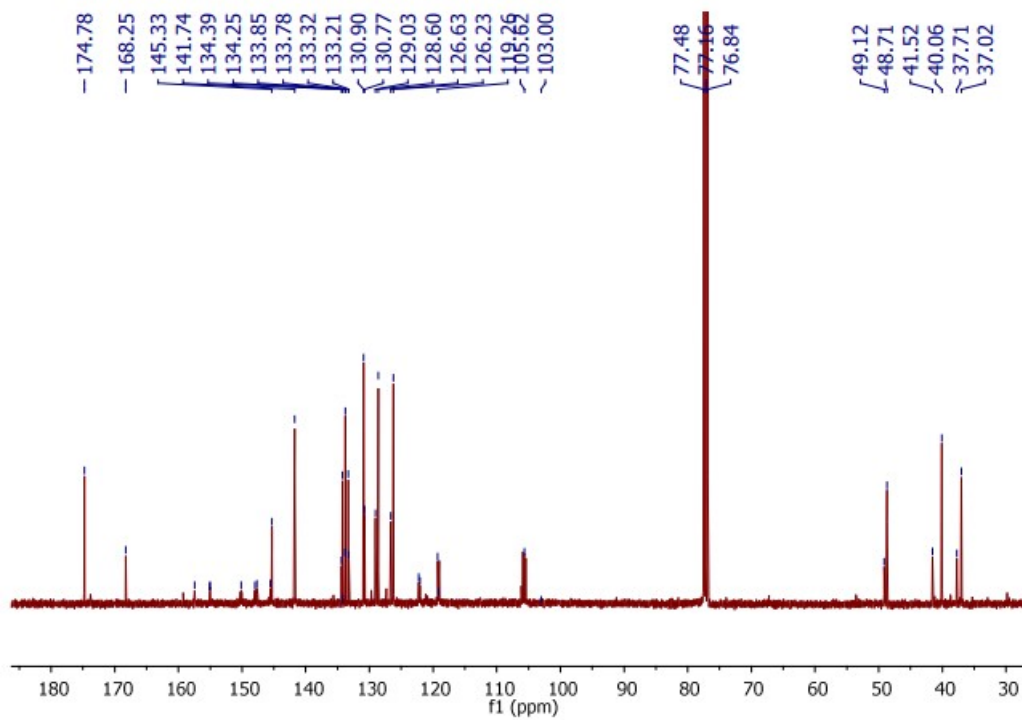
¹H-NMR spectrum of 7 (400MHz/DMSO-d₆/TMS/90°C)



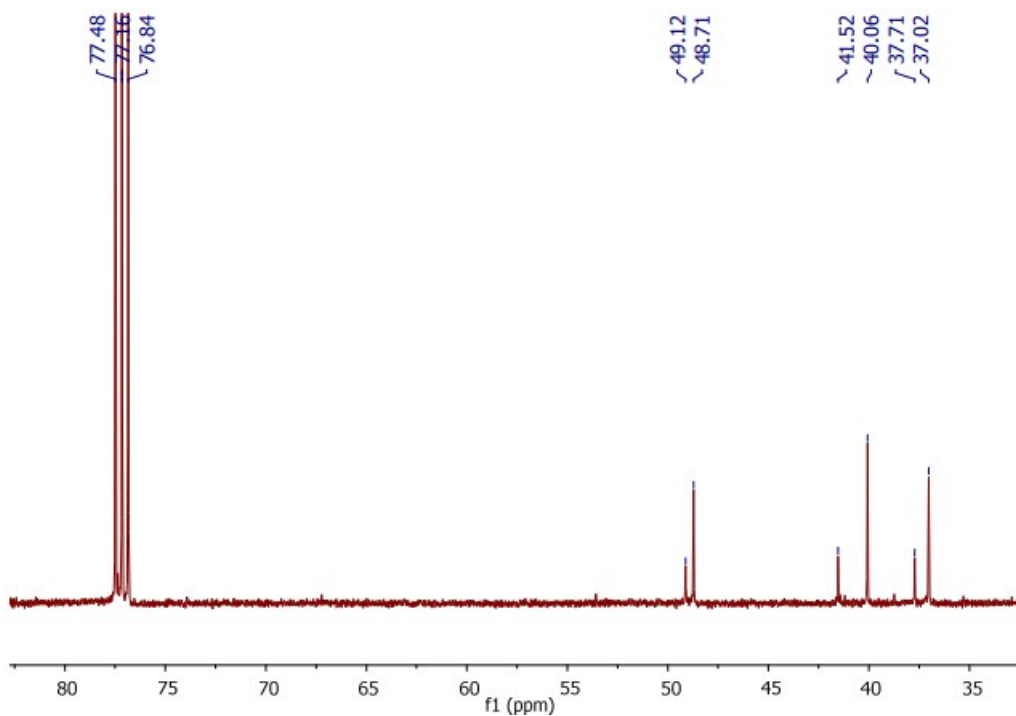
Expansion of ¹H-NMR spectrum of 7 (400MHz/DMSO-d₆/TMS/90°C)



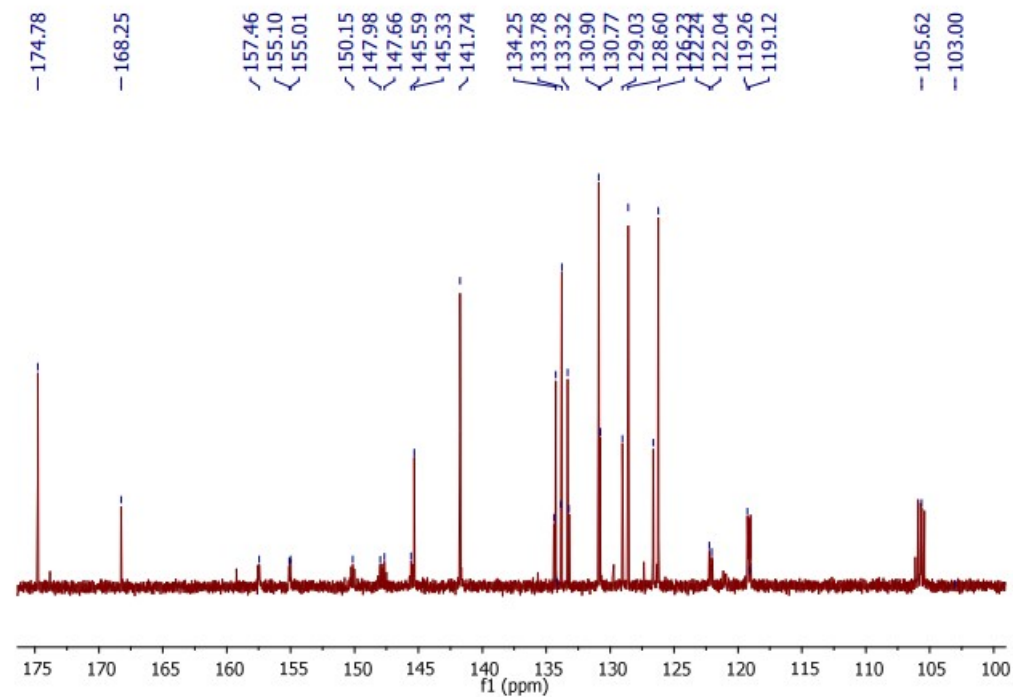
Expansion of $^1\text{H-NMR}$ spectrum of **7** (400MHz/DMSO- d_6 /TMS/90°C)



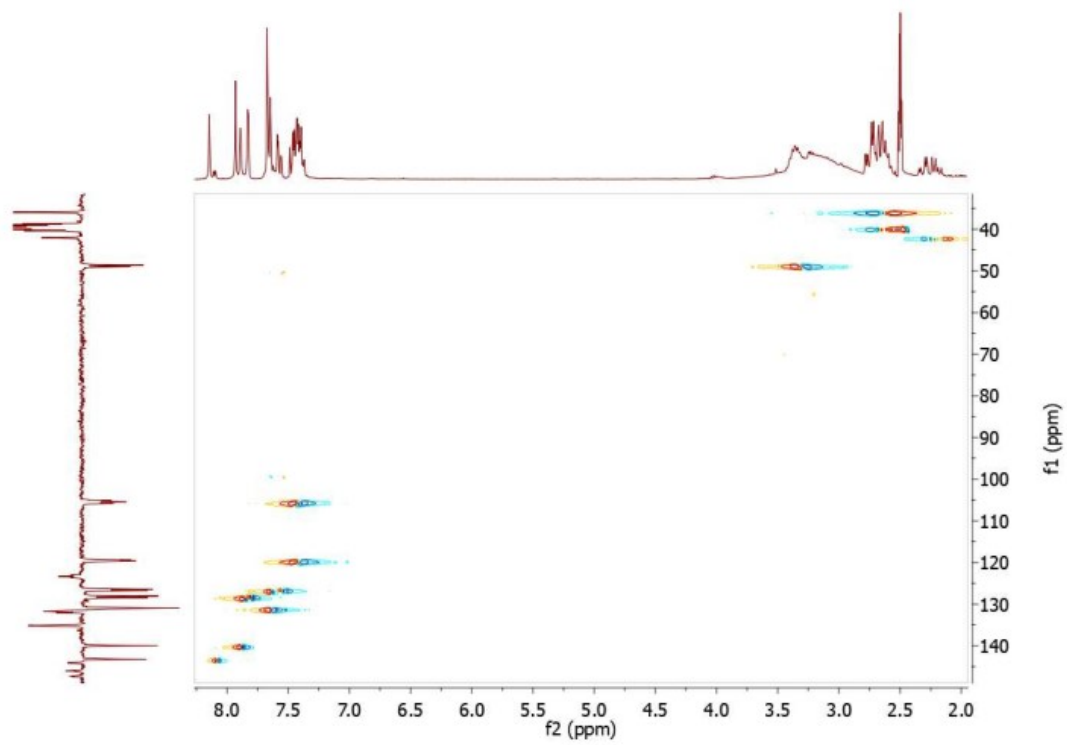
$^{13}\text{C-NMR}$ of **7** (100MHz/ CDCl_3 /TMS/25°C)



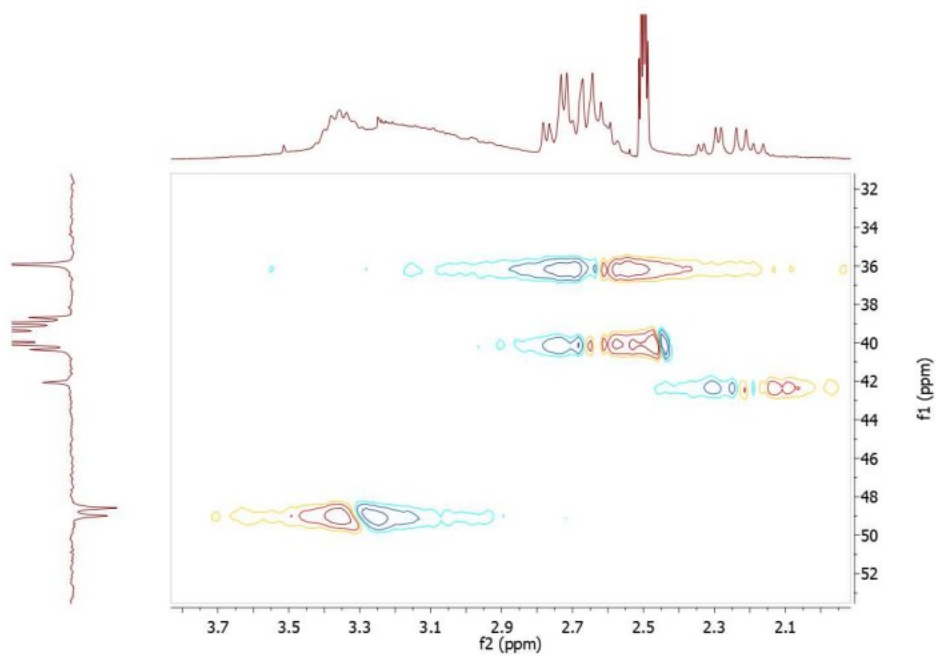
Expansion of ^{13}C -NMR of 7 (100MHz/ CDCl_3 /TMS/ 25°C)



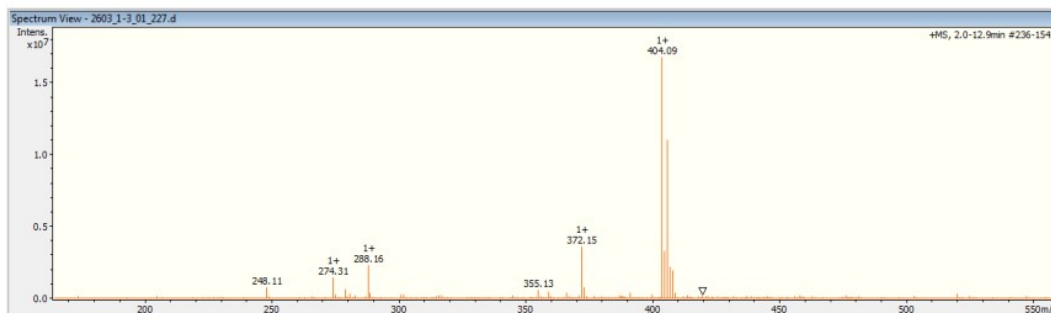
Expansion of ^{13}C -NMR of 7 (100MHz/ CDCl_3 /TMS/ 25°C)



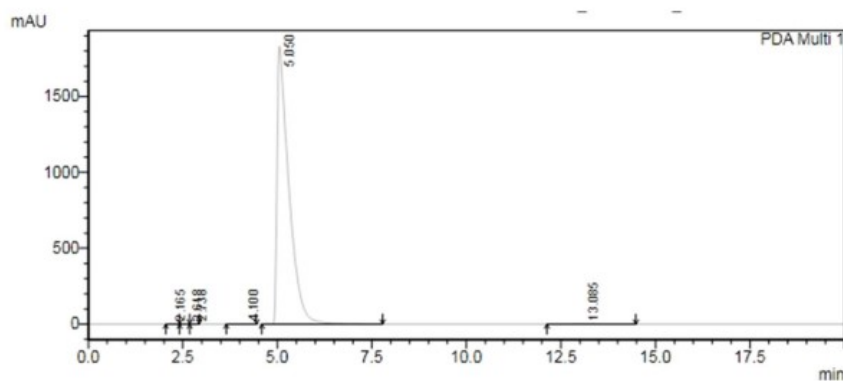
HSQC of 7 (DMSO-d₆/TMS/25°C)



Expansion of HSQC of 7 (DMSO-d₆/TMS/25°C)



Mass spectrum of 7 in positive mode (ESI, direct injection)

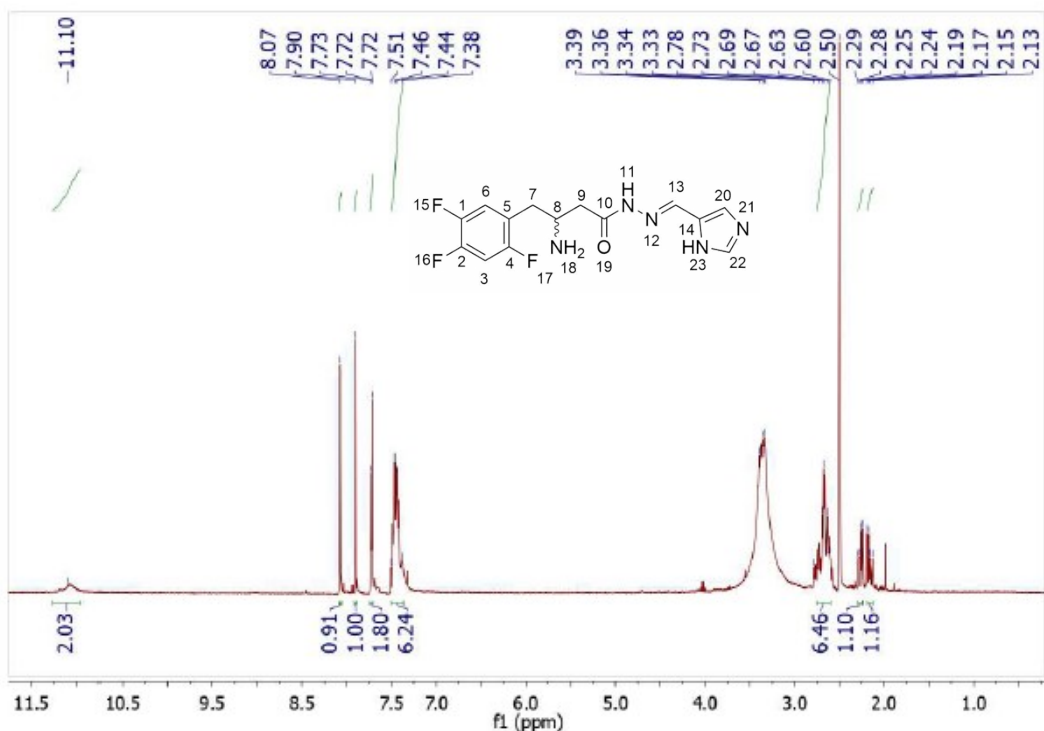


PDA Ch1 281nm 4nm

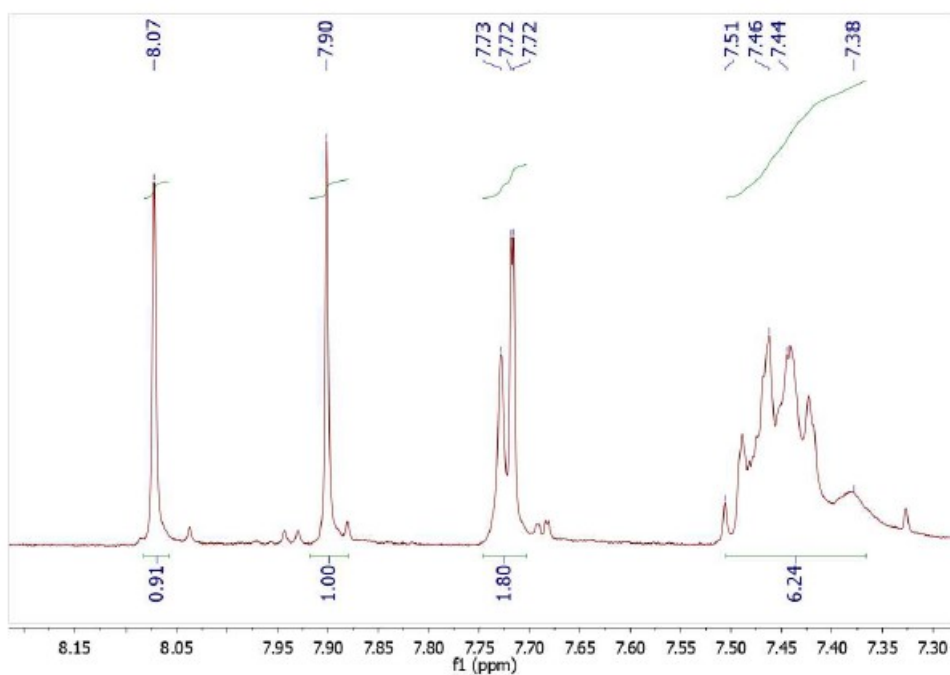
Peak#	Ret. Time	Area	Height	Area %	Height %
1	2.436	41020256	2448472	99.355	99.568
2	4.075	4113	301	0.010	0.012
3	4.512	1987	184	0.005	0.007

HPLC Purity: Kromasil Column C18 [4,6 mm x 250 mm]; detector SPD-M20A [Diode Array]; flux: 1mL/min; injection volume: 20 μ L, mobile phase: 6:4 MeCN/H₂O (pH = 9).

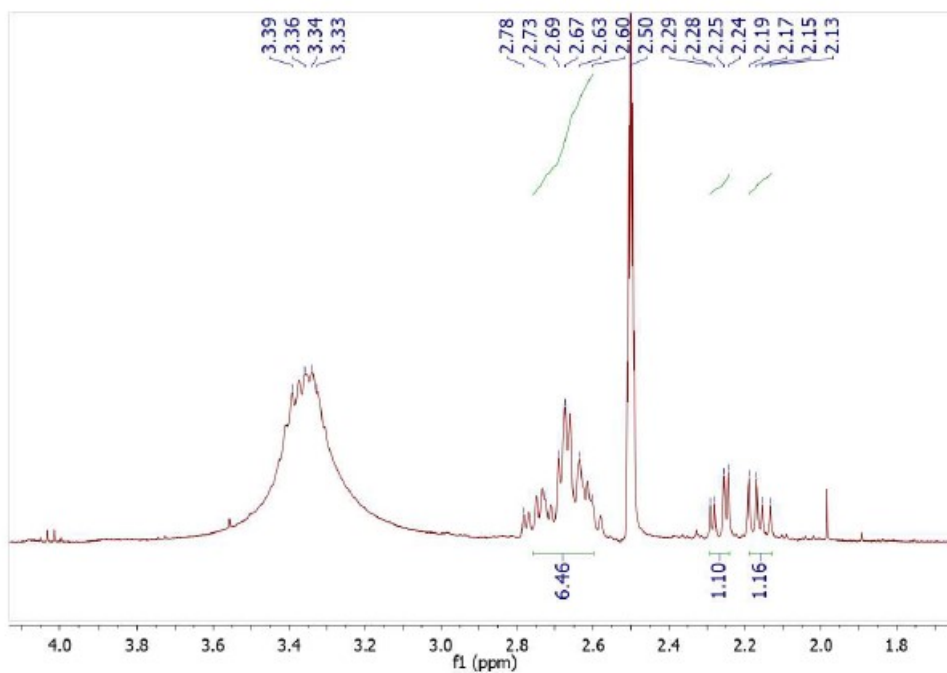
(E)-N'-((1H-imidazol-4-yl)methylene)-3-amino-4-(2,4,5-trifluorophenyl)butanehydrazide:
LASSBio-2126 (9)



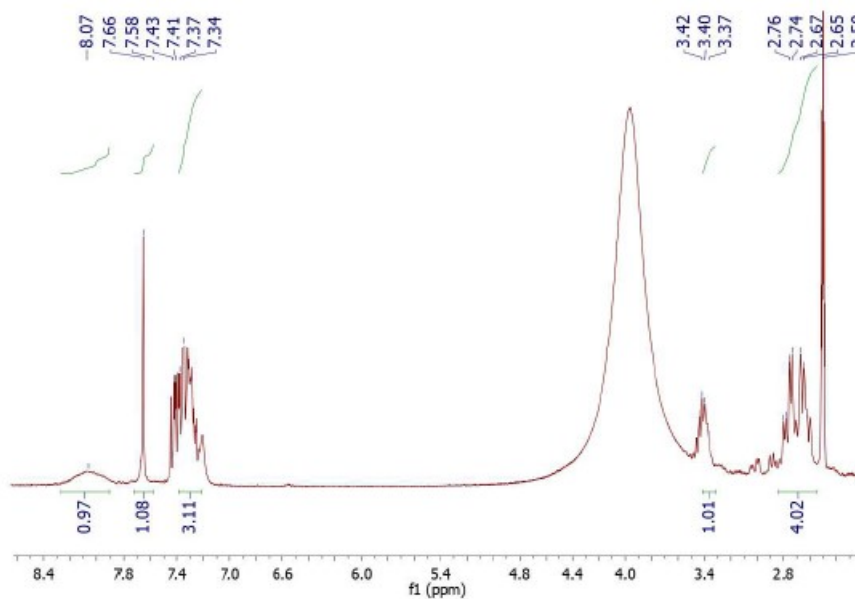
¹H-NMR spectrum of **9** (400MHz/DMSO-d₆/TMS/25°C)



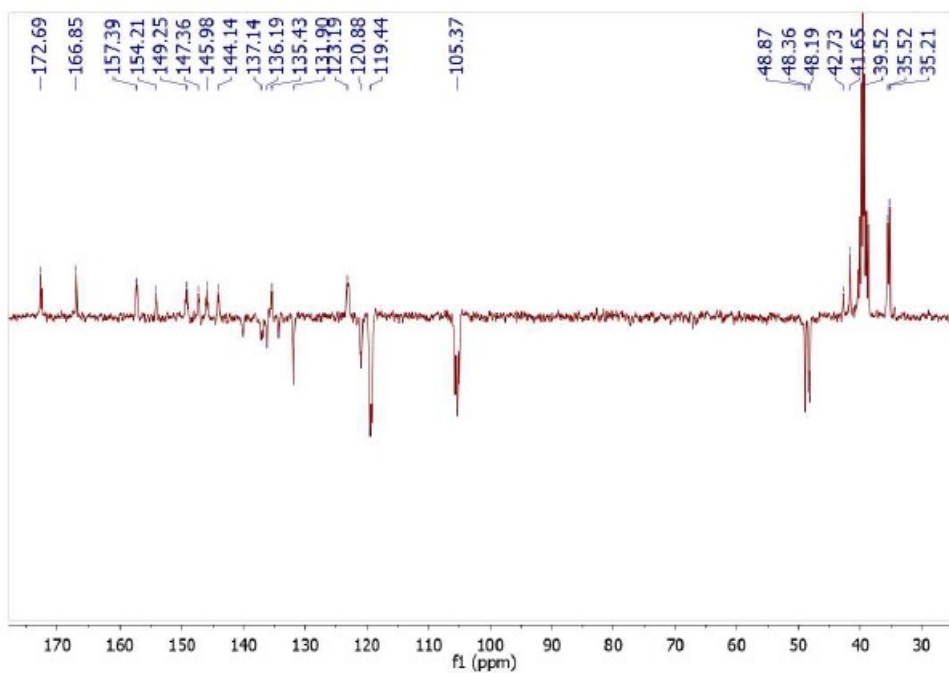
Expansion of ¹H-NMR spectrum of **9** (400MHz/DMSO-d₆/TMS/25°C)



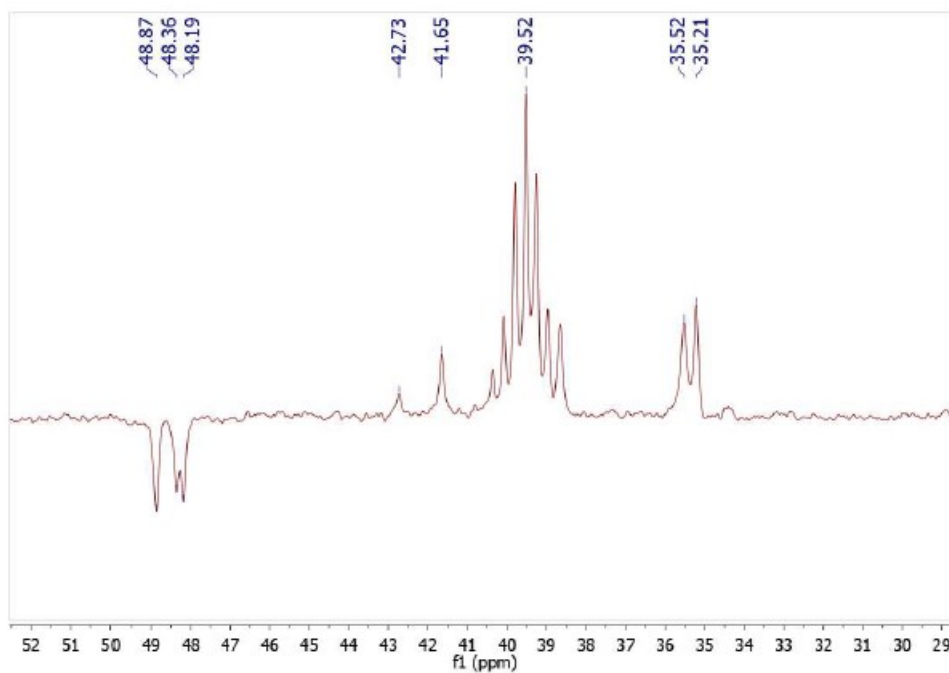
Expansion of $^1\text{H-NMR}$ spectrum of **9** (400MHz/DMSO- d_6 /TMS/25°C)



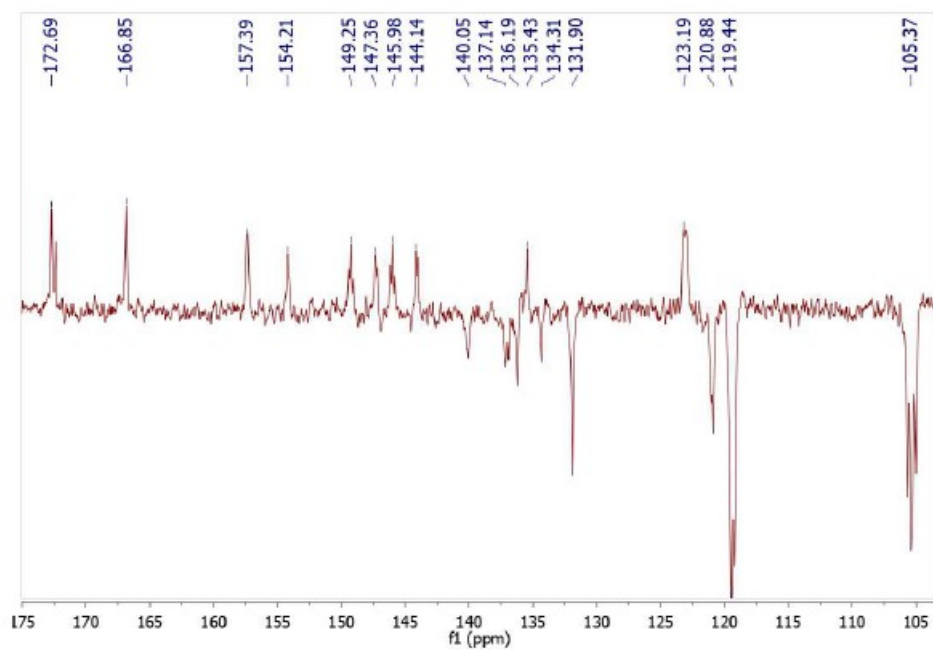
$^1\text{H-NMR}$ spectrum of **5** (400MHz/DMSO- d_6 /TMS/90°C)



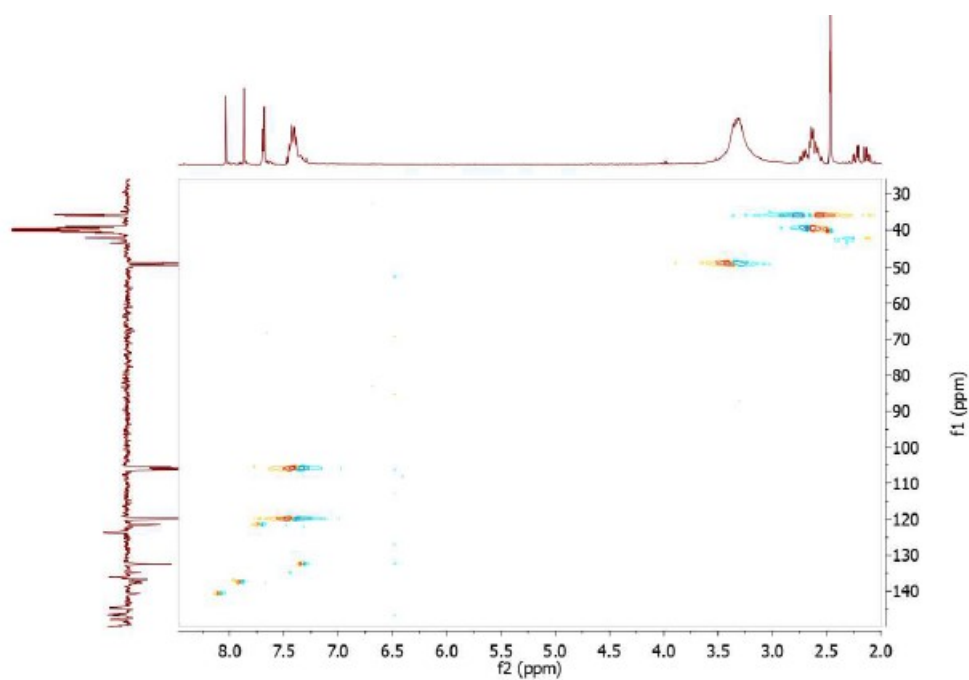
APT of **9** (100MHz/ DMSO-d₆/TMS/25°C)



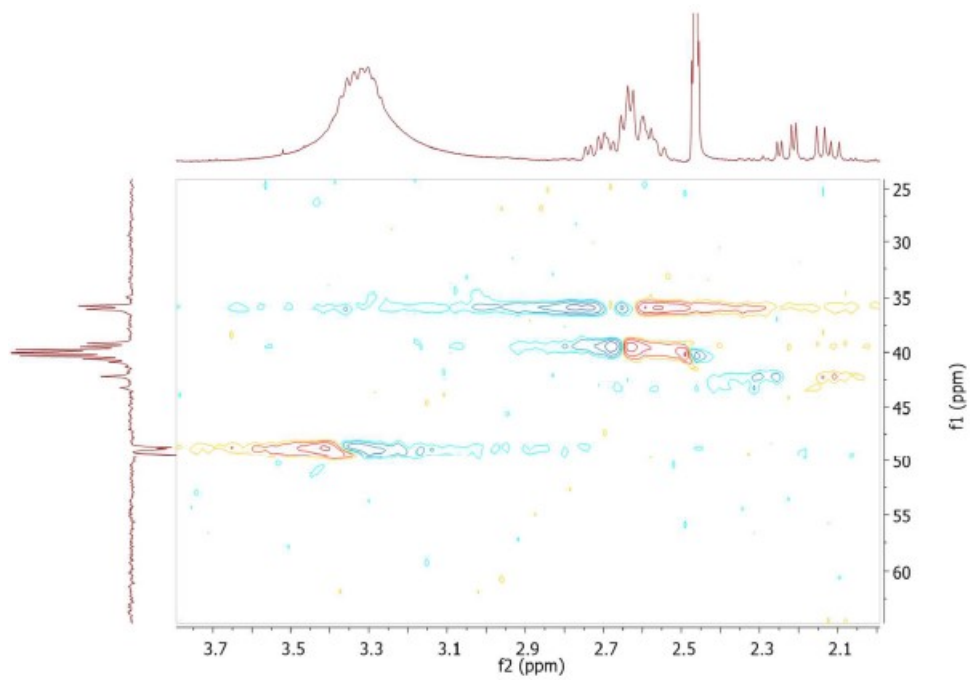
Expansion of APT of **9** (100MHz/ DMSO-d₆/TMS/25°C)



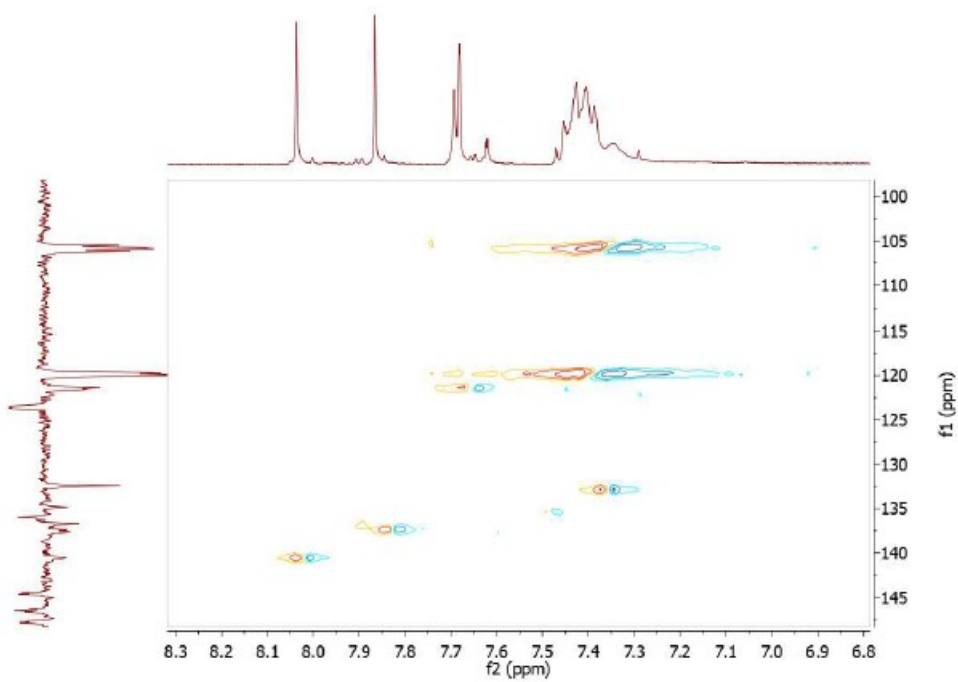
Expansion of APT of **9** (100MHz/ DMSO-d₆/TMS/25°C)



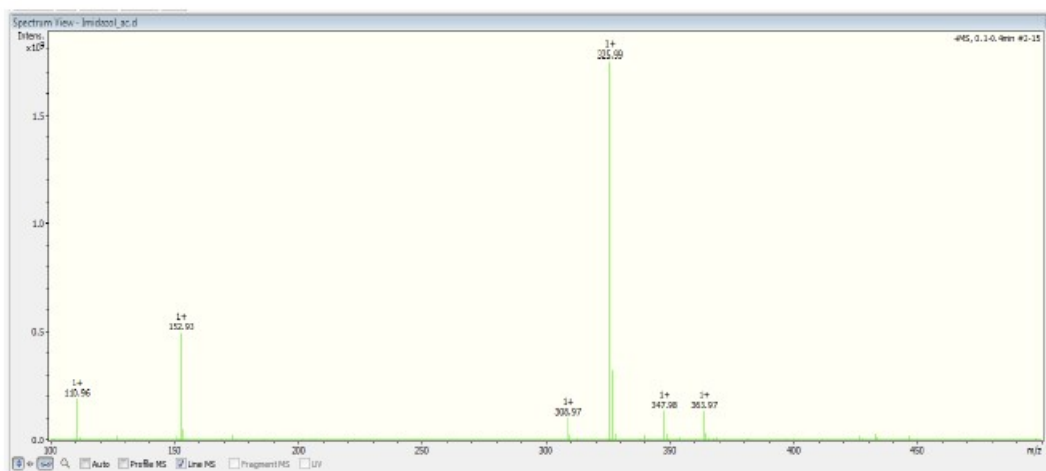
HSQC of **9** (DMSO-d₆/TMS/25°C)



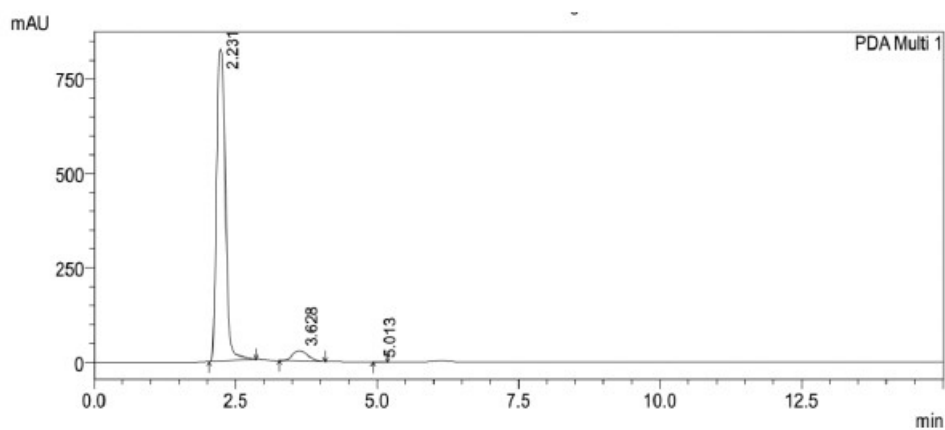
Expansion of HSQC of 9 (DMSO-d₆/TMS/25°C)



Expansion of HSQC of 9 (DMSO-d₆/TMS/25°C)



Mass spectrum of **9** in positive mode (ESI, direct injection)

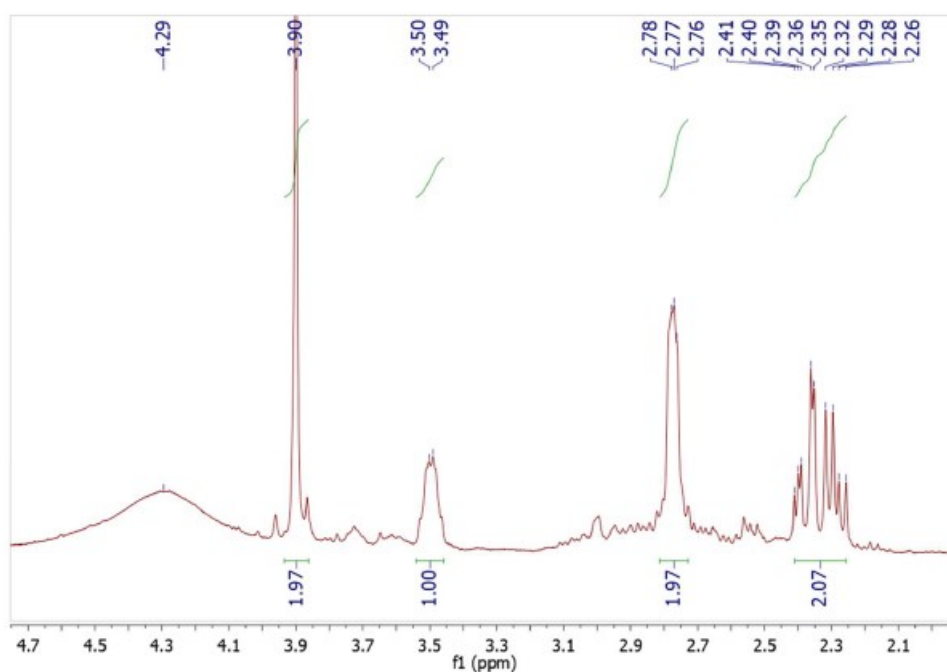
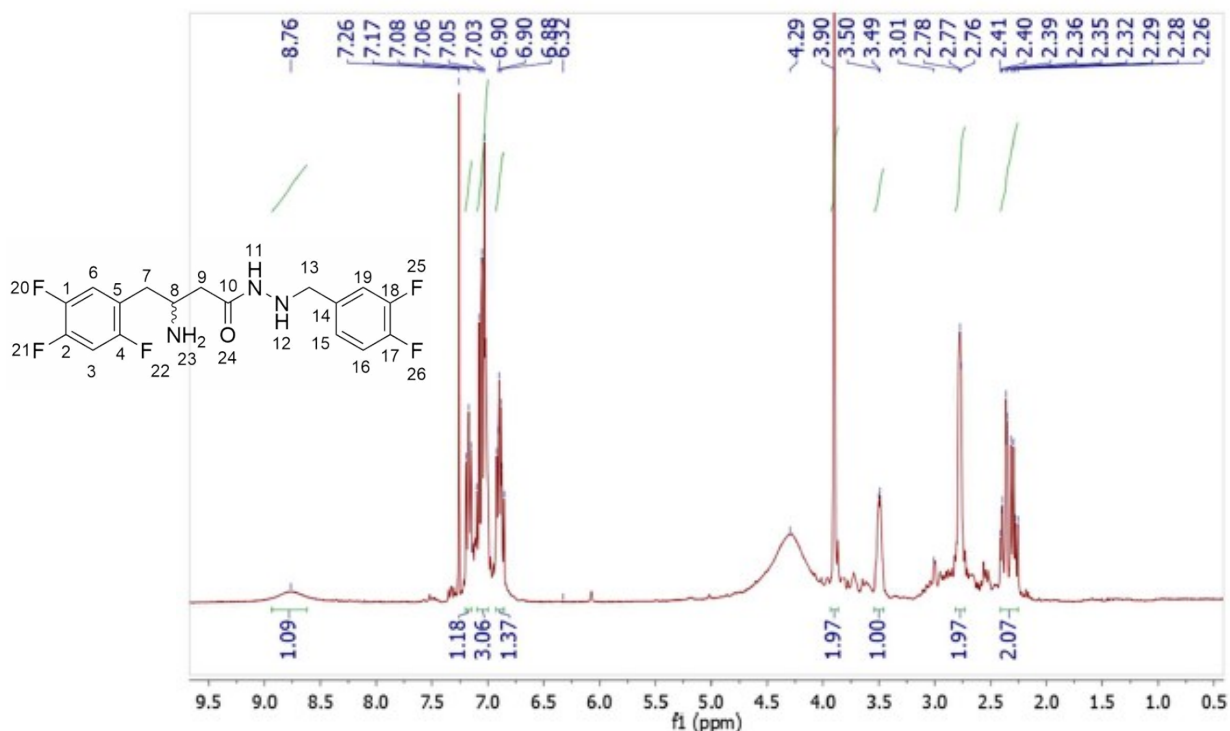


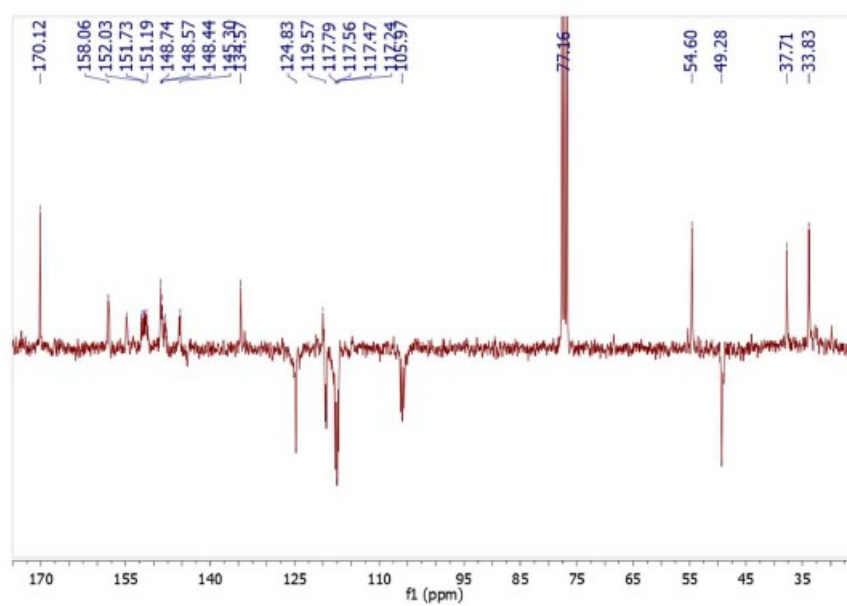
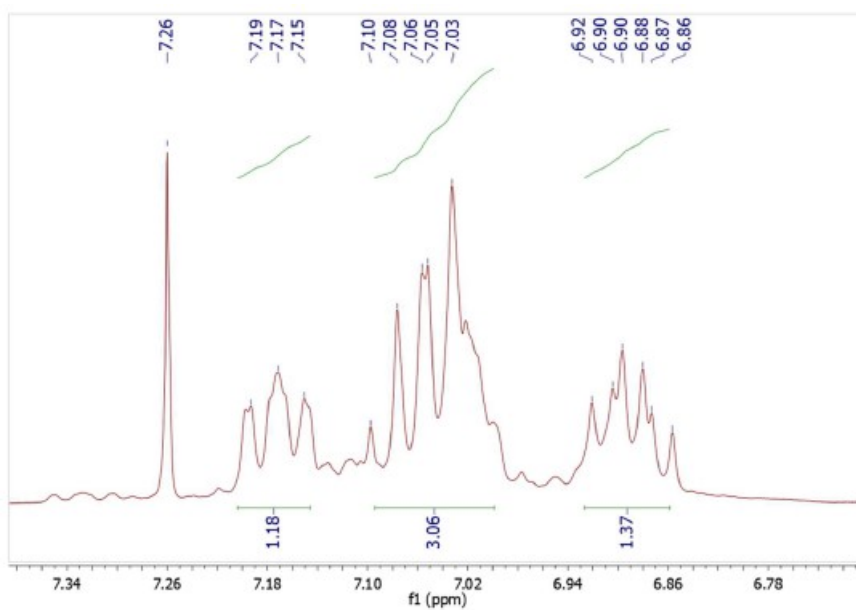
PDA Ch1 254nm 4nm

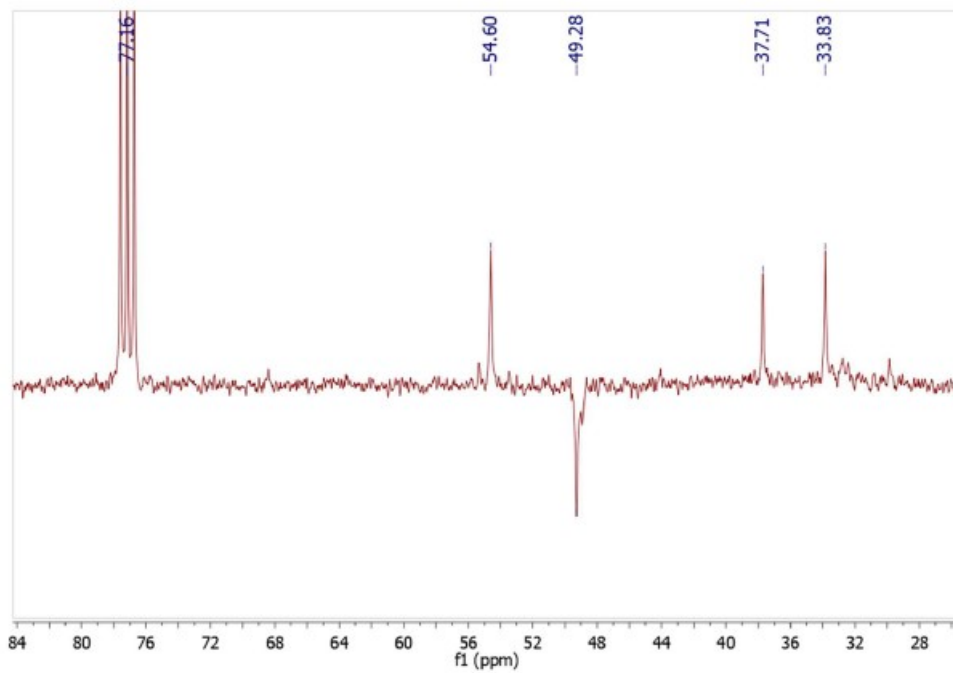
Peak#	Ret. Time	Area	Height	Area %	Height %
1	2.231	9084646	824921	95.231	97.022
2	3.628	454240	25234	4.762	2.968
3	5.013	716	84	0.008	0.010
Total		9539601	850239	100.000	100.000

HPLC Purity: Kromasil Column C18 [4,6 mm x 250 mm]; detector SPD-M20A [Diode Array]; flux: 1mL/min; injection volume: 20 μ L, mobile phase: 6:4 MeCN/H₂O (pH = 9).

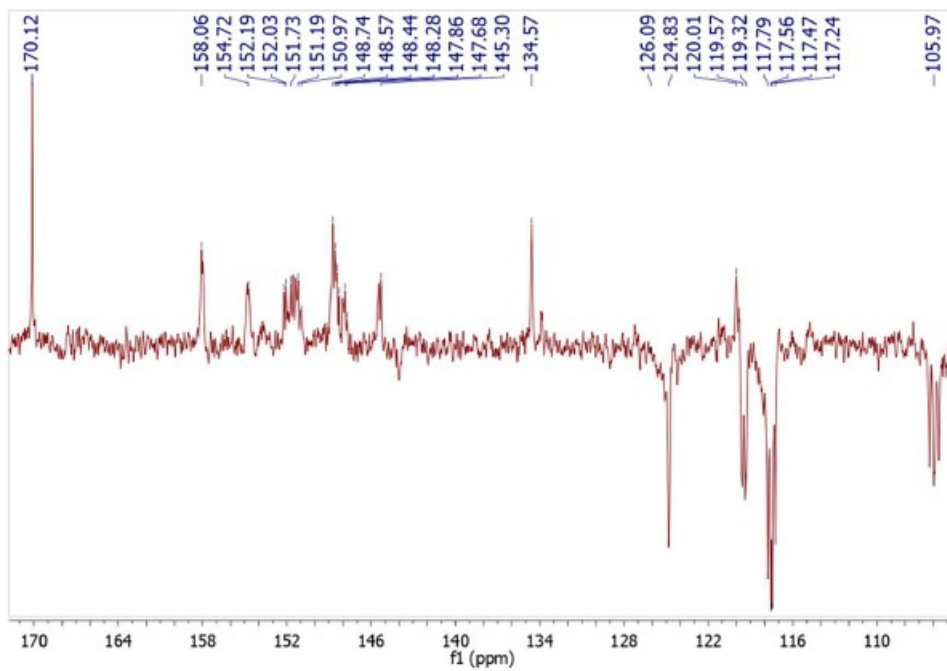
**3-amino-*N'*-(3,4-difluorobenzyl)-4-(2,4,5-trifluorophenyl)butanehydrazide:
LASSBio-2127 (13)**



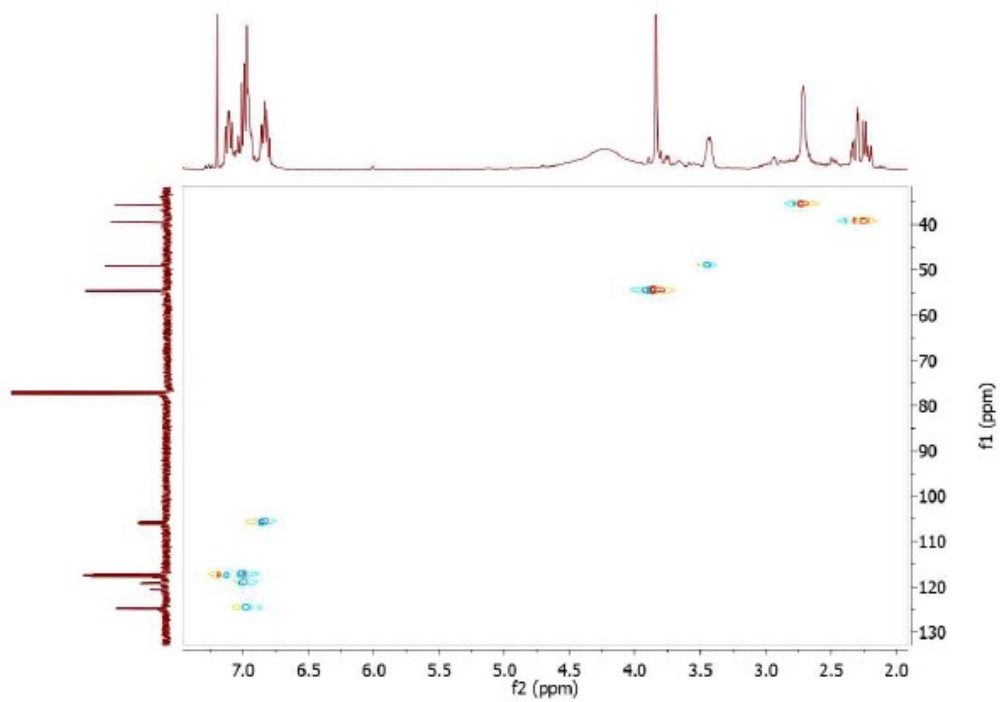




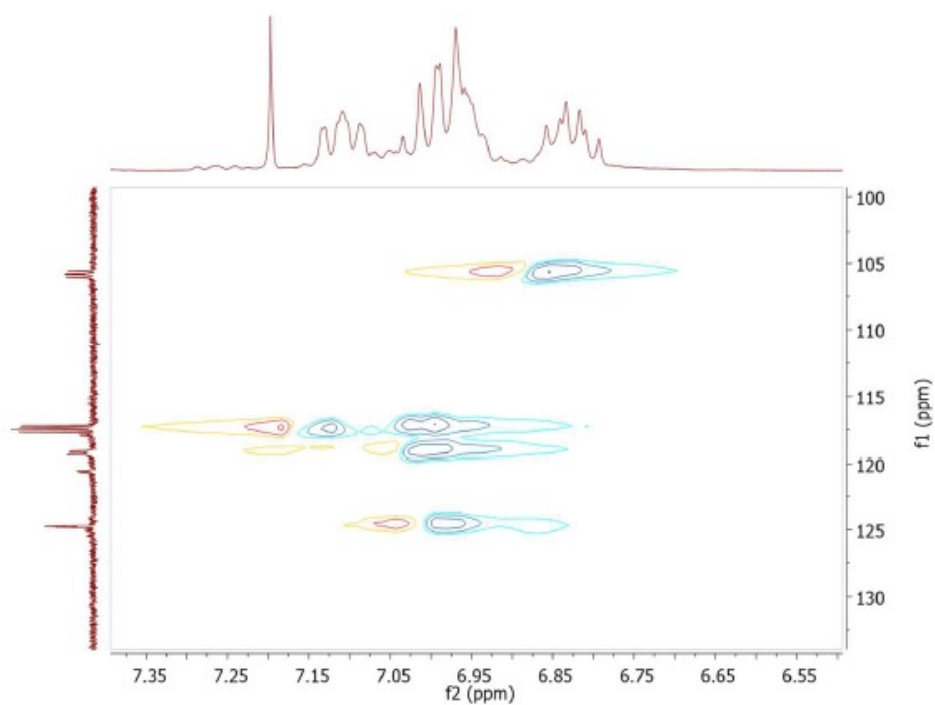
Expansion of APT of **13** (100MHz/CDCl₃/TMS/25°C)



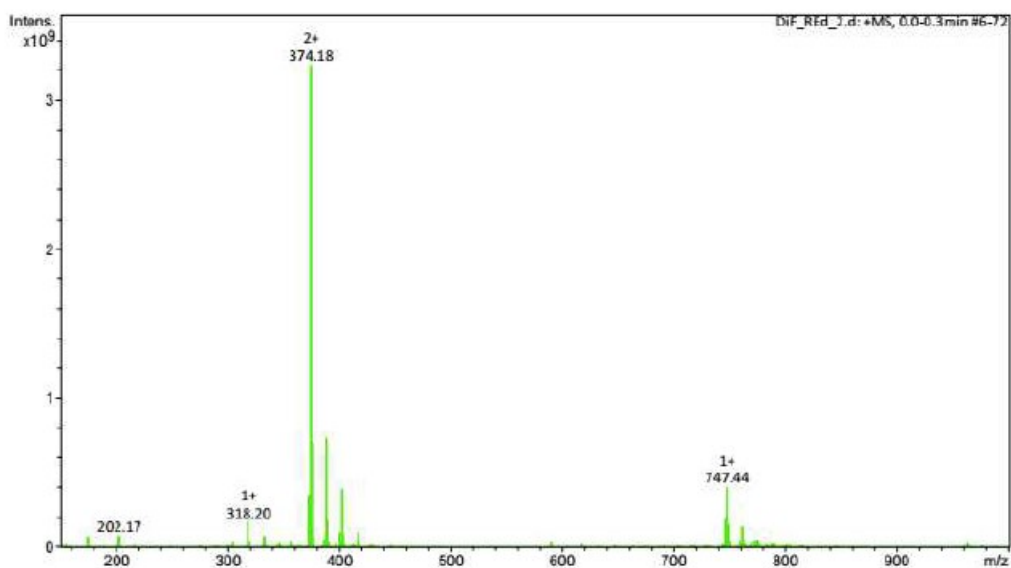
Expansion of APT of **13** (100MHz/CDCl₃/TMS/25°C)



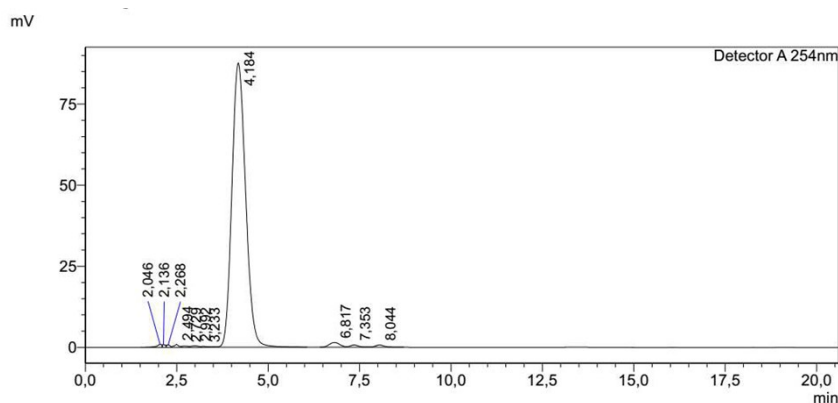
HSQC of **13** (CDCl₃/TMS/25°C)



Expansion of HSQC of **13** (CDCl₃/TMS/25°C)



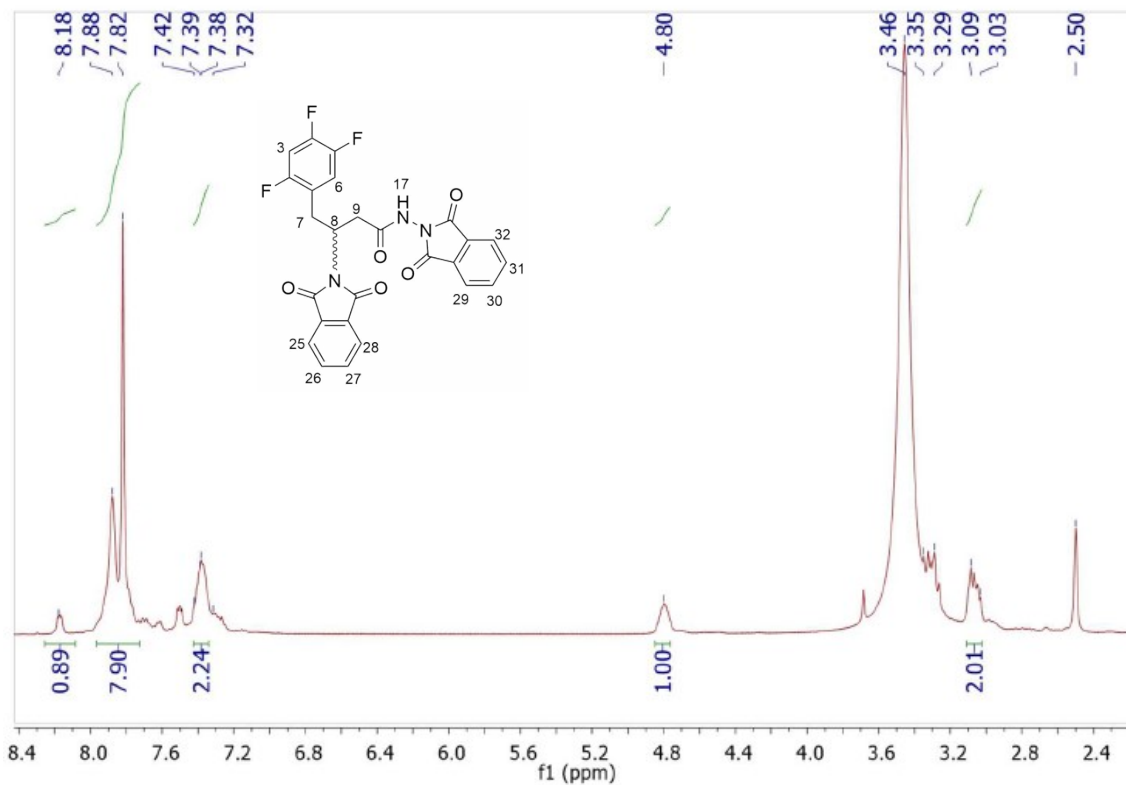
Mass spectrum of 5 in positive mode (ESI, direct injection)



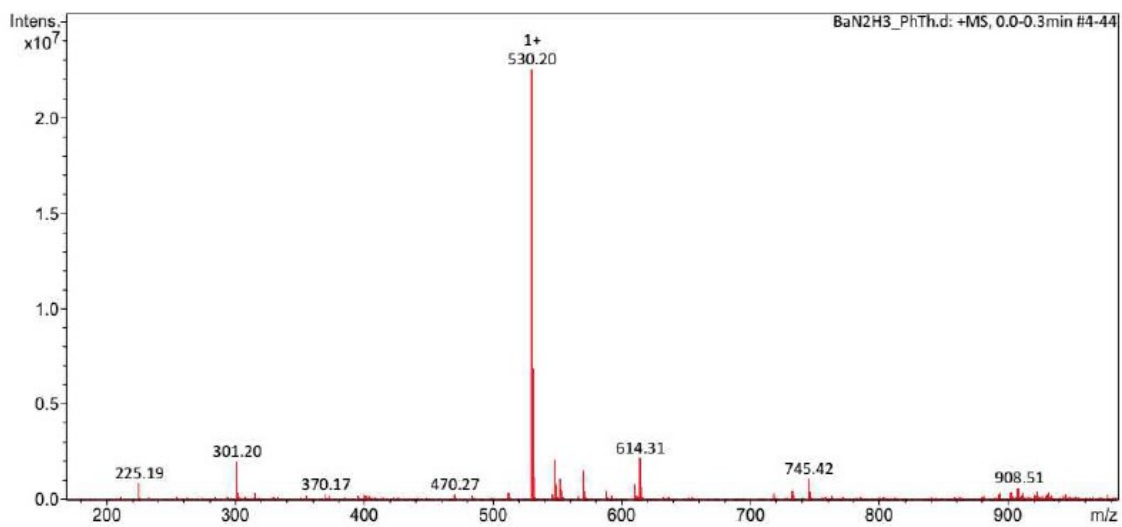
Peak#	Ret. Time	Area	Height	Area%	Height%	Area/Height
1	2,046	9001	897	0,379	0,945	10,035
2	2,136	4829	811	0,203	0,855	5,953
3	2,268	4965	781	0,209	0,823	6,355
4	2,494	7775	909	0,327	0,958	8,557
5	2,729	4673	384	0,197	0,405	12,156
6	2,992	6547	460	0,275	0,484	14,243
7	3,233	4026	276	0,169	0,291	14,576
8	4,184	2284548	87593	96,104	92,319	26,081
9	6,817	28322	1398	1,191	1,473	20,263
10	7,353	10605	679	0,446	0,716	15,609
11	8,044	11880	692	0,500	0,730	17,164
Total		2377172	94880	100,000	100,000	

HPLC Purity: Kromasil Column C18 [4,6 mm x 250 mm]; detector SPD-M20A [Diode Array]; flux: 1mL/min; injection volume: 20 μ L, mobile phase: 6:4 MeCN/H₂O (pH = 9).

***N*,3-bis(1,3-dioxisoindolin-2-yl)-4-(2,4,5-trifluorophenyl)butanamide (22a)**

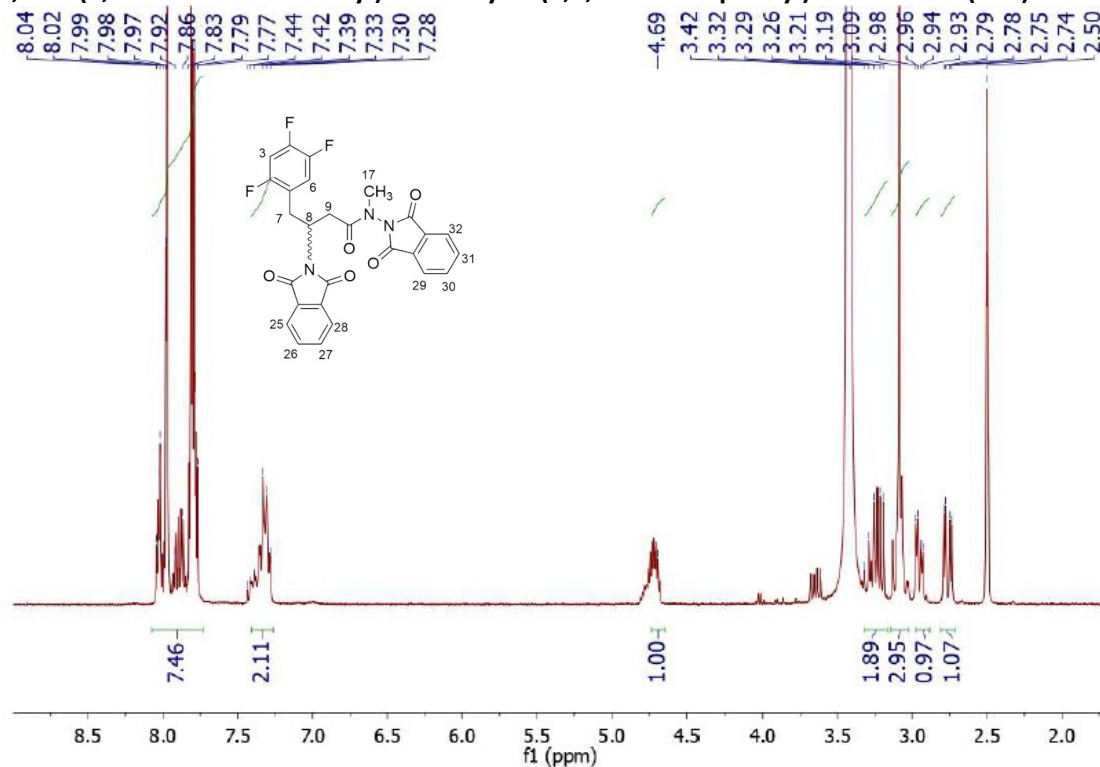


¹H-NMR spectrum of **22a** (400MHz/CDCl₃/TMS/25°C)



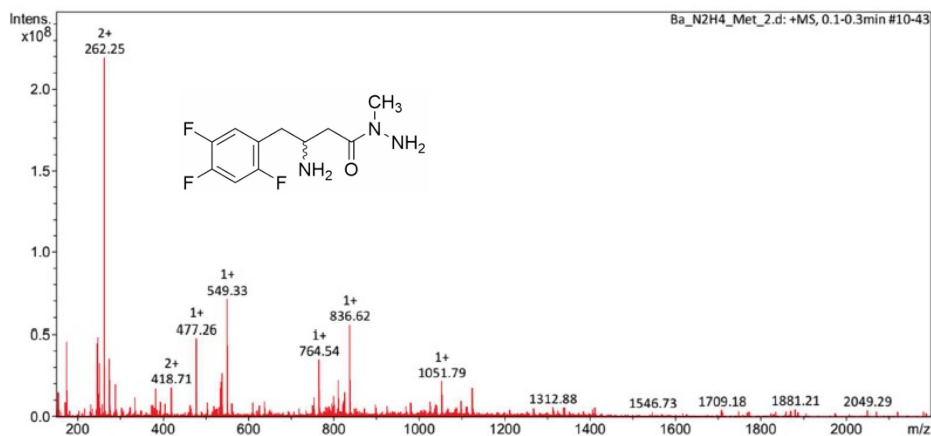
Mass spectrum of **22a** in positive mode (ESI, direct injection)

***N*,3-bis(1,3-dioxisoindolin-2-yl)-*N*-methyl-4-(2,4,5-trifluorophenyl)butanamide (22b)**



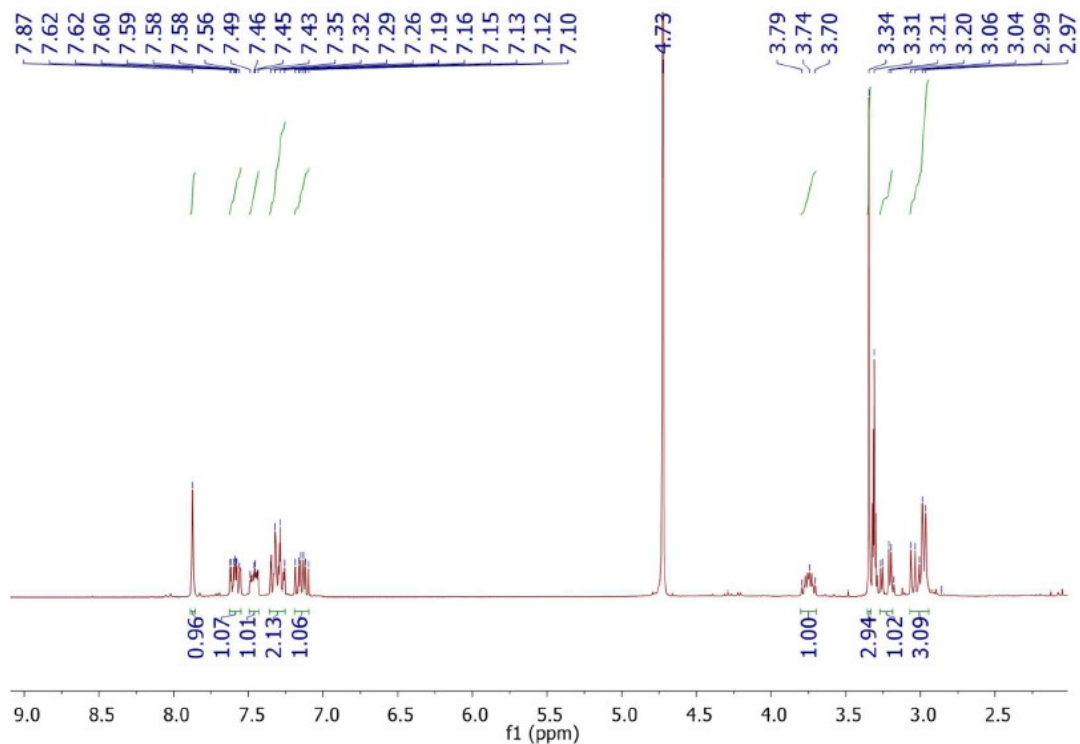
¹H-NMR spectrum of **22b** (400MHz/CDCl₃/TMS/25°C)

3-amino-*N*-methyl-4-(2,4,5-trifluorophenyl)butanehydrazide (22)

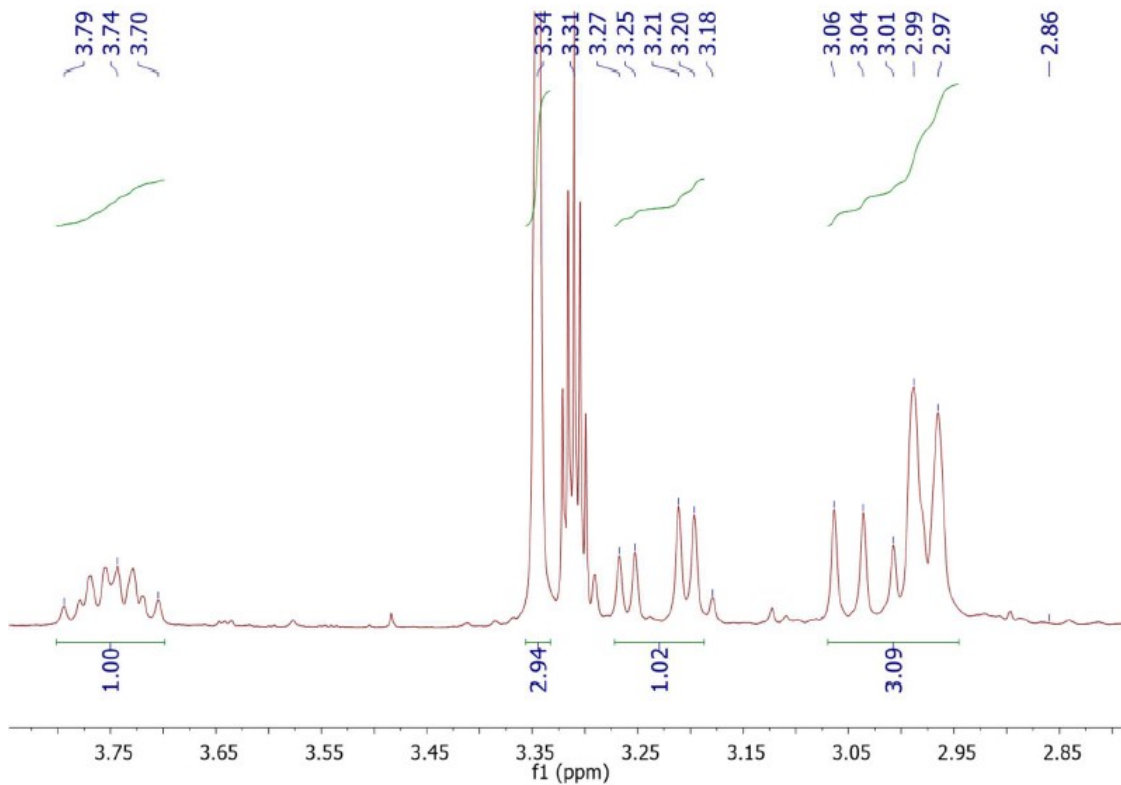


Mass spectrum of **22** in positive mode (ESI, direct injection)

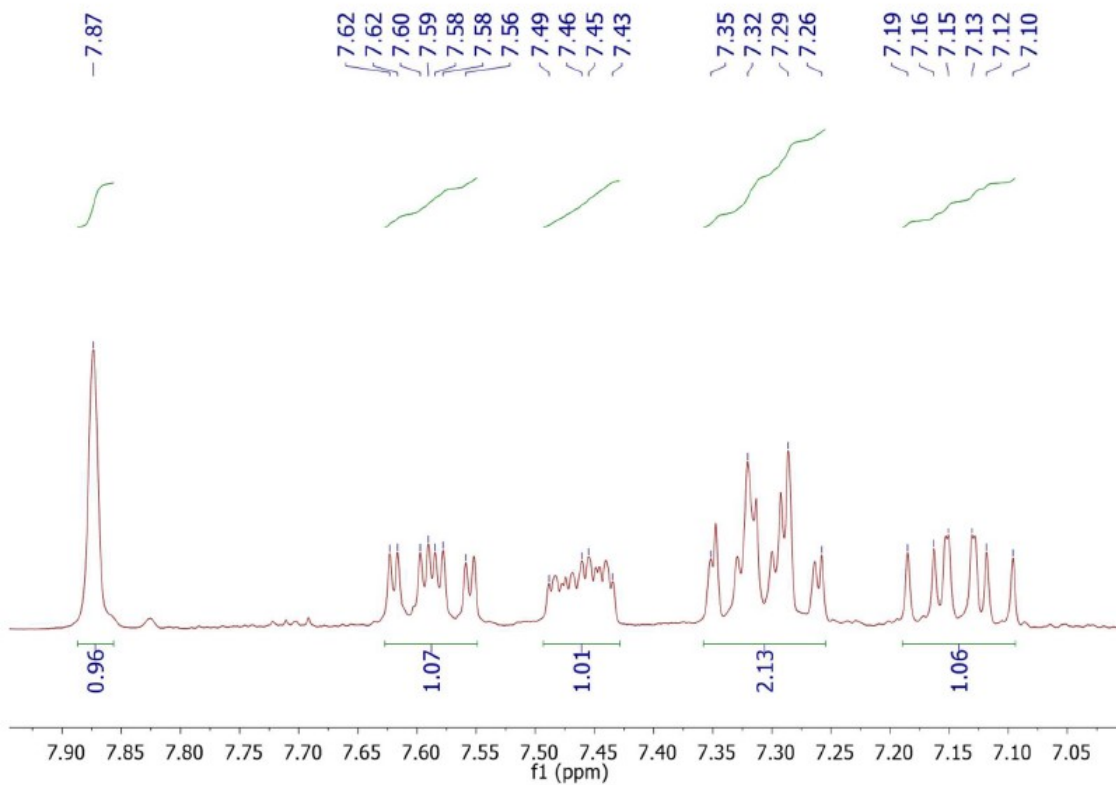
**3-amino-N'-(3,4-difluorobenzyl)-N-methyl-4-(2,4,5-trifluorophenyl)butanehydrazide:
LASSBio-2128 (14)**



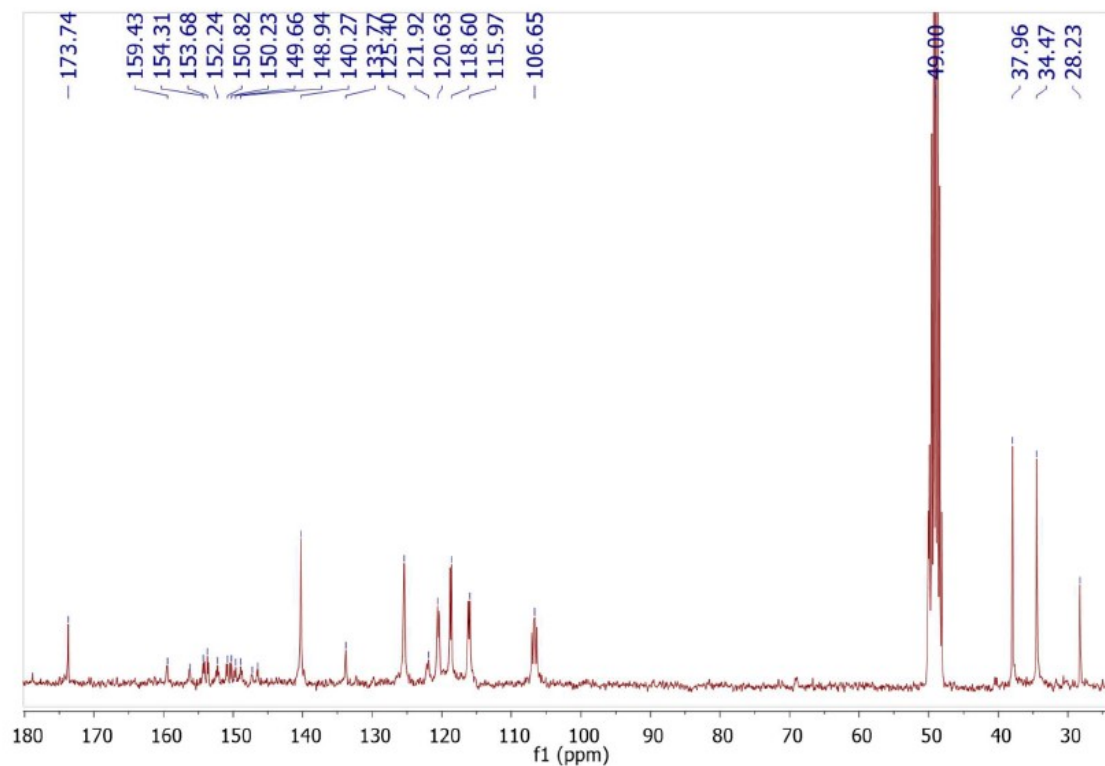
¹H-NMR spectrum of **14** (400MHz/CD₃OD/TMS/25°C)



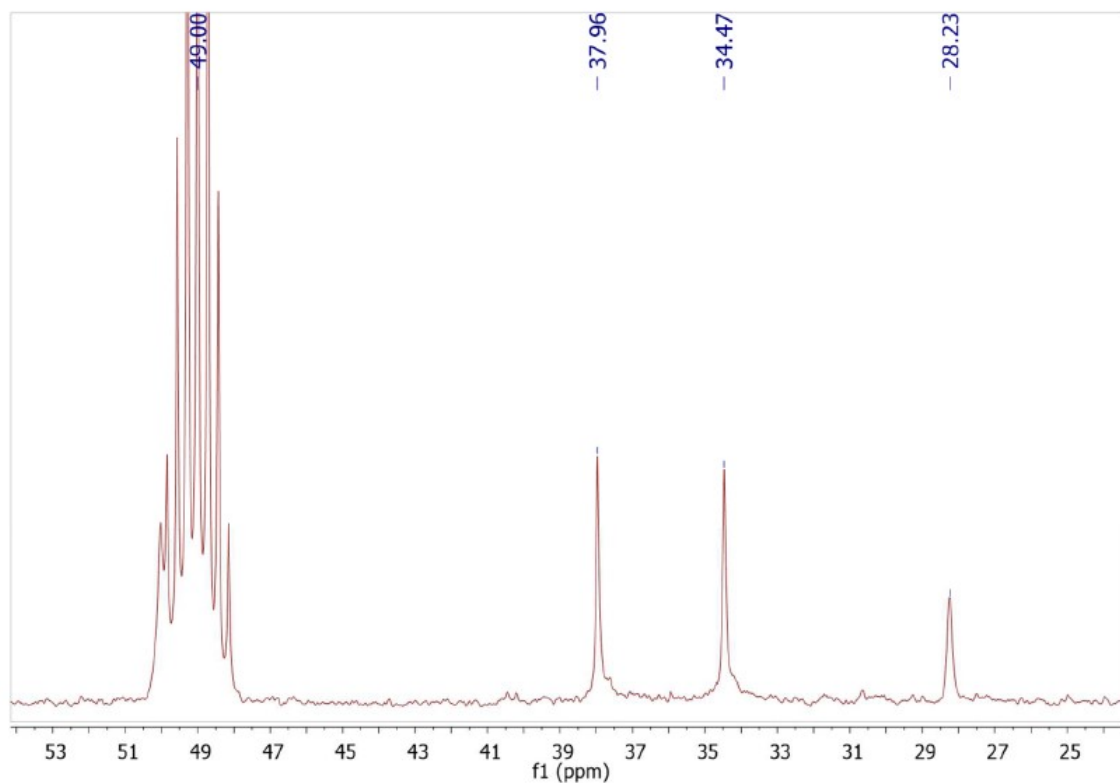
Expansion of ¹H-NMR spectrum of **14** (400MHz/CD₃OD/TMS/25°C)



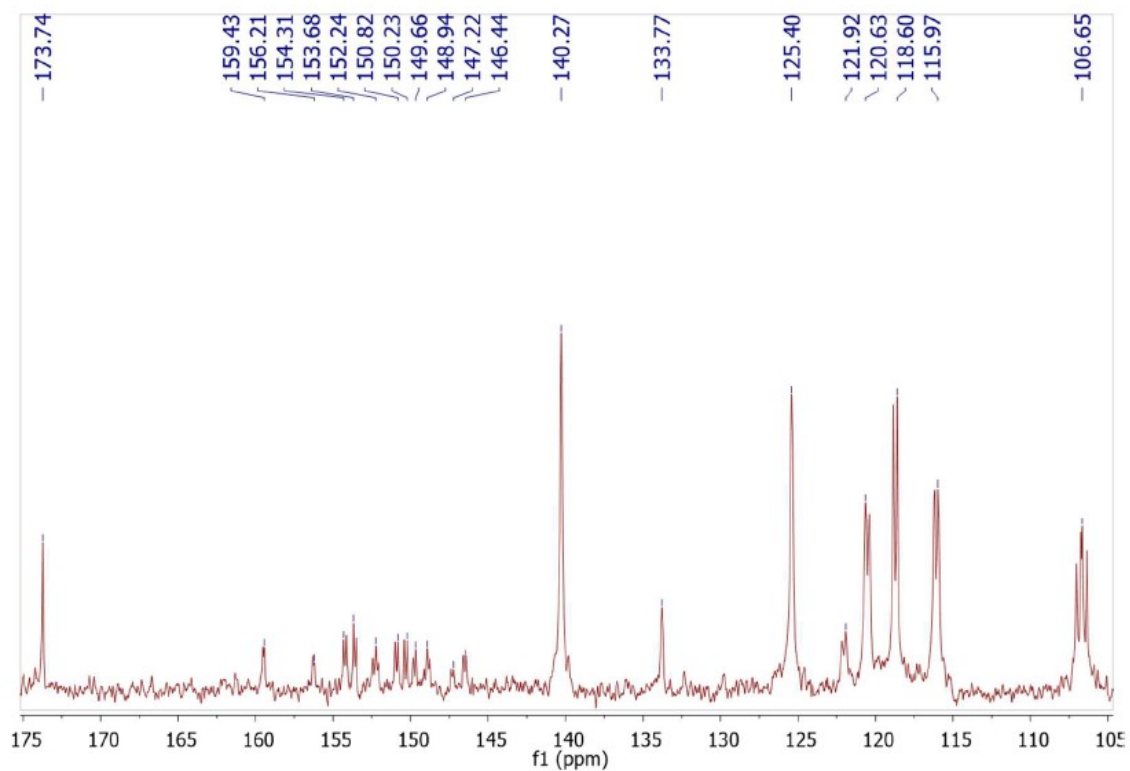
Expansion of $^1\text{H-NMR}$ spectrum of **14** (400MHz/ $\text{CD}_3\text{OD/TMS/25}^\circ\text{C}$)



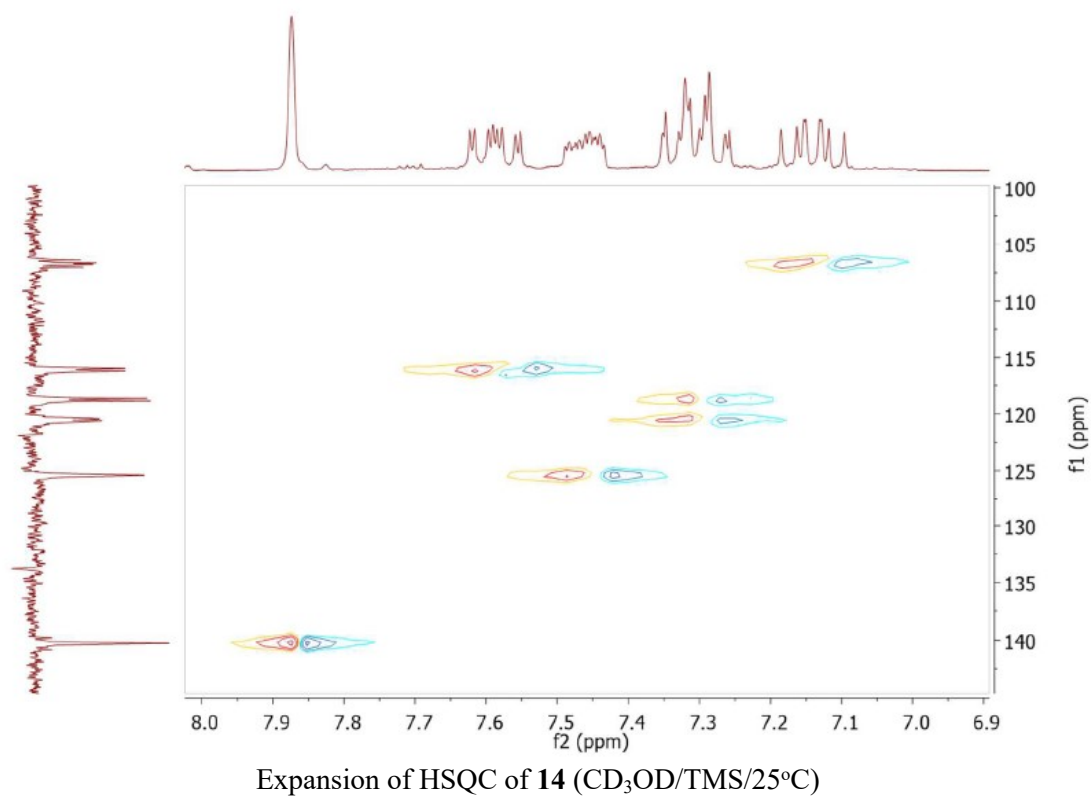
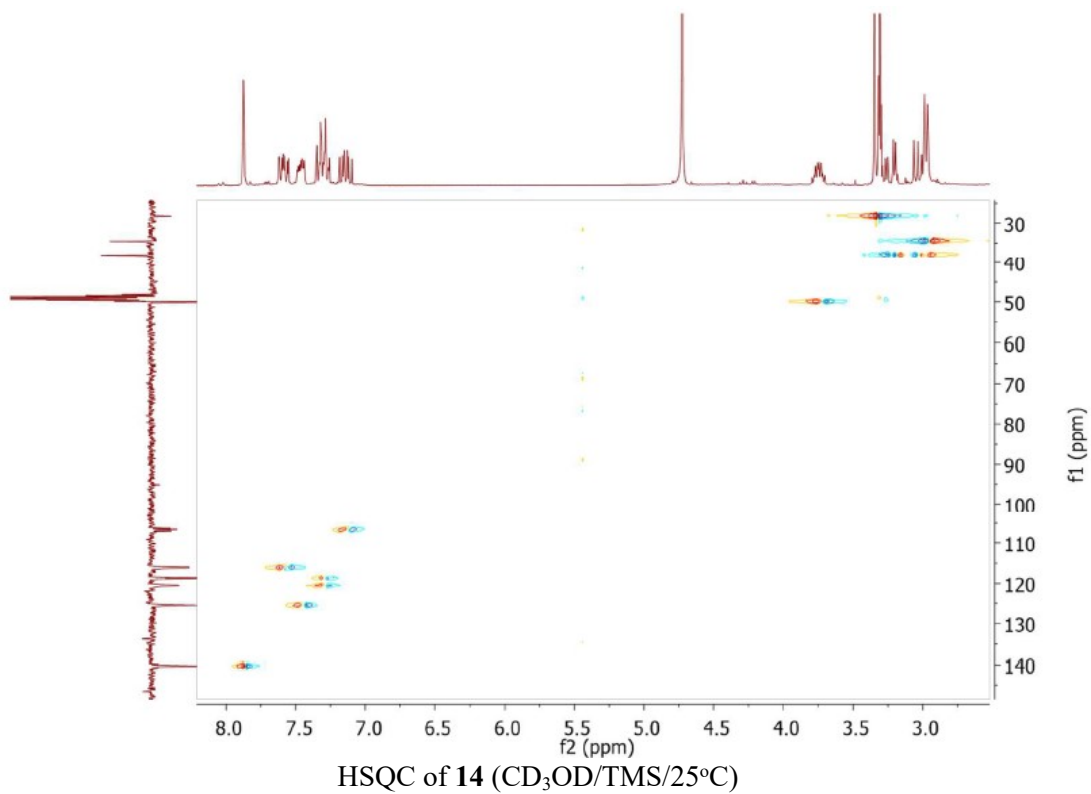
APT of **14** (100MHz/ $\text{CD}_3\text{OD/TMS/25}^\circ\text{C}$)



Expansion of APT of **14** (100MHz/CD₃OD/TMS/25°C)



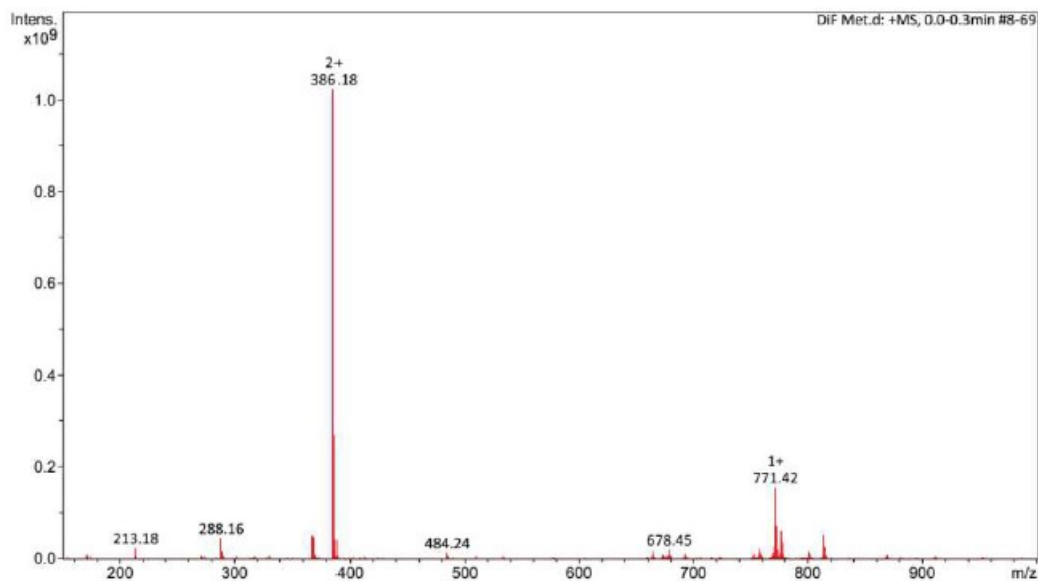
Expansion of APT of **14** (100MHz/CD₃OD/TMS/25°C)



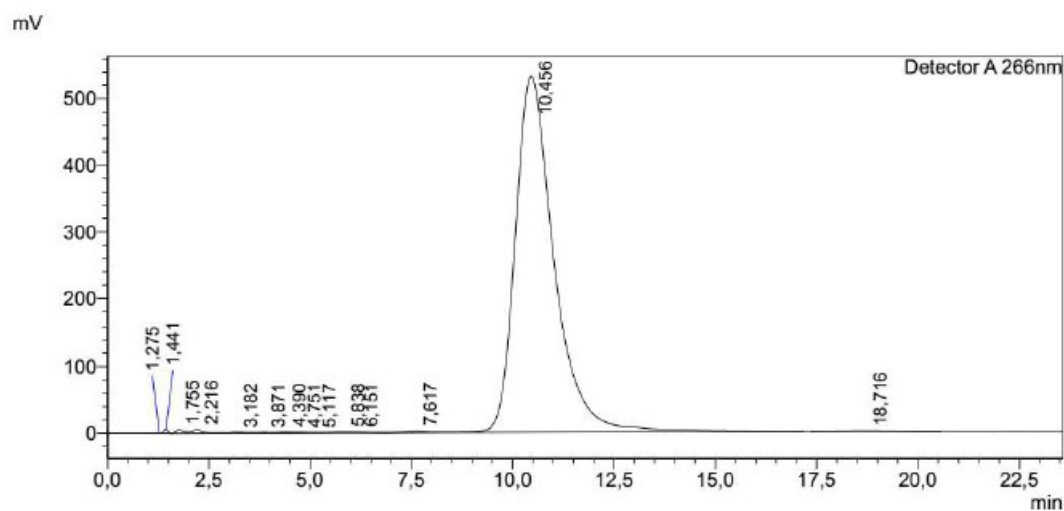
a)

b)

- a)** $^1\text{H-NMR}$ NOE-diff (400 MHz, CD_3OD) spectrum of **14**. Signal irradiated δH 7.86 (N=CH).
b) $^1\text{H-NMR}$ NOE-diff (400 MHz, CD_3OD) spectrum of **14**. Signal irradiated δH 3.36 (N- CH_3).



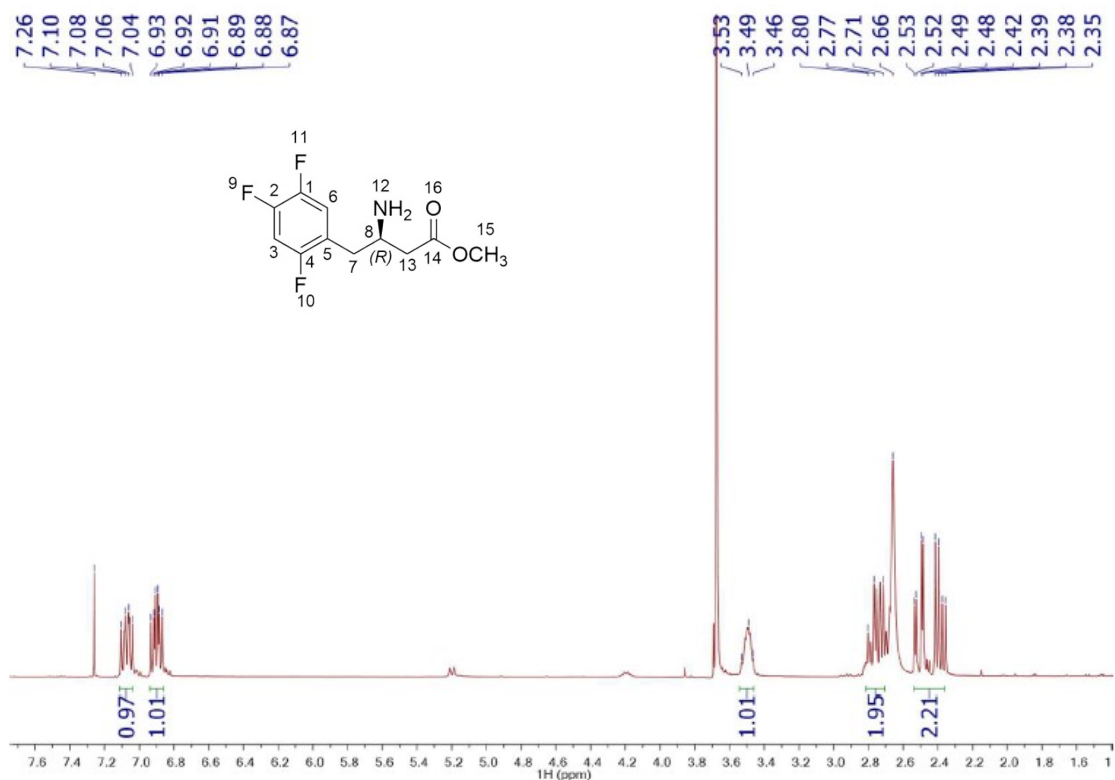
Mass spectrum of **14** in positive mode (ESI, direct injection)



Detector A 266nm					
Peak#	Ret. Time	Area	Height	Conc.	Area%
1	1,275	1213	196	0,000	0,003
2	1,441	39974	7253	0,000	0,111
3	1,755	65529	5738	0,000	0,181
4	2,216	101399	5849	0,000	0,281
5	3,182	39385	1402	0,000	0,109
6	3,871	29020	1003	0,000	0,080
7	4,390	38983	1483	0,000	0,108
8	4,751	19263	915	0,000	0,053
9	5,117	6927	573	0,000	0,019
10	5,838	42894	1366	0,000	0,119
11	6,151	30310	1285	0,000	0,084
12	7,617	97735	2363	0,000	0,271
13	10,456	35498195	532302	0,000	98,305
14	18,716	99490	1085	0,000	0,276
Total		36110318	562814		100,000

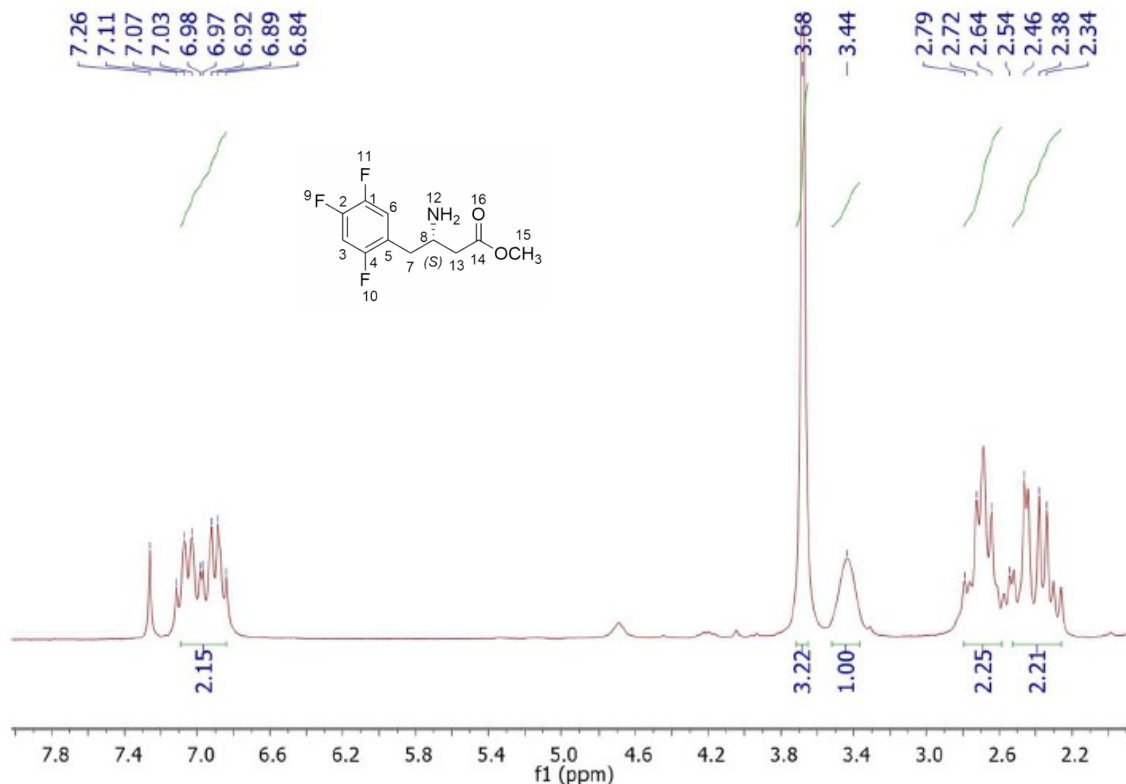
HPLC Purity: Kromasil Column C18 [4,6 mm x 250 mm]; detector SPD-M20A [Diode Array]; flux: 1mL/min; injection volume: 20 μ L, mobile phase: 6:4 MeCN/H₂O (pH = 9).

(R)-methyl 3-amino-4-(2,4,5-trifluorophenyl)butanoate (20-(R))

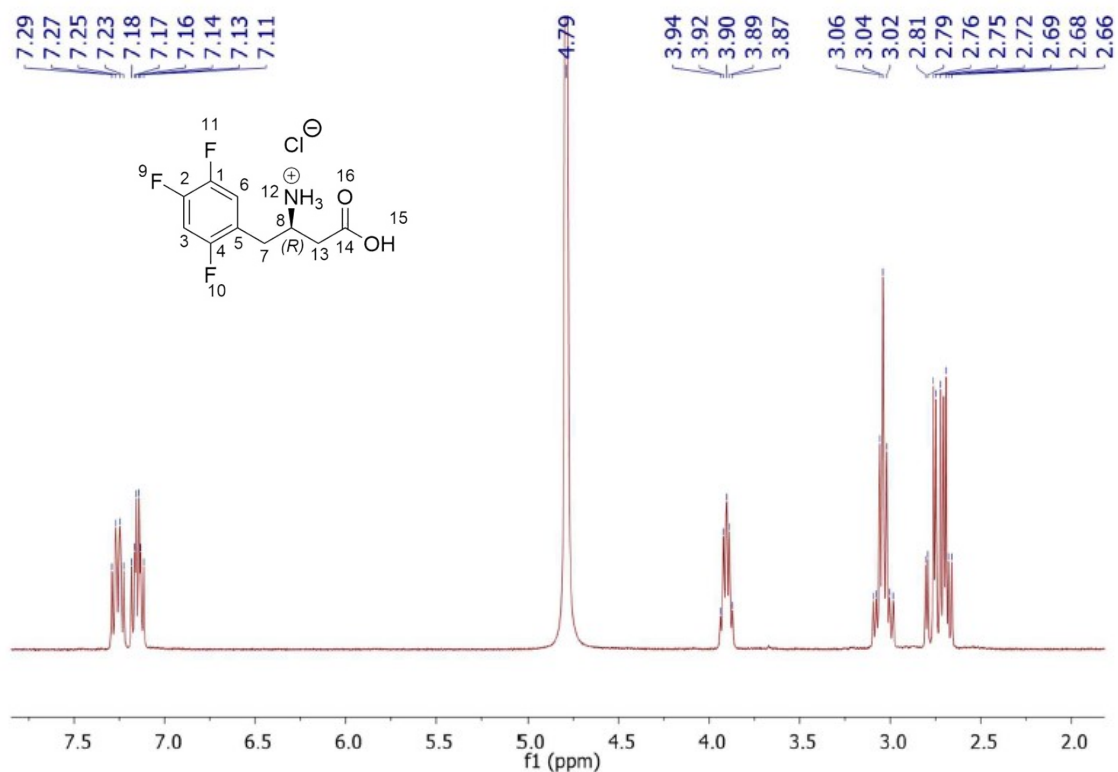


¹H-NMR spectrum of **20-(R)** (400MHz/CDCl₃/TMS/25°C)

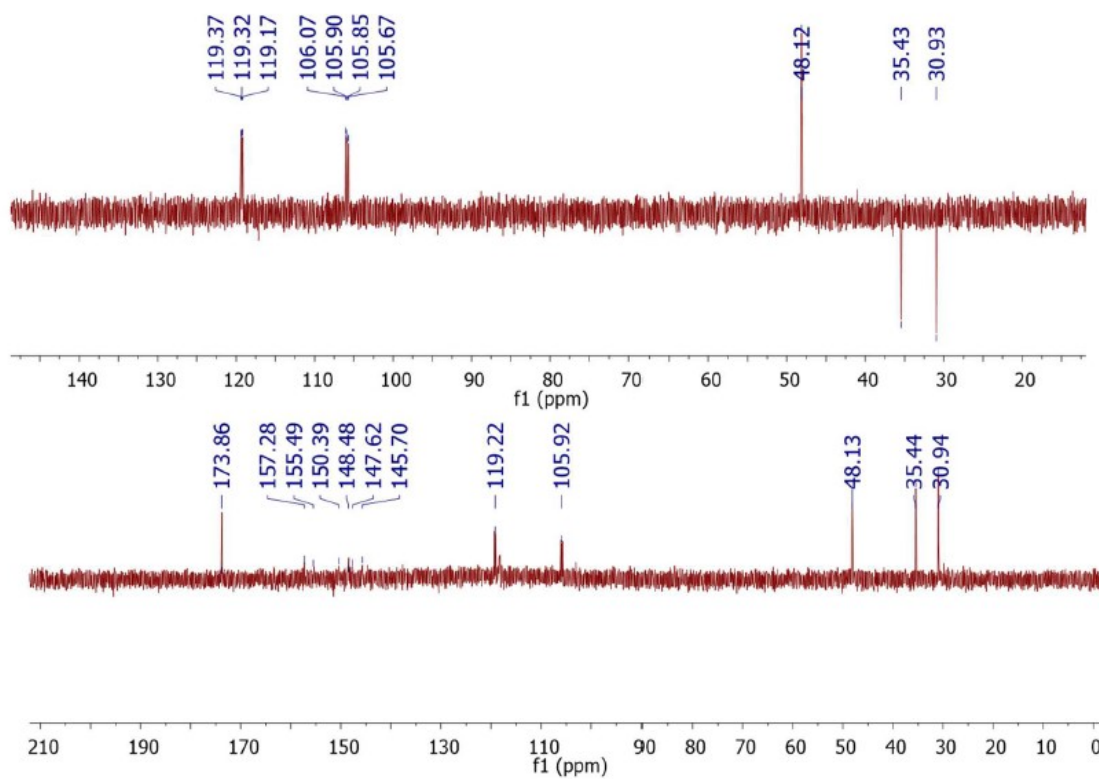
(S)-methyl 3-amino-4-(2,4,5-trifluorophenyl)butanoate (20-(S))



¹H-NMR spectrum of **20-(S)** (400MHz/CDCl₃/TMS/25°C)
(R)-1-carboxy-3-(2,4,5-trifluorophenyl)propan-2-aminium chloride (20a)

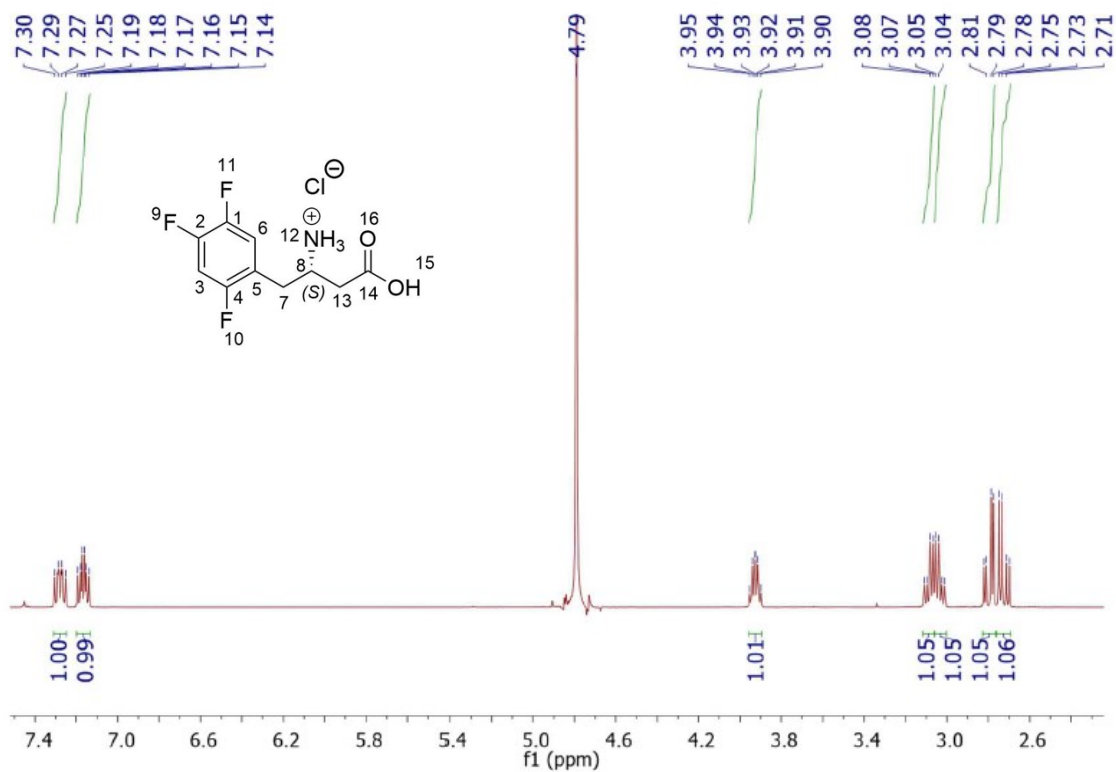


¹H-NMR spectrum of **20a** (400MHz/CDCl₃/TMS/25°C)

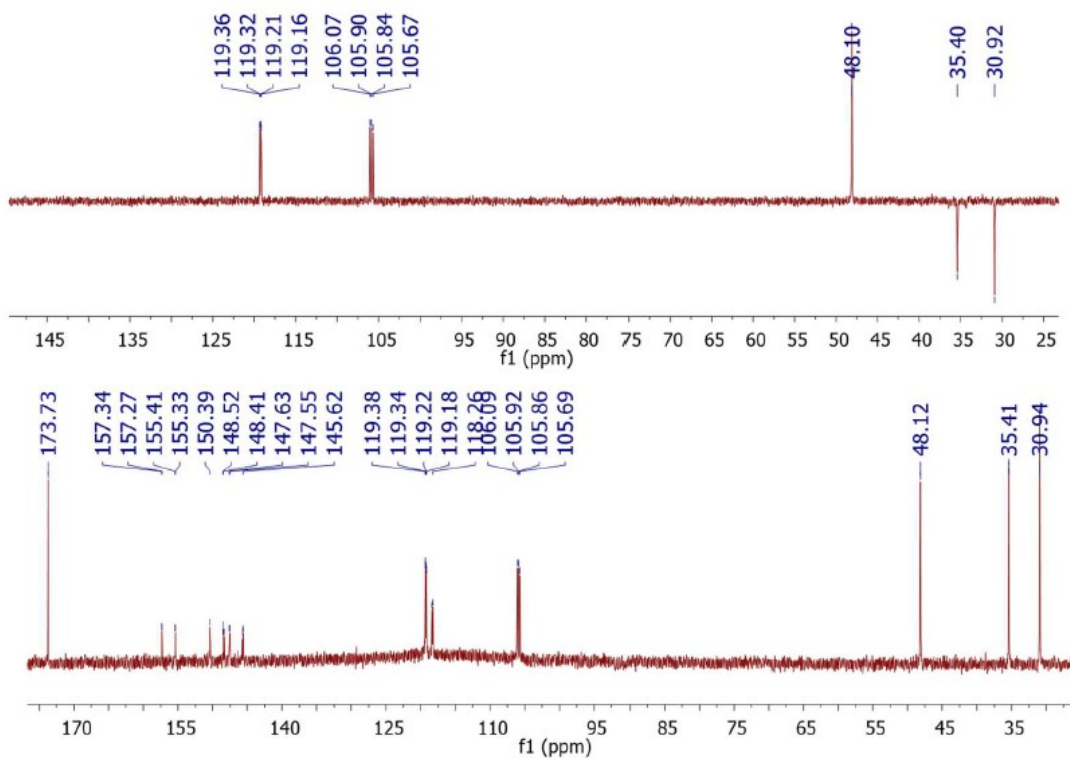


¹³C-NMR and DEPT of **20a** (100MHz/CDCl₃/TMS/25°C)

(S)-1-carboxy-3-(2,4,5-trifluorophenyl)propan-2-aminium chloride (20b)

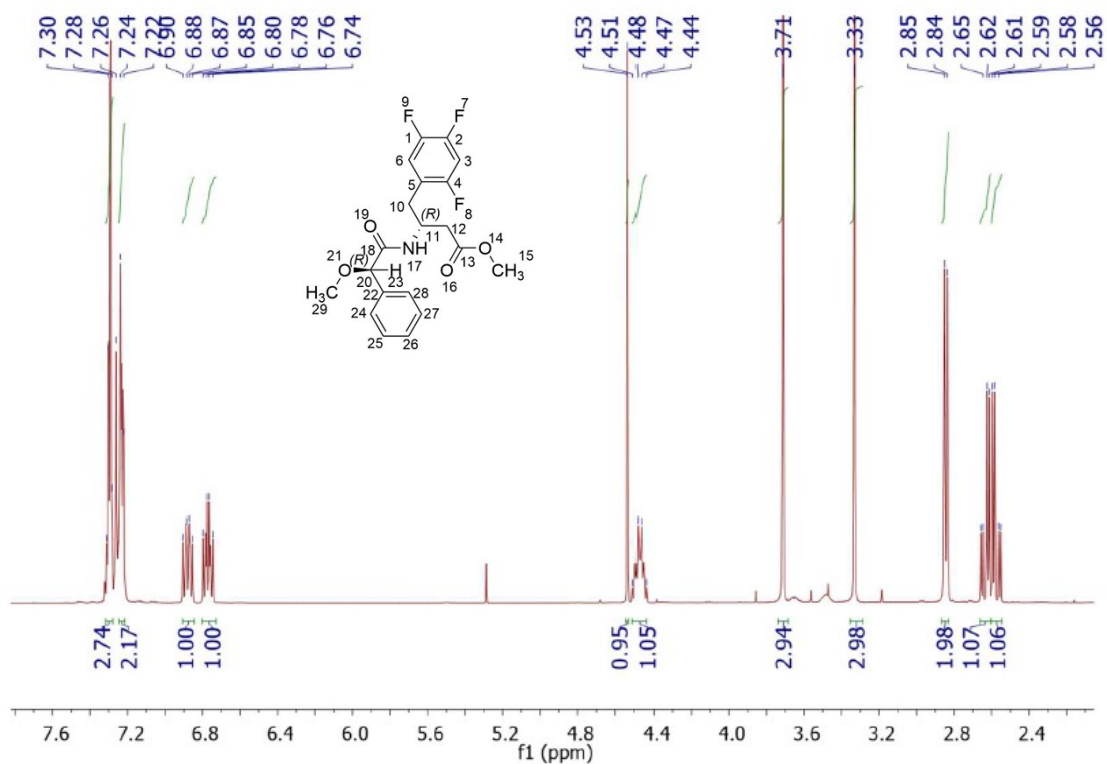


¹H-NMR spectrum of **20b** (400MHz/CDCl₃/TMS/25°C)

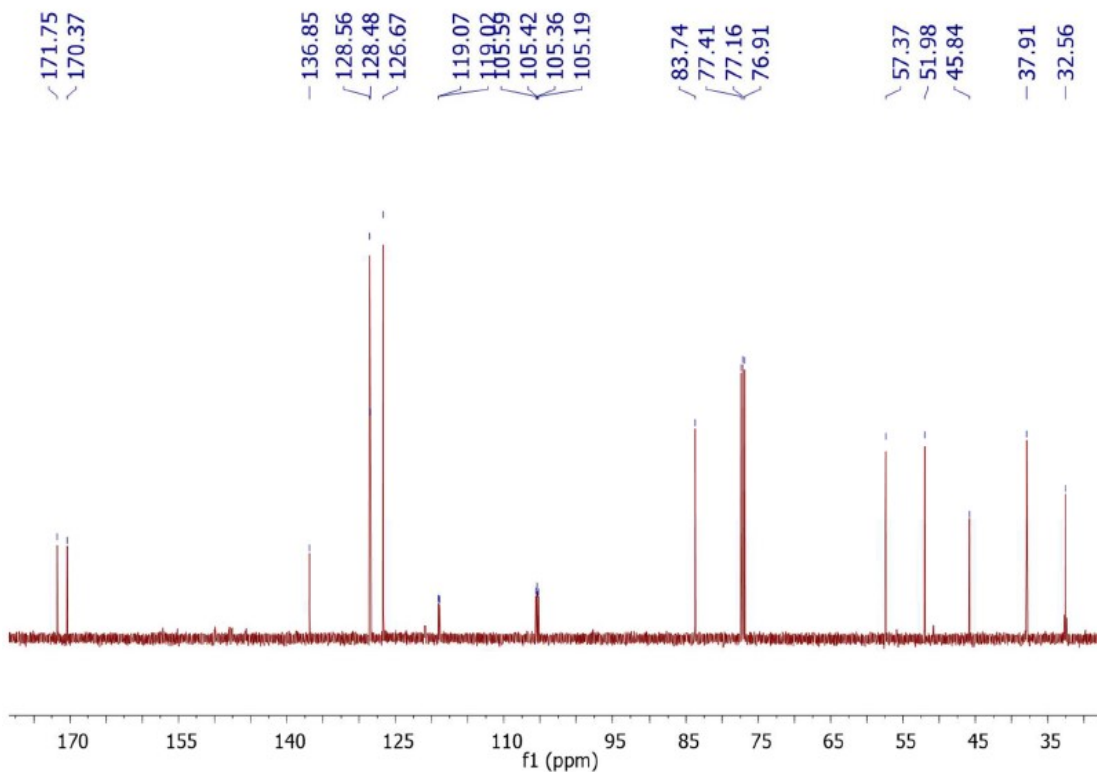


¹³C-NMR and DEPT of **20b** (100MHz/CDCl₃/TMS/25°C)

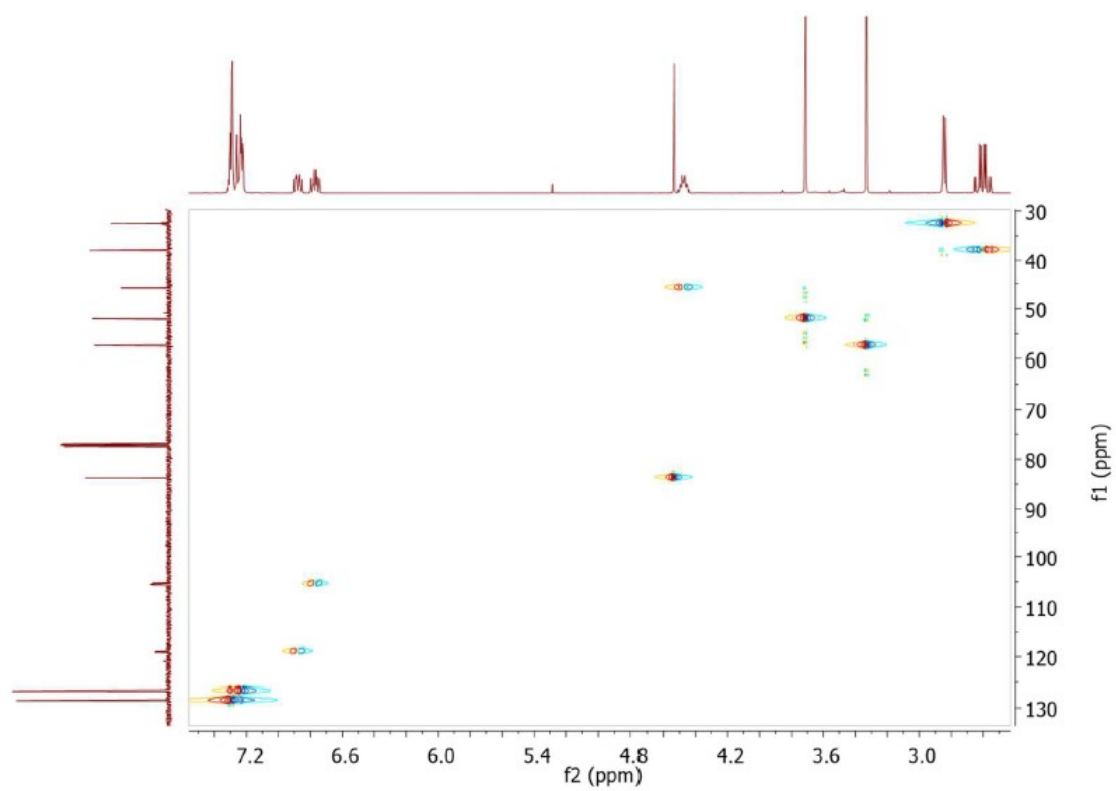
(R)-methyl 3-((R)-2-methoxy-2-phenylacetamido)-4-(2,4,5-trifluorophenyl)butanoate (23)



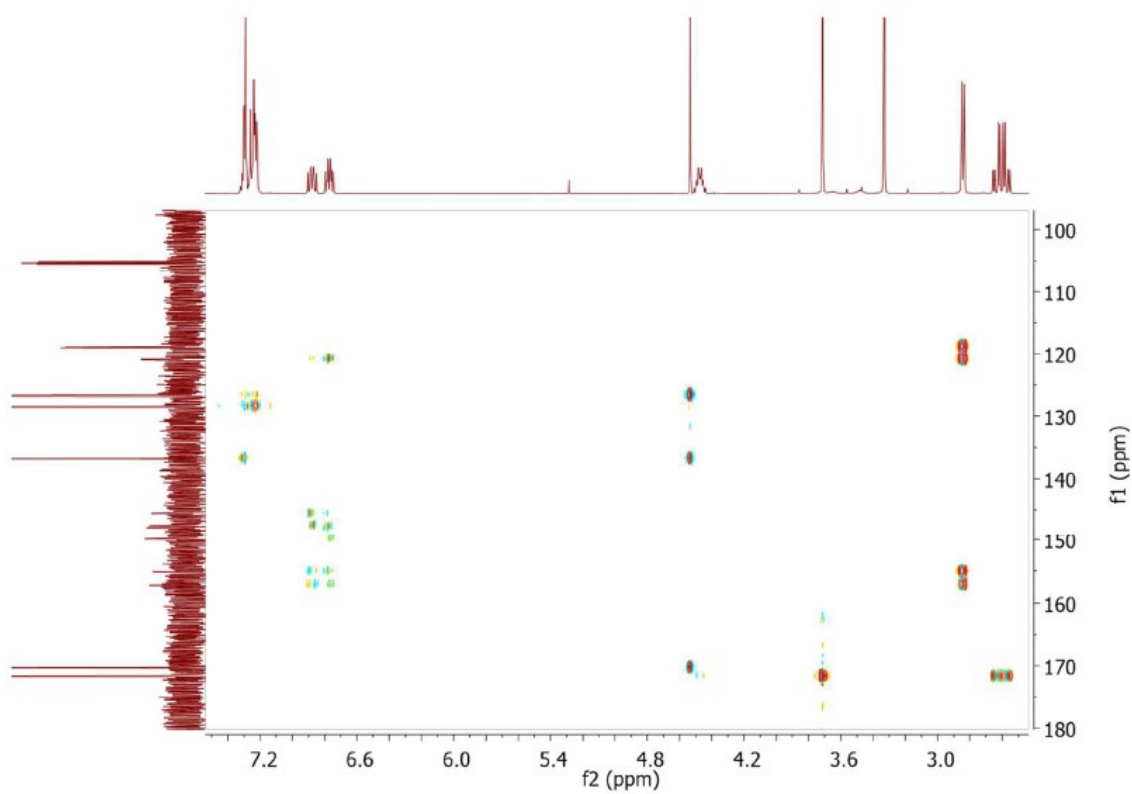
¹H-NMR spectrum of **23** (400MHz/CDCl₃/TMS/25°C)



¹³C-NMR spectrum of **23** (100MHz/CDCl₃/TMS/25°C)

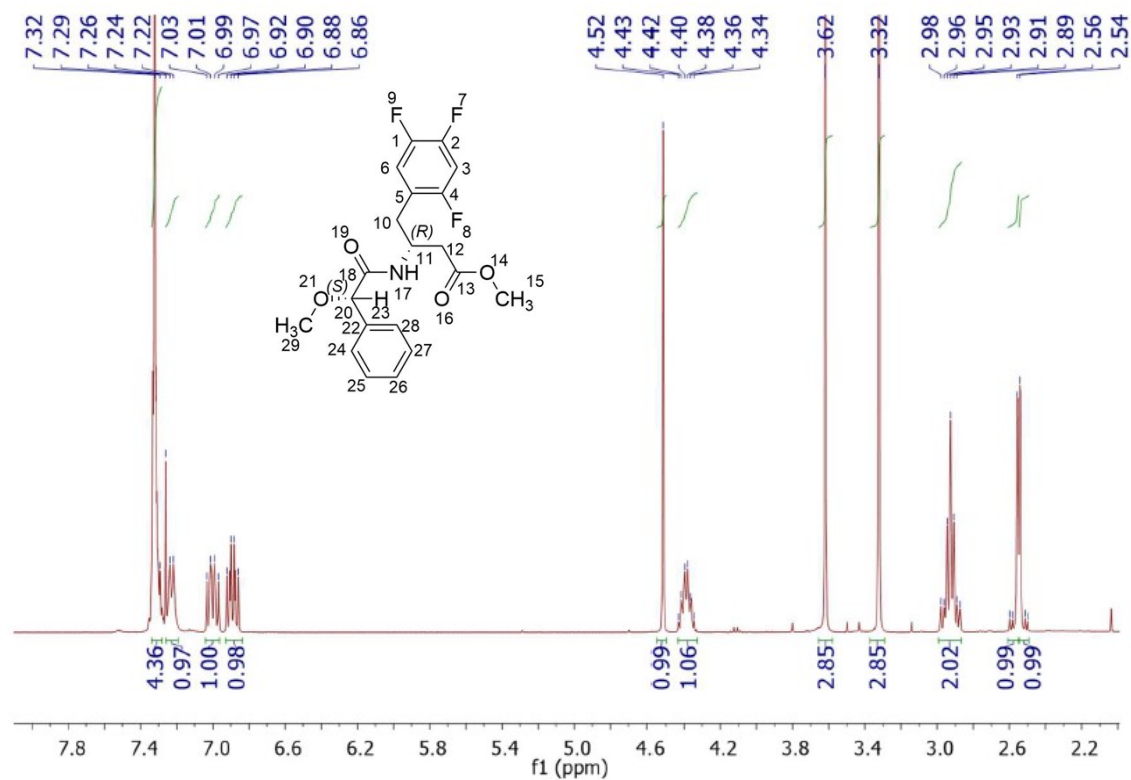


HSQC of **23** (CDCl₃/TMS/25°C)

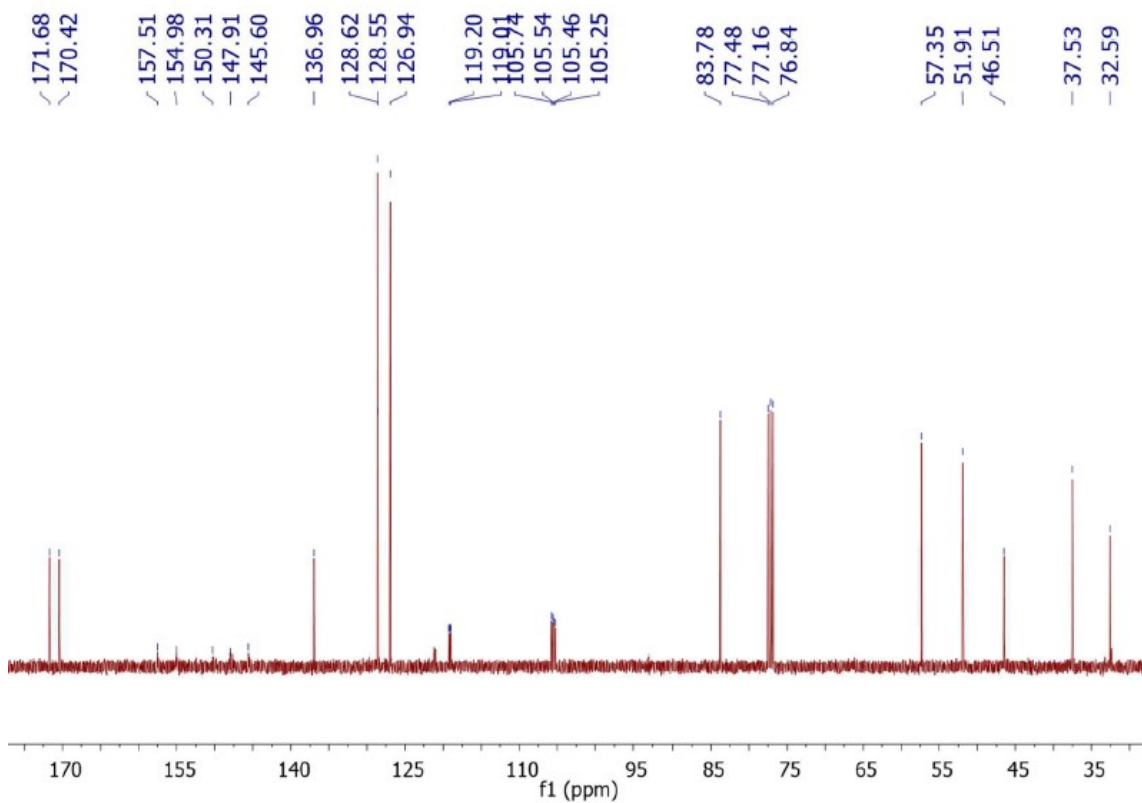


HMBC of **23** (CDCl₃/TMS/25°C)

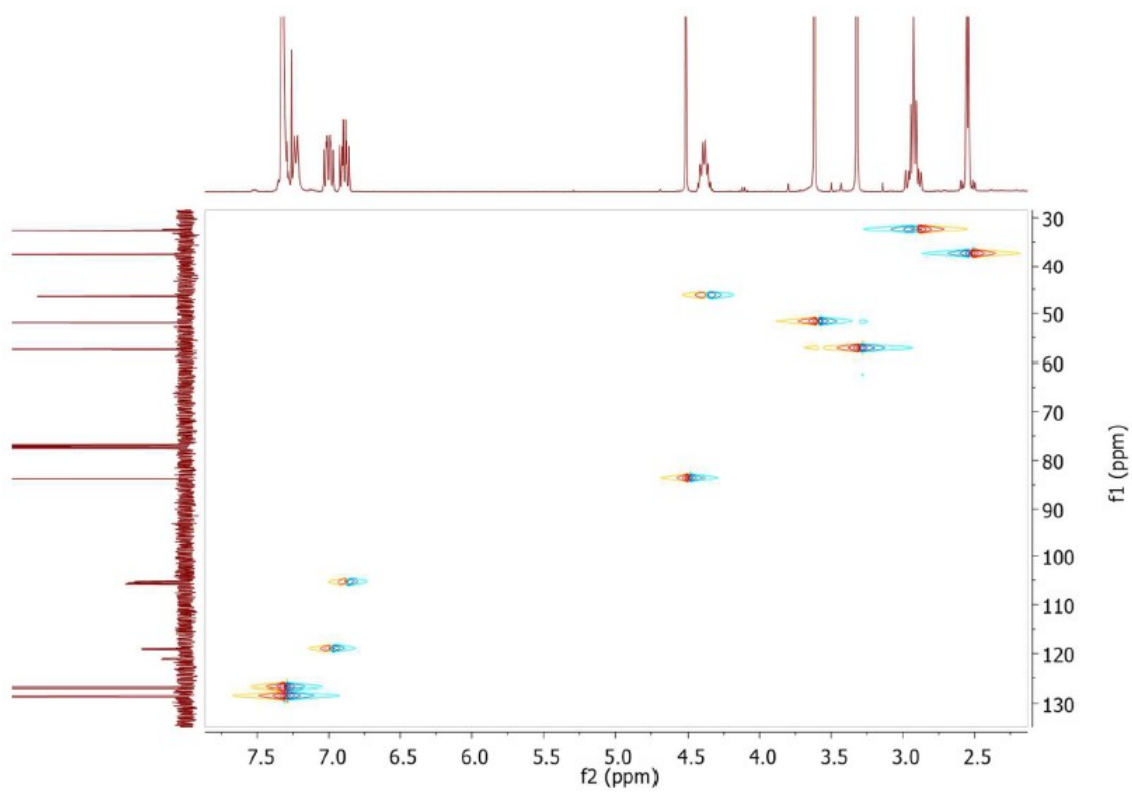
(R)-methyl 3-((S)-2-methoxy-2-phenylacetamido)-4-(2,4,5-trifluorophenyl)butanoate (24)



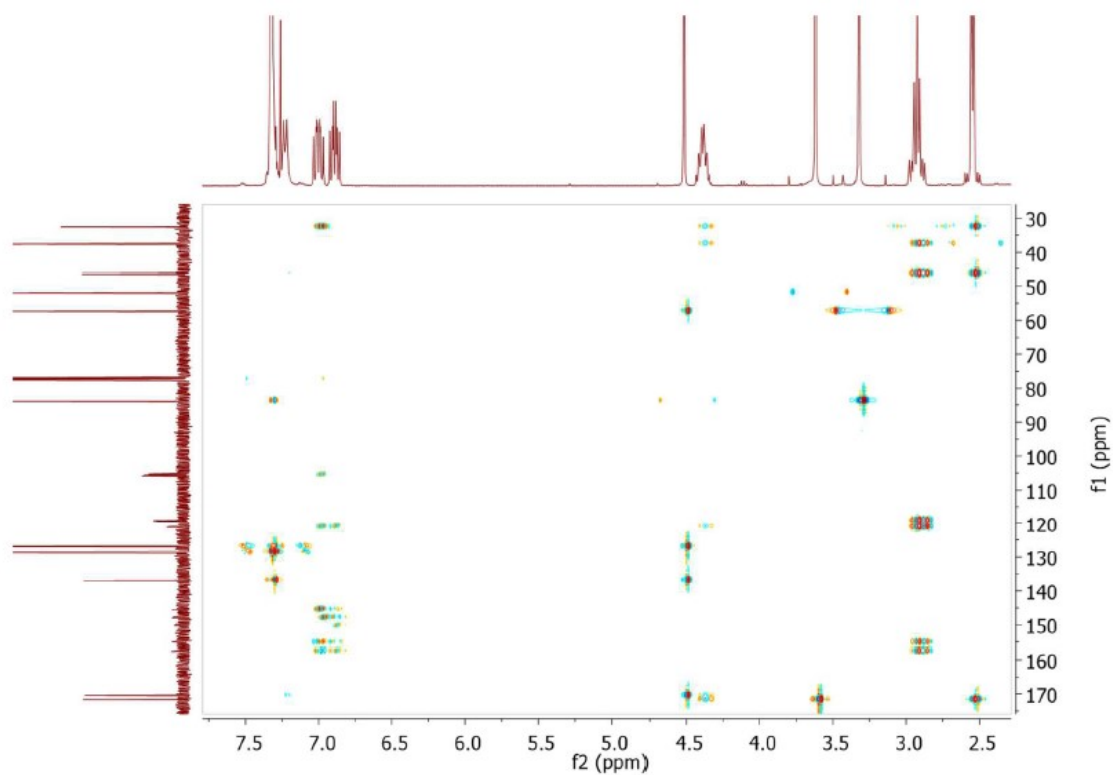
¹H-NMR spectrum of **24** (400MHz/CDCl₃/TMS/25°C)



¹³C-NMR spectrum of **24** (100MHz/CDCl₃/TMS/25°C)

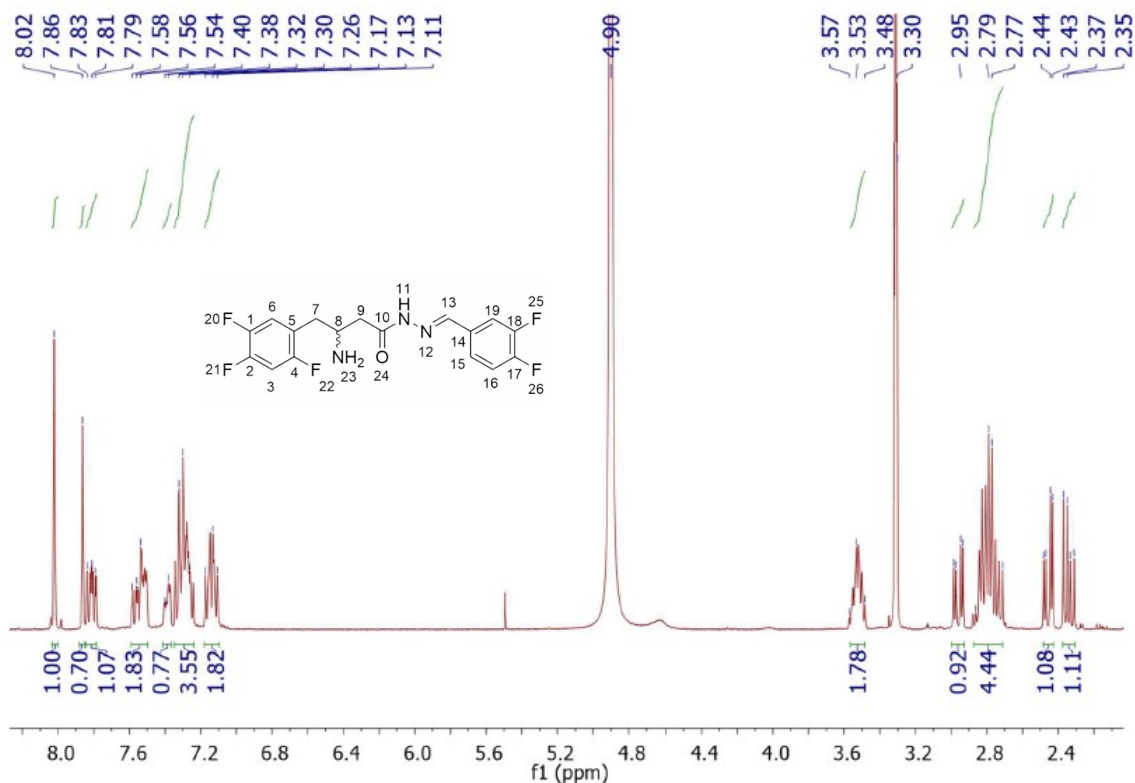


HSQC of **24** (CDCl₃/TMS/25°C)

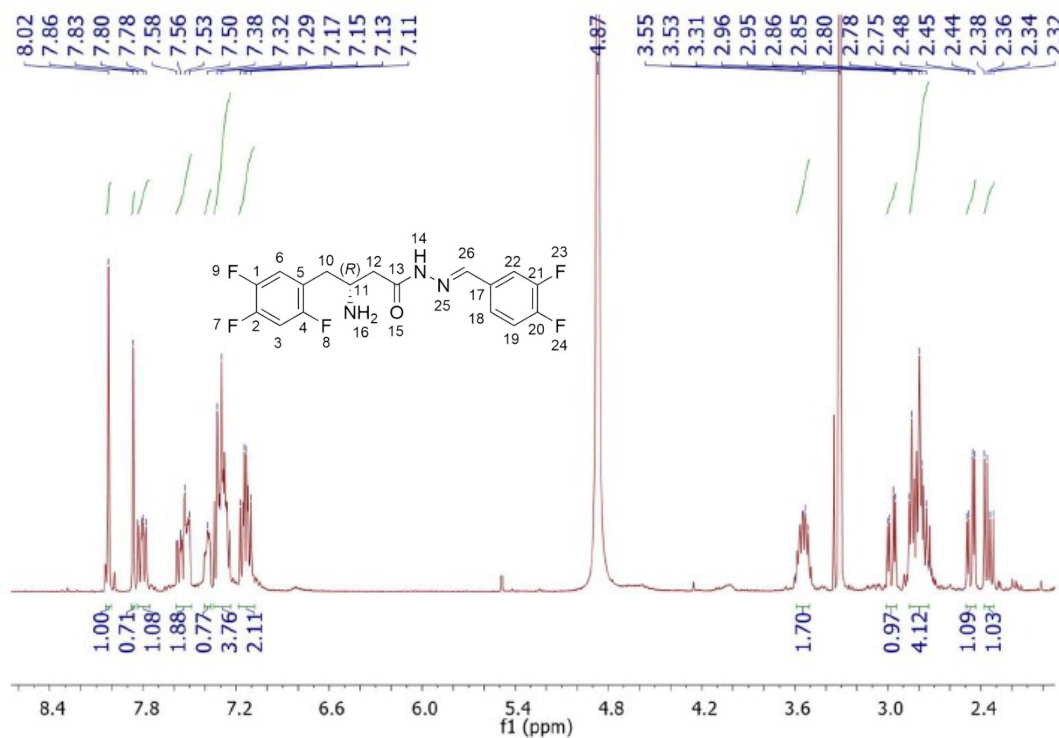


HMBC of **24** (CDCl₃/TMS/25°C)

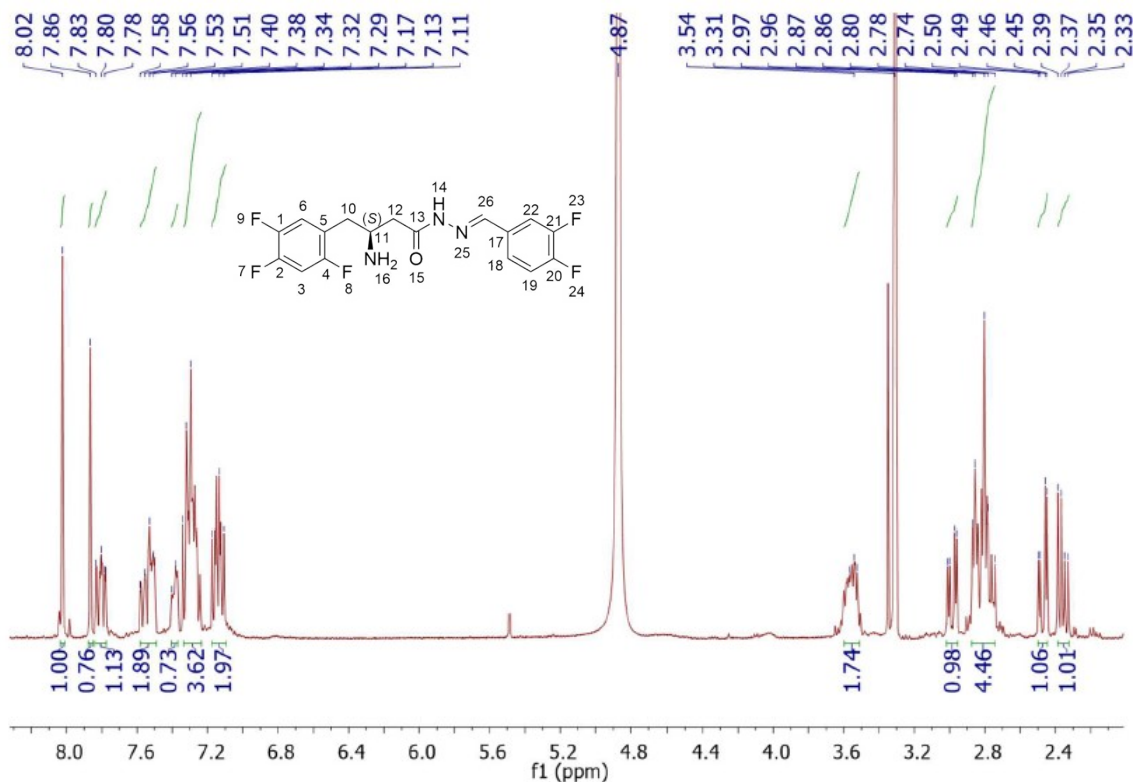
**(*R,S,E*)-3-amino-*N'*-(3,4-difluorobenzylidene)-4-(2,4,5-trifluorophenyl)butanehydrazide:
LASSBio-2124 (**6**)**



**(*R,E*)-3-amino-*N'*-(3,4-difluorobenzylidene)-4-(2,4,5-trifluorophenyl)butanehydrazide:
LASSBio-2129 (**6-(R)**)**



**(*S,E*)-3-amino-*N'*-(3,4-difluorobenzylidene)-4-(2,4,5-trifluorophenyl)butanehydrazide:
LASSBio-2130 (6-*S*)**



¹H-NMR spectrum of 6-*S* (400MHz/CD₃OD/TMS/25°C)

References

- 1 T. Zerilli and E. Y. Pyon, Clin Ther, 2007, 29, 2614–2634.
- 2 European Medicines Agency. Assessment Report For Januvia. London, 02 June 2009. Doc. Ref: EMEA/363653/2009 Available in: http://www.ema.europa.eu/docs/en_GB/document_library/EPAR_-_Assessment_Report_-_Variation/human/000722/WC500039129.pdf. Access in 02/05/2018.
- 3 P. Sun, Y. Chen, and G. YU, Process for preparing R-beta-amino phenylbutyric acid derivatives, US patent US2011/0130587 A1, 2011.
- 4 G. V. Govind et al, Sitagliptin synthesis, WO 2010131025 A1, 2010.
- 5 M. Kubryk and K. B. Hansen, Tetrahedron Asymmetry, 2006, 17, 205–209.
- 6 A. E. Kümmerle et al., J Med Chem, 2012, 55, 7525–7545.
- 7 D. A. Rodrigues et al., J Med Chem, 2016, 59, 655–670.
- 8 M. N. Khan, J Org Chem, 1995, 60, 4536–4541.
- 9 G. Tasnádi, E. Forró and F. Fülöp, Org. Biomol. Chem., 2010, 8, 793–799.
- 10 J. M. Seco, E. Quiñoá and R. Riguera, Chem Rev, 2004, 104, 17–118.
- 11 J. M. Seco, E. Quiñoá and R. Riguera, Tetrahedron Asymmetry, 2001, 12, 2915–2925.

- 12 P. Schneider, S. S. Hosseiny, M. Szczotka, V. Jordan and K. Schlitter, *Phytochem Lett*, 2009, **2**, 85–87.
- 13 P. Wiczling, M. J. Markuszewski and R. Kaliszan, *Anal Chem*, 2004, **76**, 3069–3077.
- 14 R. Konsoula and M. Jung, *Int J Pharm*, 2008, **361**, 19–25.